Spring 3-28-2022

Functionalized ?-hexalactones (FDHLs): Bio-derivable Monomers to Synthesize Renewable Polyester Thermoplastics

Atik Faysal
University of Maine, atik.faysal@maine.edu

FUNCTIONALIZED δ-HEXALACTONEs (FDHLs): BIO-DERIVABLE MONOMERS TO SYNTHESIZE RENEWABLE POLYESTER THERMOPLASTICS

By

Atik Faysal

B.Sc., University of Dhaka, Bangladesh, 2016

A DISSERTATION

Submitted in Partial Fulfillment of the

Requirements for the Degree of

Doctor of Philosophy

(in Chemistry)

The Graduate School

The University of Maine

May 2022

Advisory Committee:

William M. Gramlich, Associate Professor of Chemistry, Advisor

Barbara Cole, Professor of Chemistry

Carl P. Tripp, Professor of Chemistry

Matthew Brichacek, Assistant Professor of Chemistry

Thomas J. Schwartz, Associate Professor of Chemical and Biomedical Engineering

FUNCTIONALIZED δ-HEXALACTONEs (FDHLs): BIO-DERIVABLE MONOMERS TO SYNTHESIZE RENEWABLE POLYESTER THERMOPLASTICS

By Atik Faysal

Dissertation Advisor: Dr. William M. Gramlich

An Abstract of the Dissertation Presented
in Partial Fulfillment of the Requirements for the
Degree of Doctor of Philosophy
(in Chemistry)
May 2022

Most thermoplastics are made from limited fossil-fuel sources and these plastics have very deleterious impacts on the environment. Finding a renewable source to synthesize new thermoplastic polymers with tunable properties like biodegradability, heat resistance, and moisture resistance are ongoing research interests. Lignocellulosic biomass is a promising renewable feedstock for biobased monomers and polymers production. In this work, functionalized δ-hexalactone (FDHL) monomers are hypothesized to be synthesizable from lignocellulosic sourced hydroxymethyl furfural (HMF) and lignin-derived pendant groups, generating a variety of aliphatic polyesters and potentially overcome current polymer challenges. Achieving a higher glass transition temperature (T_g) is one of the main obstacles for the current bio-based thermoplastics. A successful FDHL monomer synthesis used commercially available methyl cyclopentanone-2-carboxylate as a starting material. Different bulky, lignin derivatives were incorporated as pendant groups (**aromatic**: phenol, 1-naphthol, and 2-phenyl phenol; **alkyl**:

cyclohexanol) in the monomer to increase the glass transition temperature (T_g) beyond that possible from poly(δ-valerolactone). Different acidic to super basic organocatalysts were screened to polymerize these novel monomers in a controlled manner. The polymerizations were carried out at room temperature via ring-opening polymerization technique using benzyl alcohol (BnOH) as an initiator. Different aliphatic polyesters with higher molecular weight and low dispersity were synthesized in a controlled manner. Typical equilibrium polymerization behavior was observed at room temperature due to the low ring strain of monomers, and the reaction was observed to be pseudo-first-order to monomer concentration in solution. By adding one phenyl group at the δ-position we found the T_g about 6 °C, and additional phenyl groups at the δ-position yielded the T_g about 40 °C which is a 105 °C increase from the unsubstituted poly(δ-valerolactone).

ACKNOWLEDGEMENTS

I would like to thank the dissertation advisor, Dr. William M. Gramlich, for the support and guidance throughout this work. I would like to give special thanks to my beloved wife, Jinhar Zahidi, for her tremendous support and motivation throughout my graduate school life. Special gratitude to Michael Flanders and Hathaithep Senkum for helping me through this whole journey. Special thanks to USDA for funding the project (USDA NIFA GRANT12439746).

TABLE OF CONTENTS

ACKNOWLEDGEMENTS v

LIST OF TABLES xi

LIST OF FIGURES xii

CHAPTER 1 : INTRODUCTION 1

1.1 Background 1

1.2 Mechanisms of ring-opening polymerization of lactones 5

1.3 Organocatalysts for ROP of lactones 7

1.4 Thermodynamics of polymerization 11

1.5 Controlled polymerization 13

1.6. Motivations and outline 15

CHAPTER 2: SYNTHESIS AND RING-OPENING POLYMERIZATION OF 6-(PHENOXYMETHYL)OXAN-2-ONE (PDHL) 18

2.1 Introduction 18

2.2. Materials and methods 20

2.2.1 Synthesis of methyl 1,4-dioxaspiro[4.4]nonane-6-carboxylate (1) 20

2.2.2 Synthesis of 1,4-dioxaspiro[4.4]non-6-ylmethanol (2) 21

2.2.3 Synthesis of 1,4-dioxaspiro[4.4]non-6-ylmethyl methanesulfonate (3) 21

2.2.4 Synthesis of 6-(phenoxymethyl)-1,4-dioxaspiro[4.4]nonane (4) 22

2.2.5 Synthesis of 2-(phenoxymethyl)cyclopentanone (5) 22

2.2.6 Synthesis of 6-(phenoxymethyl)oxan-2-one (6) 23

2.2.7 Polymerization materials and methods 23

2.2.8 General polymerization procedure for PDHL 24

2.2.9 Polymerization kinetics experiments 24

2.2.10. Polymerization thermodynamics experiments 25

2.2.11 Analysis of polymer products 26

2.3. Results and discussion 26

2.3.1. Ring-opening polymerization of PDHL lactone 34

2.3.2 Controlling the molecular weight of poly(PDHL) 36

2.3.3 Glass transition temperature (Tg) of poly(PDHL) 41

2.3.4 Thermodynamics of polymerization 42

2.3.5. Kinetics of polymerization 44

2.4 Conclusions 46

CHAPTER 3: SYNTHESIS AND RING-OPENING POLYMERIZATION OF 6-((2-PHENYLPHENOXY)METHYL)OXAN-2-ONE (2-PHPDHL) 47

3.1 Introduction 47

3.2. Materials and methods 49

3.2.1 Synthesis of 6-((2-phenylphenoxy)methyl)-1,4-dioxaspiro[4.4]nonane (7) 50

3.2.2 Synthesis of 2-((2-phenylphenoxy)methyl)cyclopentanone (8) 50

3.2.3 Synthesis of 6-((2-phenylphenoxy)methyl)oxan-2-one (9) 51

3.2.4. Polymerization materials and methods 51

3.2.6. Polymerization kinetics experiments 52

3.2.7. Polymerization thermodynamics experiments 53

3.2.8. Analysis of polymer products 54

3.3 Results and discussion 55

3.3.1 Ring-opening polymerization of 2-PhPDHL lactone 60

3.3.2 Controlling the molecular weight of poly(2-PhPDHL) 63

3.3.3 Role of TBD as an initiator in the ROP of 2-PhPDHL 66

3.3.4 Glass transition temperature (T_g) of poly(2-PhPDHL) 67

3.3.5 Thermodynamics of polymerization 69

3.3.6 Kinetics of polymerization 72

3.4 Conclusions 74

CHAPTER 4: SYNTHESIS AND RING OPENING POLYMERIZATION OF 6-((NAPHTHALEN-1-YLOXY)METHYL)OXAN-2-ONE (NDHL) 76

4.1 Introduction 76

4.2 Materials and methods 78

4.2.1 Synthesis of 6-((naphthalen-1-yloxy)methyl)-1,4-dioxaspiro[4.4]nonane (10) 79

4.2.2 Synthesis of 2-((naphthalen-1-yloxy)methyl)cyclopentanone (11) 79

4.2.3 Synthesis of 6-((naphthalen-1-yloxy)methyl)oxan-2-one (12) 80

4.2.4 Polymerization materials and methods 80

4.2.5 General polymerization procedure for NDHL 81
4.2.6 Polymerization kinetics experiments 81
4.2.7 Polymerization thermodynamics experiments 82
4.2.8 Analysis of polymer products 83
4.3 Results and discussion 84
4.3.1 Ring-opening polymerization of NDHL lactone 89
4.3.2 Controlling the molecular weight of poly(NDHL) 91
4.3.3 Glass transition temperature (T_g) of poly(NDHL) 97
4.3.4 Thermodynamics of polymerization 98
4.3.5 Kinetics of polymerization 100
4.4 Conclusions 103
CHAPTER 5: SYNTHESIS AND RING-OPENING POLYMERIZATION OF 6-((CYCLOHEXYLOXY)METHYL)OXAN-2-ONE (CDHL) 104
5.1 Introduction 104
5.2 Materials and methods 105
5.2.1 Synthesis of 6-((cyclohexyloxy)methyl)-1,4-dioxaspiro[4.4]nonane (13) 106
5.2.2 Synthesis of 2-((cyclohexyloxy)methyl)cyclopentanone (14) 106
5.2.3 Synthesis of 6-((cyclohexyloxy)methyl)oxan-2-one (15) 107
5.2.4 Polymerization materials and methods 107
5.2.5 General polymerization procedure for CDHL 108

5.2.6 Polymerization kinetics experiments 108

5.2.7 Polymerization thermodynamics experiments 109

5.2.8 Analysis of polymer products 110

5.3 Results and discussion 111

5.3.1 Ring-opening polymerization of CDHL lactone 116

5.3.2 Controlling the molecular weight of poly(CDHL) 117

5.3.3 Glass transition temperature (T_g) of poly(CDHL) 121

5.3.4 Thermodynamics of polymerization 122

5.3.5 Kinetics of polymerization 124

5.4 Conclusions 126

CHAPTER 6: FUTURE WORK 128

BIBLIOGRAPHY 131

BIOGRAPHY OF THE AUTHOR 142

LIST OF TABLES

Table 2.1. Results for acidic DPP catalyzed ROP of PDHL monomer 37

Table 2.2. Results for basic TBD catalyzed ROP of PDHL monomer 38

Table 2.3: Results for ROP of PDHL monomer with different TBD catalyst loading after 48 hours 40

Table 2.4. Observed equilibrium monomer concentration ($[M]_{eq}$) at different temperatures 42

Table 3.1. Effect of catalyst loading for ROP of 2-PhPDHL 62

Table 3.2. Results for TBD catalyzed ROP of 2-PhPDHL 66

Table 3.3. Observed equilibrium monomer concentration ($[M]_{eq}$) at different temperatures 70

Table 4.1. Amounts of 3-chloroperoxybenzoic acid (mCPBA) needed for successful (100% conversion) Baeyer-Villiger oxidation reaction 86

Table 4.2. Effect of TBD catalyst loadings for ROP of NDHL 91

Table 4.3. Results for TBD catalyzed ROP of NDHL 95

Table 4.4. Different molecular weights for poly(NDHL) obtained from ^{1}H NMR spectroscopy and SEC technique 95

Table 4.5. Effect of t-BuP_4 catalyst loadings for ROP of NDHL 97

Table 4.6. Observed equilibrium monomer concentration ($[M]_{eq}$) at different temperatures 100

Table 5.1. Effect of TBD catalyst loadings for ROP of CDHL 118

Table 5.2. Results for TBD catalyzed ROP of CDHL 121

Table 5.3. Observed equilibrium monomer concentration ($[M]_{eq}$) at different temperatures 123

LIST OF FIGURES

Figure 1.1. Modification of PLA by bulky side groups increased the T_g significantly 4

Figure 1.2. (a) Lignin-derived pendant groups added in polyacrylates. (b) Different alkyl groups are introduced at the δ-position of VL. 4

Figure 1.3. Mechanisms of anionic and cataionic ROP 6

Figure 1.4. Different acidic and basic organocatalysts system which have been reported for the successful ROP of δ-valerolactone monomers. 8

Figure 1.5. Dual activation of δ-VL monomer and initiator by TBD 10

Figure 1.6. Acid-base mechanism of TBD in ROP of δ-VL monomer[65] 11

Figure 1.7. Chain growth process for the ROP reaction 14

Figure 1.8. Initiation, propagation and undesired termination steps involve in the chain growth of ROP 14

Figure 1.9. Catalytic upgrading of HMF to functionalized δ-hexalactone (FDHL) followed by ring opening polymerization (ROP) to yield polyFDHLs. 16

Figure 1.10. Different bulky groups were introduced at the pendant position of FDHLs monomers 17

Figure 2.1. a) Alkyl substituted polyesters could not improve T_g b) Introducing bulkier pendant group at the δ-position of the six-membered lactone monomers to get higher T_g polyesters. 18

Figure 2.2. Reaction scheme for PDHL monomer synthesis 19

Figure 2.3. ^{1}H NMR spectrum of methyl 1,4-dioxaspiro[4.4]nonane-6-carboxylate (1) 27

Figure 2.4. ^{1}H NMR spectrum of 1,4-dioxaspiro[4.4]non-6-ylmethanol (2) 28

Figure 2.5. ^{1}H NMR spectrum of 1,4-dioxaspiro[4.4]non-6-ylmethyl methanesulfonate (3) 29

Figure 2.6. ^{1}H NMR spectrum of 6-(phenoxymethyl)-1,4-dioxaspiro[4.4]nonane (4). *Mineral oil from NaH washing step 30

Figure 2.7. ^{1}H NMR spectrum of 2-(phenoxymethyl)cyclopentanone (5). *Acetone solvent and mineral oil 31

Figure 2.8. ^{1}H NMR spectrum of a crude mixture of 6-(phenoxymethyl)oxan-2-one (6)..... 32

Figure 2.9. ^{1}H NMR spectrum of pure PDHL monomer (6), collected after flash column chromatography. 33

Figure 2.10. ^{13}C NMR spectrum of pure PDHL monomer (6) 34

Figure 2.11. Polymerization scheme for ring opening polymerization of PDHL..... 35

Figure 2.12. ^{1}H NMR spectrum of ring-opening polymerization of PDHL monomer using different acidic to basic organocatalysts (left). Catalysts loading ranges used to polymerize PDHL monomer (right). 36

Figure 2.13. ^{1}H NMR spectrum of crude poly(PDHL). ^{1}H NMR spectrum was collected after the polymerization reached equilibrium on day seven. (*THF solvent,**H_2O)..... 39

Figure 2.14. SEC elution curves for TBD catalyzed ROP of PDHL after reaching equilibrium conversion at different $[M]_0/[I]$ ratios. Molecular weights ($M_{n,\ SEC}$) and dispersity are in the Table 2.2..... 40

Figure 2.15. DSC thermograms of polyPDHL. Curves are shifted vertically to provide clarity. 42

Figure 2.16. Van't Hoff analysis for poly(PDHL) (red triangle). 44

Figure 2.17. a) Monomer conversion as a function of time for poly(PDHL); b) Linearized kinetics behavior for ROP of PDHL (red triangle) before reaching equilibrium, where $[M]_{eq}$ is the equilibrium monomer concentration, $[M]_0$ is the initial monomer concentration, $[M]_t$ is the monomer concentration at given a time. 45

Figure 2.18. Number average molecular weight (M_n) and dispersity (Đ) as a function of monomer conversion for poly(PDHL). Both M_n and Đ measured by SEC. Ratios of $[M]_0/[I]$ = 100/1 for poly(PDHL) used throughout this study. 46

Figure 3.1. Introducing bulkier pendant group at the δ-position of the six-membered lactone monomers to get higher T_g polyesters 48

Figure 3.2. Reaction scheme for 2-PhPDHL monomer synthesis 49

Figure 3.3. ^{1}H NMR spectrum of 6-((2-phenylphenoxy)methyl)-1,4-dioxaspiro[4.4]nonane (7). *Mineral oil from NaH washing step, #DMF, and ethyl acetate solvents 55

Figure 3.4. ^{1}H NMR spectrum of 2-((2-phenylphenoxy)methyl)cyclopentanone (8). *Mineral oil 56

Figure 3.5. ^{1}H NMR spectrum of a crude mixture of 6-((2-phenylphenoxy)methyl)oxan-2-one (9), ** 3-chlorobenzoic acid 58

Figure 3.6. ^{1}H NMR spectrum of pure 2-PhPDHL monomer (9), collected after flash column chromatography. 59

Figure 3.7. ^{13}C NMR spectrum of pure 2-PhPDHL monomer (9) 60

Figure 3.8. Polymerization scheme for the ring opening polymerization of 2-PhPDHL 61

Figure 3.9. a) Primary alcohol from the initiator initiates the polymerization instantaneously. b) Secondary alcohol of the propagating chain end acts as a slow

initiator for the upcoming monomer. c) Excess catalysts can activate the secondary alcohol of the propagating chain end and push the reaction forward. 63

Figure 3.10. ^{1}H NMR spectrum of crude poly(2-PhPDHL). ^{1}H NMR spectrum was collected after the polymerization reached equilibrium on day three. (*THF and methanol solvent) 64

Figure 3.11. SEC elution curves for ROP of 2-PhPDHL after reaching equilibrium conversion at different $[M]_0/[I]$ ratios. Molecular weights ($M_{n,\ SEC}$) and dispersity are in Table 2. 65

Figure 3.12. ^{1}H NMR spectrum of poly(2-PhPDHL) obtained by TBD catalyzed ROP in the absence of BnOH as an initiator (Table 3.2, entry 5) 67

Figure 3.13. DSC thermograms of poly(2-PhPDHL). Curves are shifted vertically to provide clarity. 68

Figure 3.14. Dependence of the glass transition temperature on molecular weight for poly(2-PhPDHL) where plot shows the T_g versus $1/M_n$ 69

Figure 3.15. Van't Hoff analysis for poly(2-PhPDHL) (green circle). 72

Figure 3.16. a) Monomer conversion as a function of time for poly(2-PhPDHL); b) Linearized kinetics behavior for ROP of 2-PhPDHL (green circle) before reaching equilibrium where $[M]_{eq}$ is the equilibrium monomer concentration, $[M]_0$ is the initial monomer concentration, $[M]_t$ is the monomer concentration at given a time. 73

Figure 3.17. Number average molecular weight (M_n) and dispersity (Đ) as a function of monomer conversion for poly(2-PhPDHL). Both M_n and Đ measured by SEC. Ratios of $[M]_0/[I] = 50/1$ for poly(2-PhPDHL) used throughout this study. 74

Figure 4.1. Introducing more sterically hindered pendant group at δ-position of the six-membered lactone monomers to get higher T_g polyesters 77

Figure 4.2. Reaction scheme for NDHL monomer synthesis 78

Figure 4.3. ^{1}H NMR spectrum of 6-((naphthalen-1-yloxy)methyl)-1,4-dioxaspiro[4.4]nonane (10). *Mineral oil from NaH washing step, DMF, and ethyl acetate solvents 84

Figure 4.4. ^{1}H NMR spectrum of 2-((naphthalen-1-yloxy)methyl)cyclopentanone (11) 85

Figure 4.5. ^{1}H NMR spectrum of a crude mixture of 6-((naphthalen-1-yloxy)methyl)oxan-2-one (12), *Mineral oils, **3-Chlorobenzoic acid. 87

Figure 4.6. ^{1}H NMR spectrum of pure 6-((naphthalen-1-yloxy)methyl)oxan-2-one (12), collected after flash column chromatography. *Ethyl acetate and DCM solvents, **impurities 88

Figure 4.7. ^{13}C NMR spectrum of pure 6-((naphthalen-1-yloxy)methyl)oxan-2-one (12) 89

Figure 4.8. Polymerization scheme for the ring-opening polymerization of NDHL 90

Figure 4.9. ^{1}H NMR spectrum of precipitated poly(NDHL). ^{1}H NMR spectrum was collected after the polymerization reached equilibrium on day three. (*Diethyl ether solvent) 92

Figure 4.10. SEC elution curves for ROP of NDHL after reaching equilibrium conversion at different $[M]_0/[I]$ ratios. Molecular weights ($M_{n,\,SEC}$) and dispersity are in Table 4.3. 93

Figure 4.11. ^{1}H NMR spectrum of poly(NDHL) obtained by TBD catalyzed ROP in the absence of BnOH as an initiator (Table 4.3, entry 4) 96

Figure 4.12. t-BuP_4 organocatalyst for ROP of lactones 97

Figure 4.13. DSC thermograms of poly(NDHL). Curves are shifted vertically to provide clarity. 98

Figure 4.14. Van't Hoff analysis for poly(NDHL) (blue diamond). 100

Figure 4.15. a) Monomer conversion as a function of time for polyNDHL b) Linearized kinetics behavior for ROP of NDHL (blue diamond) before reaching equilibrium, where $[M]_{eq}$ is the equilibrium monomer concentration, $[M]_0$ is the initial monomer concentration, $[M]_t$ is the monomer concentration at given a time. 101

Figure 4.16. Number average molecular weight (M_n) and dispersity (Đ) as a function of monomer conversion for poly(NDHL). Both M_n and Đ measured by SEC. Ratios of $[M]_0/[I] = 50/1$ for poly(NDHL) used throughout this study. 102

Figure 5.1. Introducing sterically hindered hydrogenated pendant groups at δ-position will produce a new library of monomers with tunable properties 104

Figure 5.2. Reaction scheme for CDHL monomer synthesis 105

Figure 5.3. Reaction scheme for etherification reaction which resulted in overall low yield 111

Figure 5.4. ^{1}H NMR spectrum of 6-((cyclohexyloxy)methyl)-1,4-dioxaspiro[4.4]nonane (13). 112

Figure 5.5. ^{1}H NMR spectrum of 2-((cyclohexyloxy)methyl)cyclopentanone (14). *Ethyl acetate and ethylene glycol. 113

Figure 5.6. ^{1}H NMR spectrum of a crude mixture of 6-((cyclohexyloxy)methyl)oxan-2-one (15), *DCM solvent. 114

Figure 5.7. ^{1}H NMR spectrum of pure 6-((cyclohexyloxy)methyl)oxan-2-one (15), collected after flash column chromatography. 115

Figure 5.8. ^{13}C NMR spectrum of pure 6-((cyclohexyloxy)methyl)oxan-2-one (15). 116

Figure 5.9. Polymerization scheme for the ring-opening polymerization of CDHL 117

Figure 5.10. ^{1}H NMR spectrum of crude poly(CDHL). ^{1}H NMR spectrum was collected after the polymerization reached equilibrium on day three. *1,4-Dioxane solvent, **3-chlorobenzoic acid. 119

Figure 5.11. SEC elution curves for ROP of CDHL after reaching equilibrium conversion at different $[M]_0/[I]$ ratios. Molecular weights ($M_{n,\ SEC}$) and dispersity are in Table 5.2. 120

Figure 5.12. DSC thermograms of poly(CDHL). Curves are shifted vertically to provide clarity. 122

Figure 5.13. Van't Hoff analysis for poly(CDHL) (black rectangle). 124

Figure 5.14. a) Monomer conversion as a function of time for polyCDHL b) Linearized kinetics behavior for ROP of CDHL (black rectangle) before reaching equilibrium, where $[M]_{eq}$ is the equilibrium monomer concentration, $[M]_0$ is the initial monomer concentration, $[M]_t$ is the monomer concentration at given a time. 125

Figure 5.15. Number average molecular weight (M_n) and dispersity (Đ) as a function of monomer conversion for poly(CDHL). Both M_n and Đ measured by SEC. Ratios of $[M]_0/[I] = 50/1$ for poly(CDHL) used throughout this study. 126

Figure 6.1. New recommended monomer structures for future work 128

Figure 6.2. Hydrogenated version of proposed different new monomers 129

Figure 6.3. Phosphazene base t-BuP_2 catalyst 130

CHAPTER 1: INTRODUCTION

1.1 Background

Petroleum-based thermoplastics are ubiquitous in our daily life, but the widespread use of these non-degradable plastics has created a waste management problem that has left a significant mark on the environment.[1,2] World plastic production is continuously growing from 1.7 Mton/year in 1950 to 288 Mton/year in 2012. Fossil sources are still required for the production of the majority of polymers, as only 5% of chemicals are currently produced from renewable feedstocks.[3],[4] Only about 9% of the plastic waste has been recycled, and another 12% has been incinerated for energy recovery but the remaining 79% has been discarded to the environment.[5,6,7] The overwhelming dumping of plastics cause serious ecological problems, stimulating the development of new sustainable materials. The limitation towards biodegradability of petroleum-based polymers and the exhaustible nature of the oil reserves have intensified interest in natural renewing resources for the chemical synthesis of polymers.[8] Polymers based on naturally occurring products are promising new materials, with enhanced properties like biocompatibility and biodegradability. Consequently, the production of environmentally friendly and sustainable polymers constitutes a steadily growing field of attention.[8,9] PHB (poly-3-hydroxybutyrate), PHA (polyhydroxyalkanoates), poly(lactic acid) (PLA) are the major thermoplastics synthesized from biomass for the last few decades.[10,11,12] The motivation behind the synthesis of these thermoplastic materials is the development of polymers having characteristics comparable to those of the industrial polymers or better but synthesized from renewable raw materials like biomass.[8]

Lignocellulosic biomass, the most abundant biomass source, is a promising feedstock for biobased monomer production, and polymers derived from lignocellulosic biomass can provide

sustainability and performance advantages.[5] Lignocellulose does not compete with the food industry and is readily available as a part of various waste streams of the agriculture, forestry, and the paper industry.[3] Therefore, lignocellulose is likely to be the main renewable source of carbon to substitute hydrocarbons in the future. Sustainable polymers from lignocellulosic biomass have the potential to reduce the environmental impact of commercial plastics while also offering significant performance benefits relative to petrochemical-derived macromolecules.[5]

Cellulose, hemicellulose, and lignin are the three primary components of lignocellulosic biomass, which can be transformed into platform chemicals like 5-hydroxymethylfurfural (HMF)[13,14,15] and lignin-derived phenols[16,17,18,19] that can be used as building blocks for the production of various bio-based monomers.[20,21] A variety of approaches have been reported in the literature to prepare HMF from cellulose: the most common methods are using ionic liquids[22] as the solvent, water as a solvent[23], and a biphasic system.[24,25] Lignin is a major component of woody biomass and a renewable source of aromatic compounds. Several processes are known for refining lignin including, supercritical water[26], formic acid hydrolysis[27], reactions in ionic liquids[28], and pyrolysis[29]. Pyrolysis has been shown the most promising method to generate small molecules from lignin, but the typical pyrolysis method has a low yield problem. DeSisto et al. have developed formate assisted fast pyrolysis (FAsP) of lignin, which overcame the low yields issue by pyrolysis method, to extract methyl and ethyl functionalized phenols, cresols, catechols, and naphthols.[30],[31] Vithanage et al. showed the formate assisted fast pyrolysis (FAsP) of lignin yielded a bio-oil consisting of alkylated phenol compounds and phenol rich monomer mixture.[32]

HMF is particularly attractive in this regard because it possesses both a hydroxyl group and an aldehyde that can undergo reactions independently. Illustrating the ability of HMF to undergo

selective upgrading, Allen et al. recently showed that zeolite catalysts can be used to etherify the hydroxyl group in HMF with a variety of alcohols, including phenols that can be obtained from lignin,[33] which opens the door to the production of HMF-based polymers with tunable pendant groups.

Current bio-based thermoplastics such as polylactic acid (PLA) are commercially relevant, but they cannot replace all petroleum-based thermoplastics because they suffer from low glass transition temperatures, toughness, and moisture resistance.[34,35,36,37] Like PLA, most aliphatic polyesters cannot be used at high temperatures and lack mechanical properties appropriate for all applications.[38] By introducing different pendant functional groups we can tune the properties and expand the versatility of aliphatic polyesters. Rotational barriers of the polymer backbone can be increased by adding bulky groups to polymer chain, which results in higher T_g. Relatively flexible backbone polymers like polylactide have been modified by introducing bulky side groups to increase the T_g (Figure 1.1).[39,40,41] Lignin is an abundant natural polymer and a renewable source of bulky aromatic compounds[42] and lignin pendant groups have been incorporated in polyacrylates to significantly increase the glass transition temperature (Figure 1.2a).[41,43] Similarly, we hypothesize that incorporating these lignin-derived aromatic molecules as pendant groups in aliphatic polyesters will increase the glass transition temperature of aliphatic polyesters.

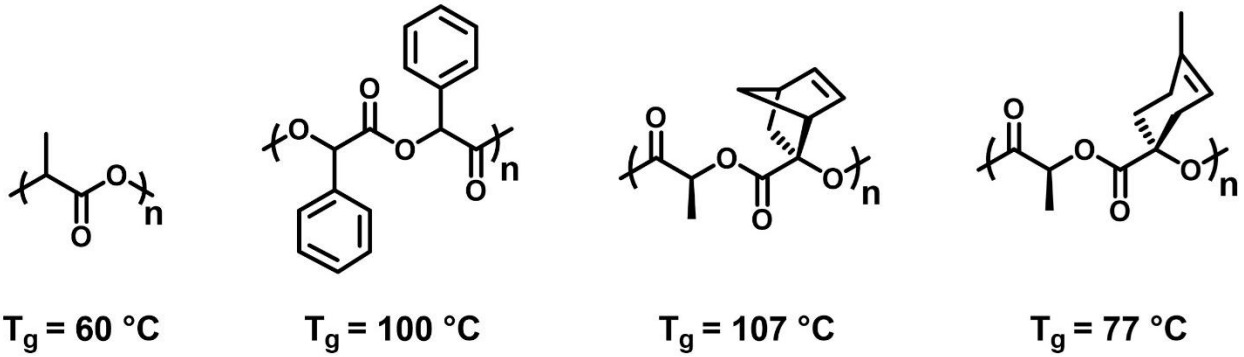

Figure 1.1. Modification of PLA by bulky side groups increased the T_g significantly

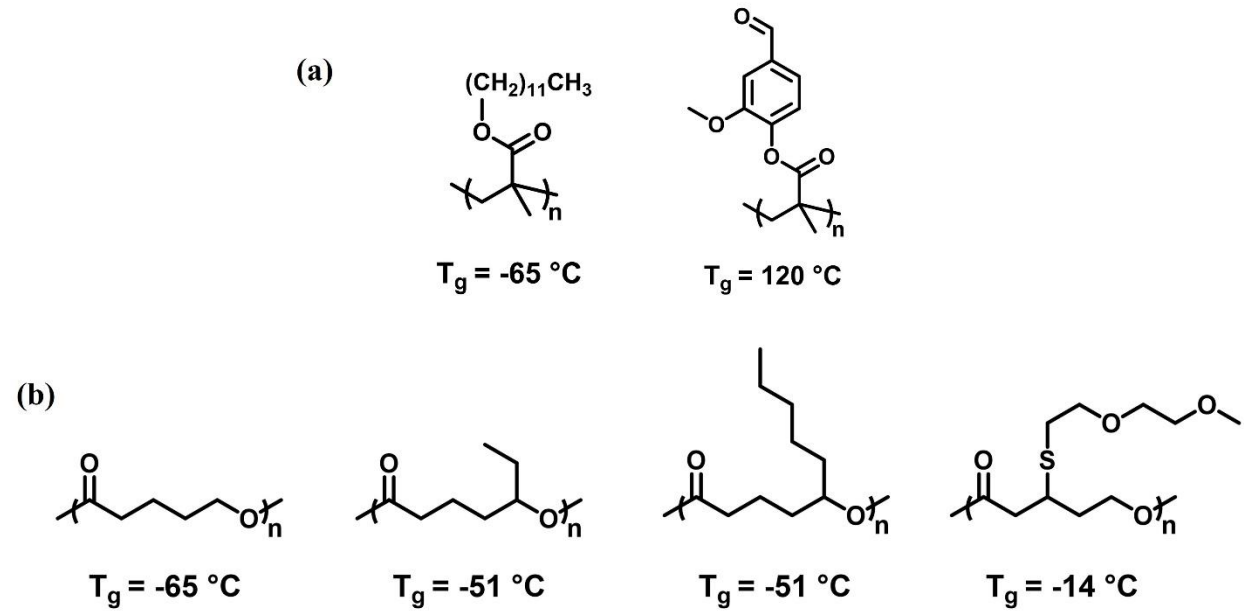

Figure 1.2. (a) Lignin-derived pendant groups added in polyacrylates. (b) Different alkyl and thiol groups are introduced at VLs.

The synthesis and ring-opening polymerization (ROP) of functionalized lactones is a powerful strategy for generating functionalized polyesters[44] and their well-known depolymerization methods such as ester hydrolysis and transesterification could provide a recyclable methodology to mitigate concerns about end-of-life plastic disposal.[45] Six membered lactones have low ring

strain but can be polymerized at room temperature using different organocatalysts.[46,47] Six membered lactones bearing different pendant groups have not been studied thoroughly due to the limited availability of diverse monomers. Mostly alkyl groups have been attached at the δ-position of the six-membered lactone monomers. The ring-opening polymerization of six-membered lactones is enthalpically favored (indicated by a negative ΔH_p) and entropically disfavored (indicated by a negative ΔS_p). Generally, polymerized six- or seven-membered lactones have low T_g (around -70 to -60 °C), and incorporating pendant alkyl groups at the δ-position of six-membered δ-valerolactone (DVL) did not substantially change the T_g of the corresponding polyester (Figure 1.2b).[48] Different chain length alkyl groups at the δ-position of six-membered δ-valerolactone have been attached to figure out the impact on T_g of the polymers. The low T_g of functionalized polyesters restricts the end application of these thermoplastics. To our knowledge there are not yet any reports of a systematic method except for alkyl chains as pendant groups to yield higher T_g by introducing different pendant groups off the fixed polymer backbone, while maintaining a fully renewable origin with the potential for polymer recycling.

1.2 Mechanisms of ring-opening polymerization of lactones

Ring-opening polymerization is a chain-growth polymerization that offers the advantages of providing more precise control over the molecular weight and molecular weight distribution with the advent of living polymerization reactions.[49] ROP mechanisms are divided into cationic and anionic polymerization depending on the ionic charge of active propagating species.[49,50] For anionic polymerization nucleophiles such as organometallics, alkoxides, and alcohols are used as initiators (Figure 1.3a). Nucleophilic attack by initiators at the carbonyl carbon in the lactone monomer opens the ring and yields a propagating anionic chain end. Cationic ROP proceeds either

by a monomer-activated mechanism via protonated monomer (Figure 1.3b) or a chain-end activated mechanism via cationic oxonium chain ends (Figure 1.3c).[2] Both monomer activated and chain-end activated mechanisms sometimes compete with each other and result in uncontrolled polymerization.

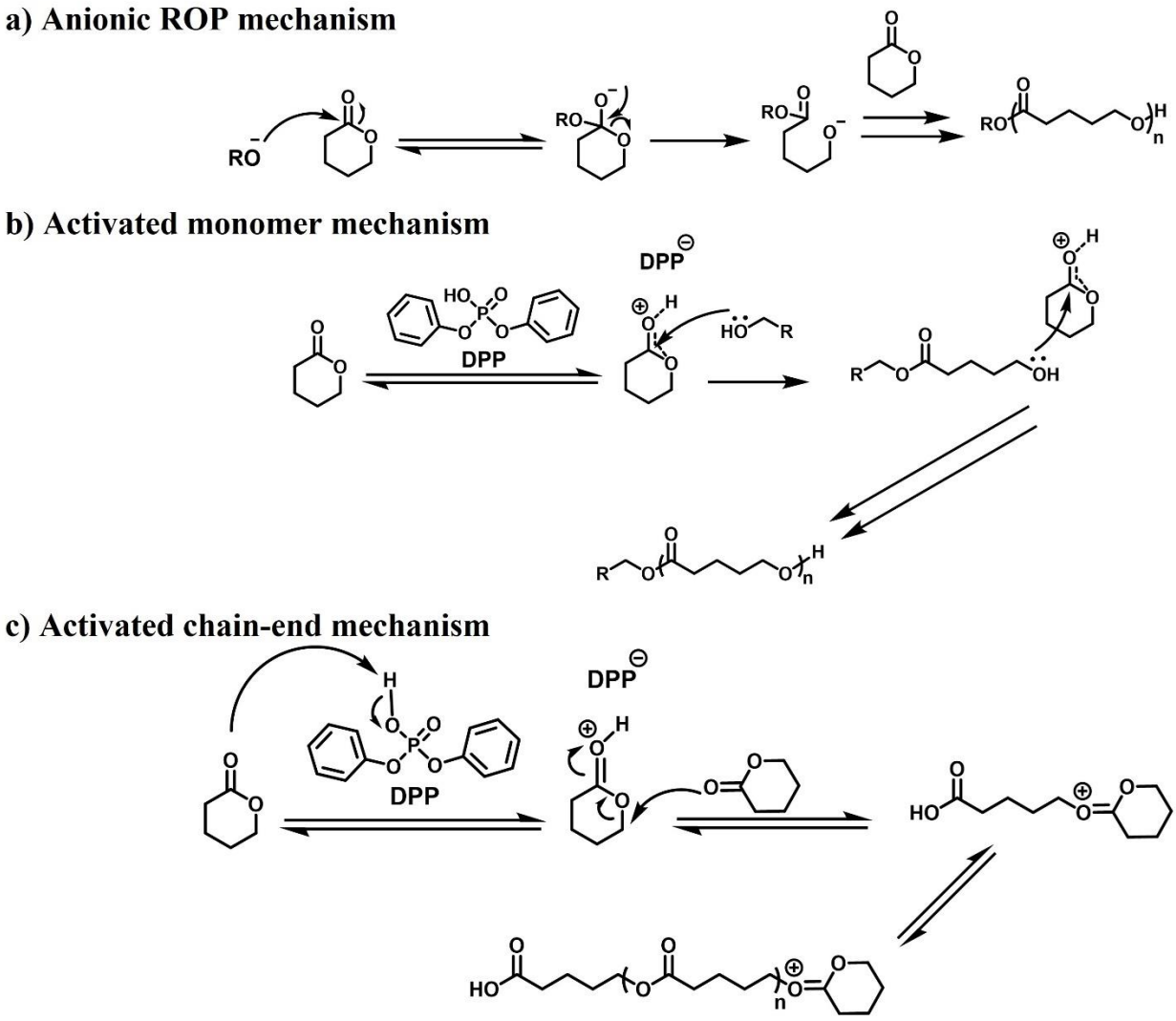

Figure 1.3. Mechanisms of anionic and cataionic ROP

1.3 Organocatalysts for ROP of lactones

A broad variety of metal complexes have been evaluated as catalysts for the ring-opening polymerization (ROP) of lactones, but a metal-free approach is desirable when the resulting polyesters are to be used within medicinal, food packaging, or microelectronic devices.[51] Significant progress has been achieved over the past few years in organo-catalyzed ROP to overcome this issue and to find an alternate way to polymerize these lactones.[52] Hedrick and Waymouth have developed a variety of acidic and basic catalytic systems: 4-aminopyridines, *N*-heterocyclic carbenes, thiourea/amine combinations, guanidines, phosphazenes that can efficiently promote the ROP of lactide via nucleophilic, basic, or dual activation.[53,54,55,56] Fastnacht et al., showed the catalytic activity of the bis- and tris-urea as hydrogen bond donors for ring-opening polymerization of δ-valerolactones in the presence of a co-catalyst system.[57,58] Makiguchi et al., also polymerized δ-valerolactones and ε-caprolactone successfully by using diphenyl phosphate (DPP) as an acidic organo-catalyst.[59] (Figure 1.4) DPP is an excellent acidic catalyst for ring opening polymerization of different lactones and lactams have been reported in the literature.

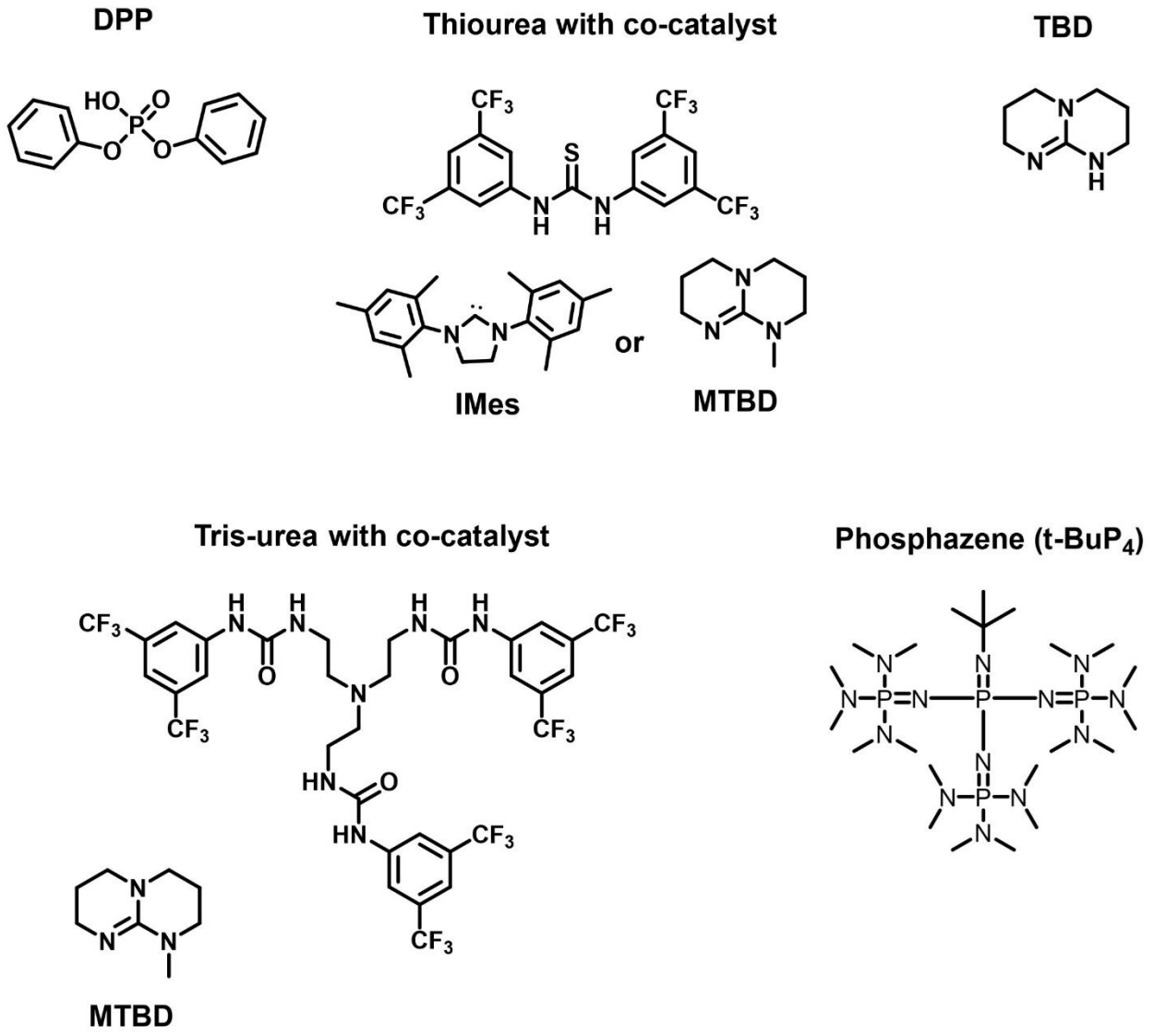

Figure 1.4. Different acidic and basic organocatalysts system which have been reported for the successful ROP of δ-valerolactone monomers.

Among these catalysts basic guanidine 1,4,7-triazabicyclodecene (TBD) drawn attention by polymerizing various lactones with high molecular weights and narrow PDIs.[60,61,62] TBD contains tertiary and secondary nitrogen atoms that act as a hydrogen bond donor and acceptor. This allows the activation of the monomer and initiator simultaneously. Such a phenomenon is commonly called a bifunctional mode of action.[63] Cyclic esters such as δ-VL and ε-CL can be polymerized

by TBD in the absence of any co-catalysts, unlike thiourea or urea catalysts due to the dual activation mechanism. Waymouth and Hedrick proposed the bifunctional nucleophilic mechanism of TBD. The nucleophilic attack of the imine nitrogen of TBD at the carbonyl would generate an intermediate. The adjacent protonated nitrogen of TBD is ideally suited for proton transfer to the incoming alkoxide to generate the TBD amide.[64] Hydrogen-bond activation of the incoming alcohol should facilitate esterification, liberating the ester and regenerating TBD (Figure 1.5). Simon and Goodman reported that TBD-catalyzed ROP proceeds by either a nucleophilic or acid-base catalytic mechanism, where the nucleophilic catalytic mechanism predominates when the alcohol concentration is low compared to the catalyst loading.[65] Lactone intermediate is formed instead of amide during acid-base catalytic mechanism reported by Simon and Goodman (Figure 1.6).[65] Both mechanisms can compete with each other during propagation step of the polymerization.

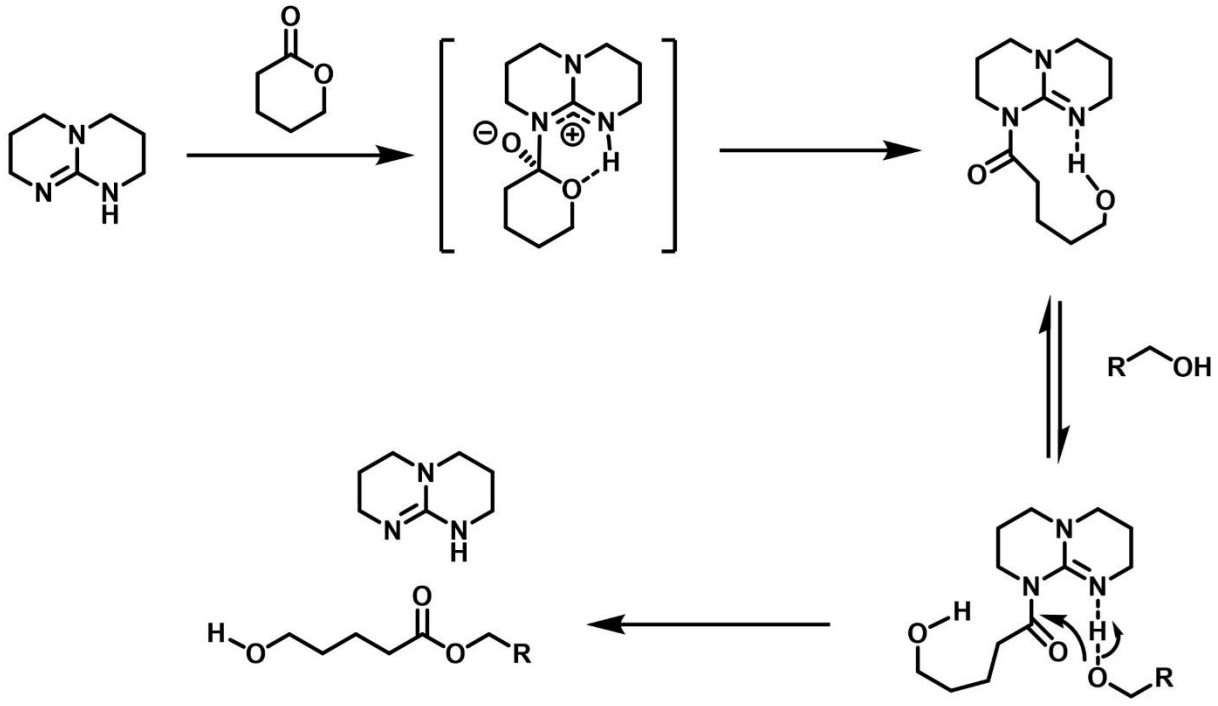

Figure 1.5. Dual activation of δ-VL monomer and initiator by TBD[64]

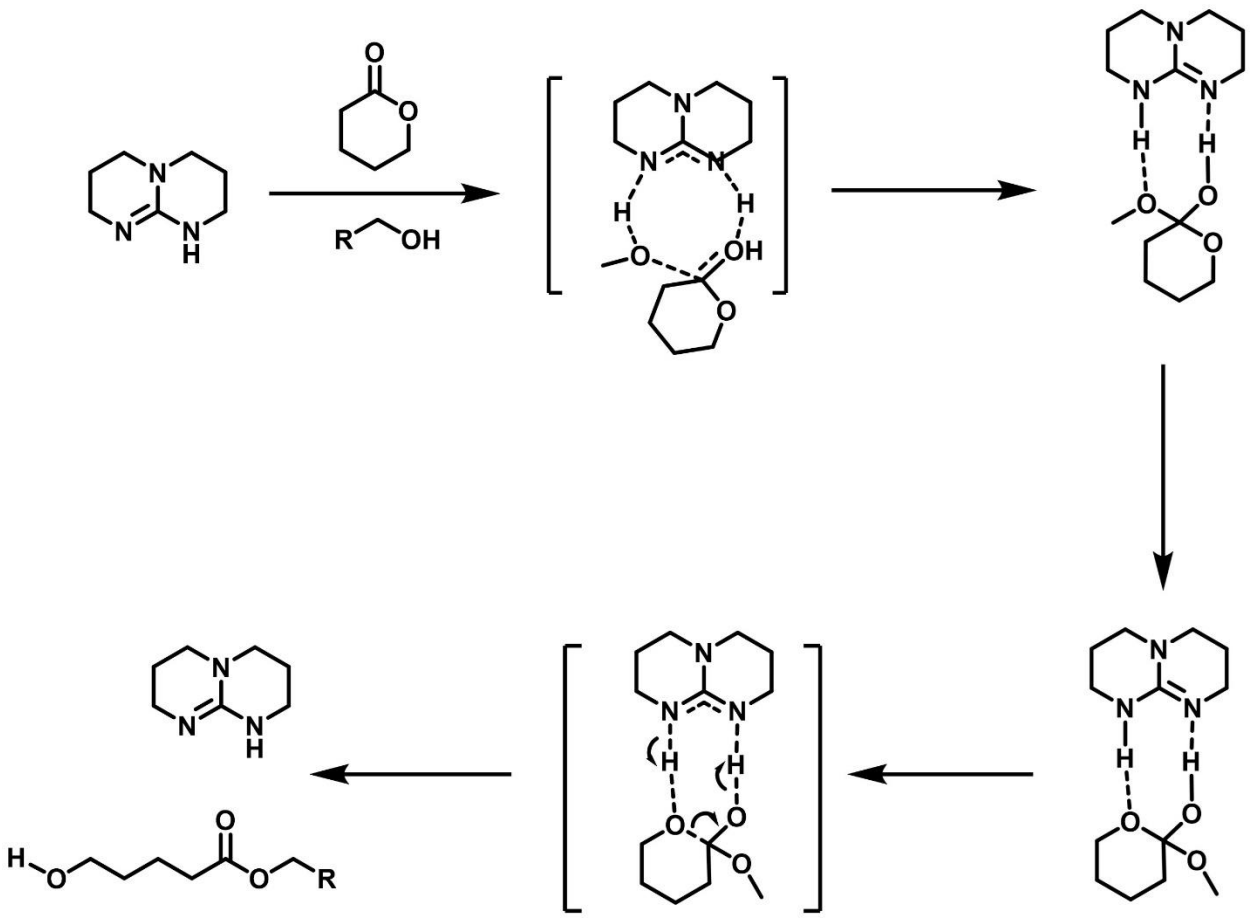

Figure 1.6. Acid-base mechanism of TBD in ROP of δ-VL monomer[65]

1.4 Thermodynamics of polymerization

Polymerization can be viewed from the change in Gibbs free energy (ΔG) upon transformation (Equation 1.1). When ΔG < 0, the polymerization is favored, whereas if ΔG > 0, the polymerization is disfavored. The magnitude of ΔG does not describe how fast the reaction will occur but rather the lowest energy state. Depending on the catalytic system, different routes through the transition states are realized, although this will not change the fundamental features of the system.[66]

$$\Delta G_p = \Delta H_p - T\Delta S_p \quad \text{(Equation 1.1)}$$

Here, ΔH_p is the enthalpy of polymerization, T is the temperature of polymerization, and ΔS_p is the entropy of polymerization. The maximum conversion of the monomer is dependent on the intrinsic thermodynamic features (ΔH_p and ΔS_p) of the polymerization, and as a function of temperature.[67]

The driving force for the polymerization of cyclic compounds is their ring strain. Non-distorted bond angle values, bond stretching and/or compression, repulsion between eclipsed hydrogen atoms, and nonbonding interactions between substituents (angular, conformational and transannular strain, respectively) cause the ring strain for cyclic compounds.[68] The angle and bond deformations are most common for the three and four-membered rings, and this results in a high ring strain. The five and six-membered cycles are the least strained but the presence of the ester in the six-membered ring increases the strain so that, for example, δ-valerolactone (DVL), lactides (LA), morpholine-2,6-dione (MDO) can be readily polymerized. In general, the ring-opening polymerization of six-membered lactones is enthalpically favored (indicated by a negative ΔH_p) and entropically disfavored (indicated by a negative ΔS_p).[69] For a typical ROP, it reaches an equilibrium over time where the rate of polymerization equals the rate of depolymerization. This results in an equilibrium monomer concentration, $[M]_{eq}$. At low temperatures, the enthalpy of the polymerization overcomes the entropic penalty of polymerization but at a certain temperature, the entropic penalty outweighs the ring strain. This temperature is called ceiling temperature (T_c) when the rates of polymerization and depolymerization are equal. The fundamental thermodynamic description behind this was explained by Dainton and Irvin, who concluded that this phenomenon was independent of the catalytic system but dependent on the monomer concentration, leading to the development of the more familiar Dainton's equation (Equation 1.2).[66,70,71,72]

$$T_c = \frac{\Delta H_p}{\Delta S_p + R \ln [M]_{eq}} \qquad \text{(Equation 1.2)}$$

where T_c is the ceiling temperature, R is the gas constant and $[M]_{eq}$ is the equilibrium monomer concentration. At lower temperature, Equation 1.2 can be rearranged to Equation 1.3 which is known as van 't Hoff analysis to estimate enthalpy (ΔH_p) and entropy (ΔS_p) for the polymerization:

$$\ln \left(\frac{[M]_{eq}}{[M]_{ss}}\right) = \frac{\Delta H_p}{RT} - \frac{\Delta S_p}{R} \qquad \text{(Equation 1.3)}$$

where T is the polymerization temperature, R is the ideal gas constant, and $[M]_{ss}$ is a standard state monomer concentration which is 1 M typically. So, ROP technique is enthalpy driven which is dictated by the ring strain of cyclic monomers and low entropic penalty is desired for ROP of cyclic monomers.

1.5 Controlled polymerization

Step growth and chain-growth are two general strategies for generating polymers or macromolecules. Chain-growth strategies have the advantage of providing more control over the molecular weight and molecular weight distribution during polymerization reactions. Step-growth polymerizations are less atom economical as condensation or cross-coupling reactions are involved.[73,74] An elementary reaction of the macromolecular chain growth for the ROP can be written as in Figure 1.7:

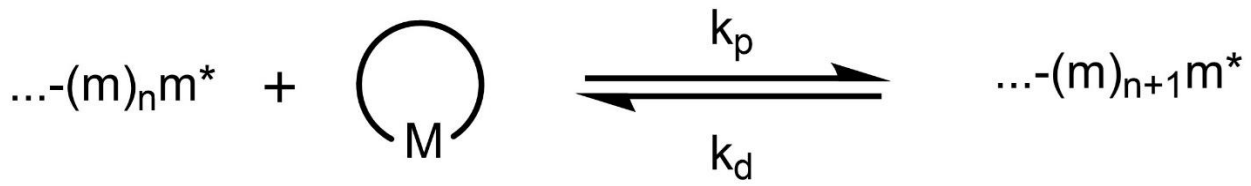

Figure 1.7. Chain growth process for the ROP reaction

where M denotes the monomer molecule, m is the macromolecule repeating unit derived from the M monomer and m* denotes the active species. In an ROP reaction, initiation, propagation and undesirable termination steps are involved. In the initiation step, the initiator (denoted as I) reacts with monomer, and this results in active species (denoted as m*) which are capable of adding new monomer molecules. In the propagation step, more successive addition of monomers occurs where the active center remains intact in the polymer chain end (Figure 1.8). The rate constants of initiation, propagation, and depropagation are denoted as k_i, k_p and k_d respectively.

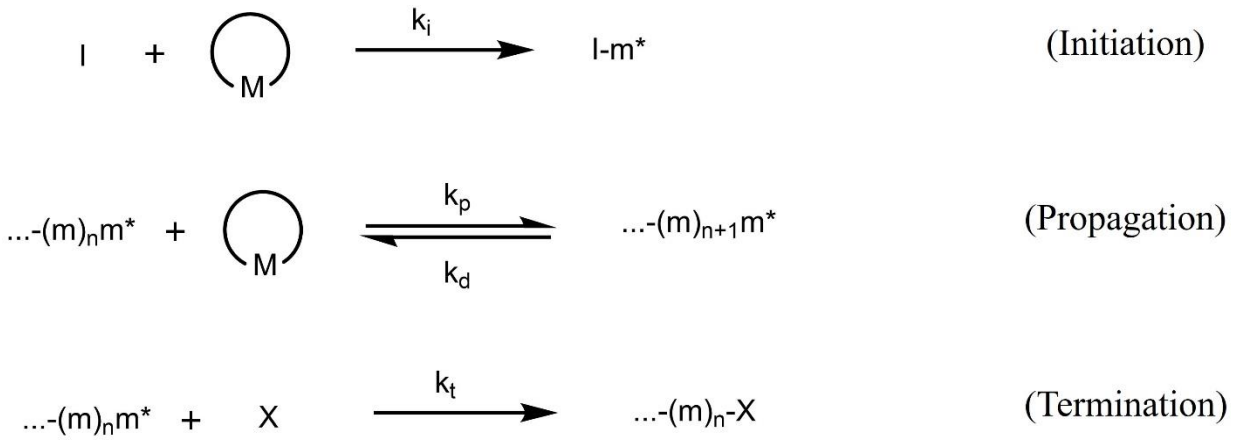

Figure 1.8. Initiation, propagation and undesired termination steps involve in the chain growth of ROP

For an idealized, living polymerization the initiation is instantaneous and all initiator molecules introduced to the system produce an equal number of polymer chains. Characteristics of a living chain-growth polymerization include the first-order kinetics in monomer concentration and a linear relationship between molecular weight and monomer conversion. Deviations from the linear dependence refers to the presence of slow initiation or side reactions. The initiation should be faster than any side reactions, such as termination and the rate constants of termination (k_t) will be equal to zero, where X is the terminating species. The resultant polymers will show a narrow molecular weight distribution with a uniform chain length.

1.6. Motivations and outline

The motivation of the work was to create novel lactone monomers by selectively functionalizing HMF with lignin-based pendant groups[33] in the first track by Dr. Thomas J. Schwartz's research group from the University of Maine. This track involved etherification of hydroxyl group and oxidation of aldehyde group in HMF and then hydrogenation using bifunctional catalysts to get functionalized δ-hexalactones (FDHLs) monomers. In the second track (this work), functionalized aliphatic polyesters were made by the ring-opening polymerization (ROP) of these new FDHLs (Figure 1.9). The second track involved the design of the monomers and their synthesis, investigating the reactivity of different organo-catalysts towards these new lactone monomers, optimization of the polymerization conditions (solvent effects, temperature, catalyst loadings, etc.) to increase rate and conversion, understanding how the pendant group affects the polymerization kinetics and thermodynamics and studying the influence of sterically hindered pendant groups on glass transition temperature (T_g) for these new lactone monomers.

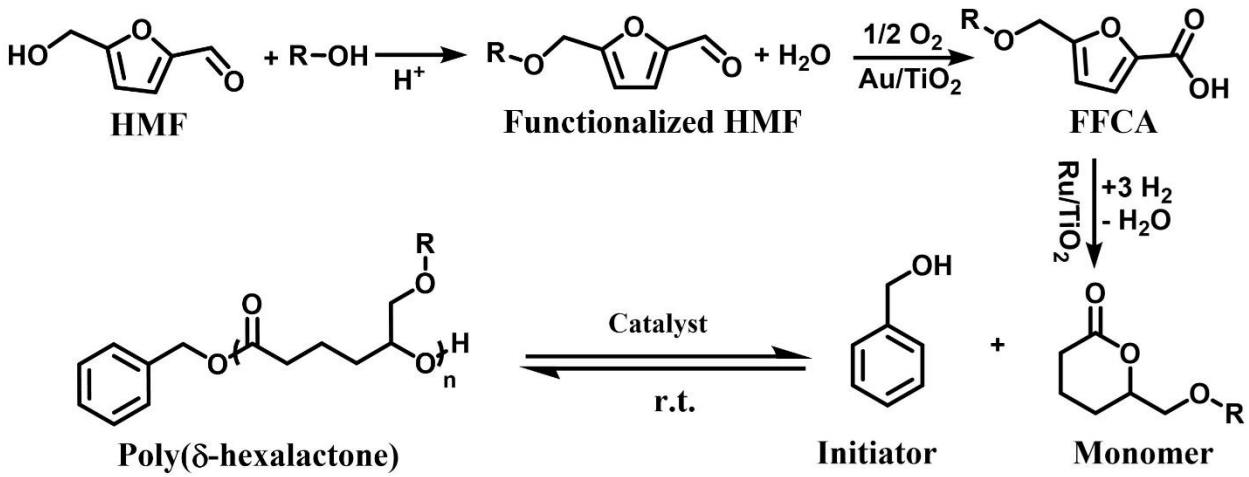

Figure 1.9. Catalytic upgrading of HMF to functionalized δ-hexalactone (FDHL) followed by ring opening polymerization (ROP) to yield polyFDHLs.

Parallel to the catalytic studies to produce FDHLs, six-membered lactone monomers bearing different pendant groups were synthesized from commercially available methyl cyclopentanone-2-carboxylate.. Different phenol groups and their hydrogenated versions which can be lignin-derived potentially were introduced as a pendant group in the FDHLs monomers (Figure 1.10). Four monomers: 6-(phenoxymethyl)oxan-2-one (**PDHL** – chapter 2), 6-((2-phenylphenoxy)methyl)oxan-2-one (**2-PhPDHL** – chapter 3), 6-((naphthalen-1-yloxy)methyl)oxan-2-one (**NDHL** – chapter 4) and 6-((cyclohexyloxy)methyl)oxan-2-one (**CDHL** – chapter 5) were synthesized successfully and reported in the next chapters.

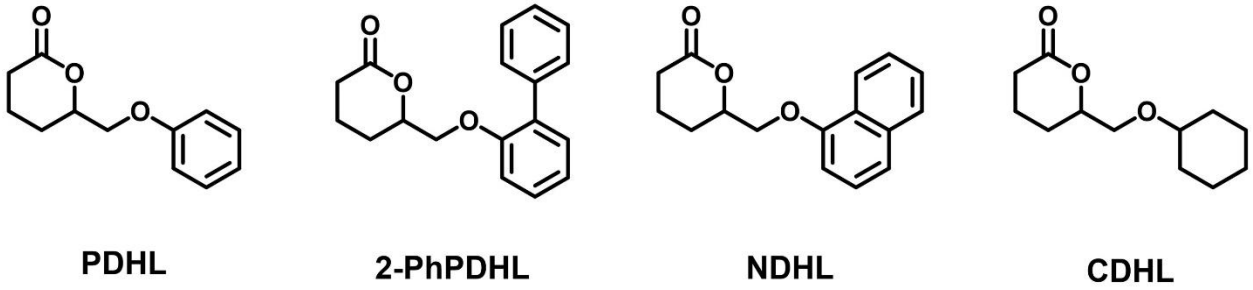

Figure 1.10. Different bulky groups were introduced at the pendant position of FDHLs monomers

Sustainable polymers from biomass can solve the waste management issue of current fossil fuel-based plastics. Introducing lignin-derived aromatic groups at the pendant position of polymers has the ability to give high T_g and other degradation properties. In the next chapters, the detailed synthetic steps for FDHLs monomers and their polymerizations conditions are described.

CHAPTER 2

SYNTHESIS AND RING-OPENING POLYMERIZATION OF 6-(PHENOXYMETHYL)OXAN-2-ONE (PDHL)

2.1 Introduction

By introducing different pendant functional groups, the properties of aliphatic polyesters can be tuned. Ring-opening polymerization (ROP) of functionalized lactones is a powerful strategy for generating functionalized aliphatic polyesters. Mostly alkyl functional groups have been introduced at δ-position of the valerolactone (VL) and their ROP could not change different properties significantly (e.g., glass transition temperature) (Figure 2.1a).

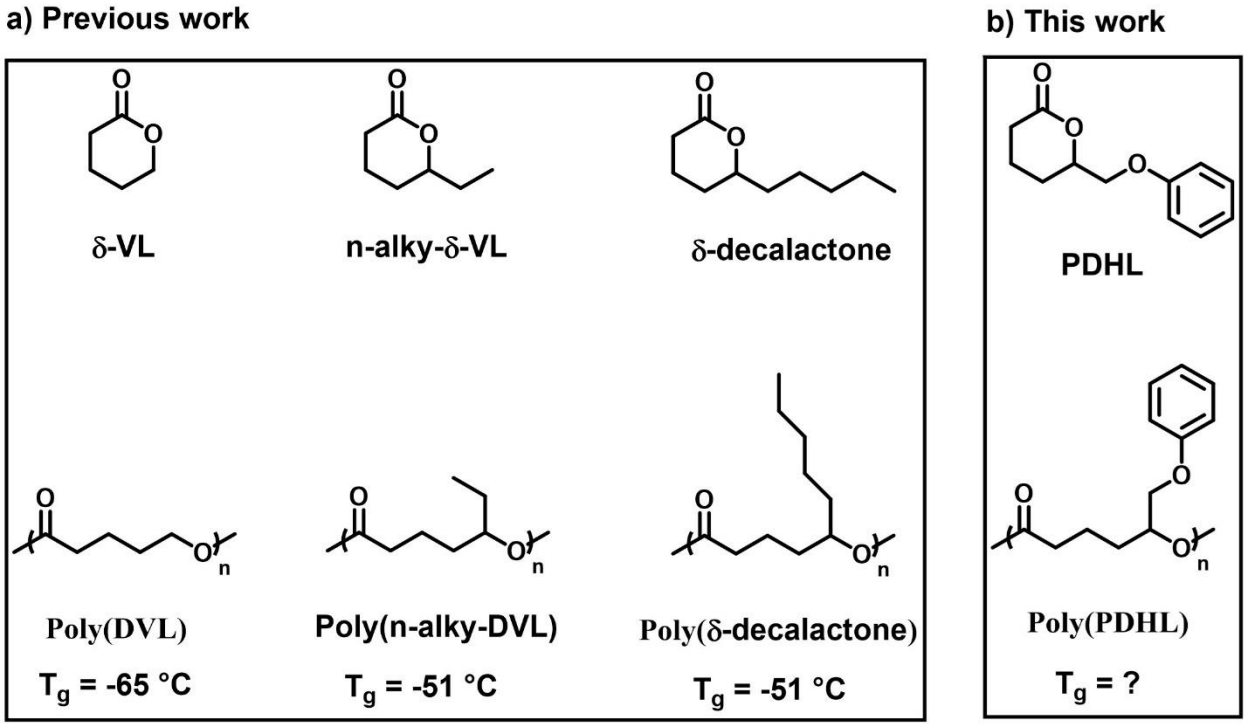

Figure 2.1. a) Alkyl substituted polyesters could not improve T_g b) Introducing bulkier pendant group at the δ-position of the six-membered lactone monomers to get higher T_g polyesters.

By introducing bulky aromatic groups at the δ-position of the lactone, pendant diverse novel lactone monomers were synthesized from commercially available methyl cyclopentanone-2-carboxylate. In this chapter, one phenol group was added at the δ-position of the lactone monomer by following six steps reaction scheme (Figure 2.2) to study how the pendant group affects polymerization and polymer properties (Figure 2.1b). Different acidic to basic organocatalysts were screened to find a catalytic system for polymerizing the new monomer in a controlled manner. Finally, full thermodynamics and kinetics studies were conducted for the new monomer and polymeric system.

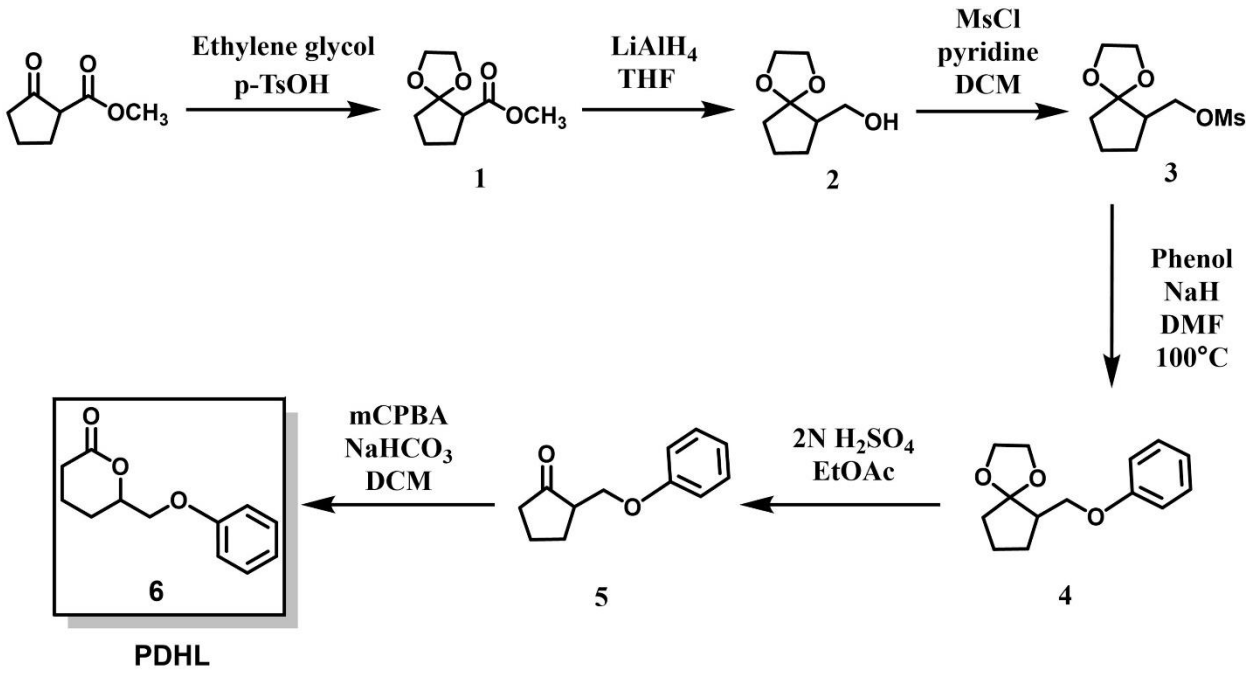

Figure 2.2. Reaction scheme for PDHL monomer synthesis

2.2. Materials and methods

Reagents, including methyl cyclopentanone-2-carboxylate (TCI), p-toluenesulfonic acid (Acros), lithium aluminum hydride (Aldrich), potassium sodium tartrate tetrahydrate (Aldrich), sodium hydride (Acros), methanesulfonyl chloride (Fisher), phenol (Aldrich), potassium hydroxide (Aldrich), 3-chloroperoxybenzoic acid (Acros), sodium bicarbonate (Fischer), DPP: diphenyl phosphate (Acros), Schreiner′s Thiourea: *N*,*N*′−bis[3,5−bis(trifluoromethyl)phenyl] (Aldrich), MTBD: 7-methyl-1,5,7 triazabicyclo[4.4.0]dec-5-ene (TCI), thiourea: 1,3-diisopropyl-2-thiourea (Aldrich), IMes: 1,3-dimesitylimidazol-2-ylidene (Fisher), tris(2-aminoethyl)amine (Aldrich), 3,5-bis(trifluoromethyl)phenyl isocyanate (Aldrich), 1,3-diaminopropane (Aldrich), TBD: 1,5,7-triazabicyclo[4.4.0]dec-5-ene (Fisher), benzyl alcohol (Aldrich), 1,4-dioxane (extra dry) (Acros), dichloromethane (anhydrous) (Acros), and N,N-dimethylformamide (anhydrous) (Aldrich) were used as received. All the other solvents and reagents were used as received from commercial suppliers without further purification unless stated otherwise.

2.2.2 Synthesis of methyl 1,4-dioxaspiro[4.4]nonane-6-carboxylate (1)

First, *p*-toluene sulfonic acid (37 g, 0.22 mol) was dissolved in ethylene glycol (120 mL) and stirred at 30 °C for 30 minutes. After 30 minutes, molecular sieves (3Å, 4 to 8 mesh) (40 g) were added to the mixture and the ethylene glycol solution was separated from the sieves. The methyl cyclopentanone-2-carboxylate (25 mL, 0.2 mol) was added into the solution and stirred for 3 hours at room temperature. After the reaction time, the mixture was poured into 1 M potassium hydroxide solution (100 mL) saturated with sodium chloride (NaCl) and extracted with diethyl ether (3 x 100 mL). After collecting the organic layer, the solution was washed with brine solution (100 mL) and

dried over anhydrous Na_2SO_4. The solvent was removed on a rotary evaporator to give **1** as a colorless product (24.2 g, 65% yield).

^{1}H NMR (Chloroform-*d*) δ (ppm): 3.9 - 4.0 (m, 4H), 3.70 (s, 3H), 2.92 (t, 1H), 1.6 - 2.2 (m, 6H).

2.2.3 Synthesis of 1,4-dioxaspiro[4.4]non-6-ylmethanol (2)

Lithium aluminum hydride ($LiAlH_4$) (4 g, 0.11 mol) was added to tetrahydrofuran (THF) solvent (150 mL) and stirred at 0 °C. After 30 minutes, synthesized **1** (24.2 g, 0.13 mol) was added dropwise into the $LiAlH_4$ suspension and stirred overnight at room temperature. Ethyl acetate (200 mL) was added very slowly to quench excess $LiAlH_4$ in an ice bath and then the reaction mixture was poured into ice-cold saturated sodium potassium tartrate solution (100 mL). The organic layer was separated and dried over anhydrous Na_2SO_4. The solvent was removed on a rotary evaporator to obtain the desired product **2a** (14.8 g, 72% yield).

^{1}H NMR (Chloroform-*d*) δ (ppm): 3.92 (m, 4H), 3.62 (m, 2H), 2.65 (t, 1H), 2.11 (m, 1H), 1.5-1.95 (m, 7H).

2.2.4 Synthesis of 1,4-dioxaspiro[4.4]non-6-ylmethyl methanesulfonate (3)

Pyridine (14.5 mL, 0.18 mol) and methanesulfonyl chloride (5.1 mL, 0.07 mol) were added into the solution of **2** (9.4 g, 0.06 mol) in dichloromethane (50 mL). The mixture was stirred for 24 h at room temperature forming a white precipitate. The mixture was filtered, then washed with NaCl saturated 1N HCl (15 mL, 0.03 mol) and extracted with dichloromethane (2 x 50 mL). The organic layer was separated and dried over $MgSO_4$. The solvent was removed on a rotary evaporator to give **3** (9.21 g, 65% yield).

^{1}H NMR (Chloroform-*d*) δ (ppm): 4.30 (dd, *J* = 9.8, 6.2 Hz, 1H), 4.14 (dd, *J* = 9.8, 7.7 Hz, 1H), 3.90 (m, 4H), 3.00 (s, 3H), 2.37 (m, 1H), 1.4 - 2.02 (m, 5H).

2.2.5 Synthesis of 6-(phenoxymethyl)-1,4-dioxaspiro[4.4]nonane (4)

NaH (4.68 g, 60% dispersion in mineral oil) was washed with THF (3 x 10 mL) in 500 mL round-bottom flask to remove mineral oil and then the NaH was suspended in DMF (50 mL) solvent. Phenol (5.5 g or 0.058 mol in 20 mL DMF) solution was added dropwise into the NaH suspension under an ice bath and stirred for 30 min at room temperature to deprotonate the phenol. After deprotonation, the round-bottom flask was sealed with a septum, flushed with N_2, and connected to a bubbler. **3** (9.21 g, 0.039 mol) was added into the mixture using a plastic syringe and placed in a 100 °C preheated oil bath and stirred for 18 h. After the reaction time, the round-bottom flask was removed from the oil bath and excess NaH was quenched by adding deionized water (100 mL). The mixture was extracted with ethyl acetate (3 x 50 mL) and washed with 5 M KOH solution (100 mL). The organic layer was dried over Na_2SO_4 and removed on a rotary evaporator to give **4** (7.5 g, 55% yield).

^{1}H NMR (Chloroform-*d*) δ (ppm): 7.27 (m, 2H), 6.91 (m, 3H), 3.84-4.1 (m, 6H), 2.46 (m, 1H), 2.04 (m, 1H), 1.52 - 1.9 (m,, 6H).

2.2.6 Synthesis of 2-(phenoxymethyl)cyclopentanone (5)

In this synthesis, a 2N H_2SO_4 (19 mL, 0.35 mol) solution was added into a mixture of **4** (7.5 g**,** 0.032 mol) in ethyl acetate (30 mL) solvent and stirred overnight at room temperature. Brine solution (50 mL) was poured into the mixture the next morning and extracted with ethyl acetate (3

x 50 mL). The extracted organic layer was dried over Na_2SO_4 and removed on a rotary evaporator to give **5** (3.1 g, 51% yield).

^{1}H NMR (Chloroform-*d*) δ (ppm): 7.26 (m, 3H), 6.92 (m3H), 4.19 (dd, *J* = 9.3, 3.7 Hz, 1H), 4.10 (dd, *J* = 9.3, 6.3 Hz, 1H), 2.56 (m, 1H), 2.4 – 1.8 (m, 7H).

2.2.7 Synthesis of 6-(phenoxymethyl)oxan-2-one (6)

In this synthesis, 3-chloroperoxybenzoic acid (mCPBA, 70%) (7.9 g, 0.032 mol) and sodium bicarbonate (3.4 g, 0.04 mol) were added to dichloromethane (50 mL) and stirred for 15 mins at room temperature. **5** (3.1 g, 0.016 mol) was added into the mixture and stirred for 9 h. After the reaction time, extra dichloromethane (50 mL) solvent was added into the reaction mixture. The organic layer was washed with saturated Na_2SO_3 (20 mL), saturated $NaHCO_3$ (50 mL), then brine solution (20 mL) and separated. The organic layer was dried over anhydrous Na_2SO_4 and removed on a rotary evaporator to get the crude product (δ-substituted 93.5% major and α-substituted 6.5% minor product). The resulting solid was purified via silica gel flash column chromatography using 72:28 hexane:ethyl acetate mobile phase. After running flash column chromatography, 1.3 g of pure PDHL (**6**) was collected at a 40% yield.

^{1}H NMR (Chloroform-*d*) δ (ppm): 7.27 (m, 2H), 7.0 – 6.87 (m 3H), 4.68 (m, 1H), 4.14 (dd, *J* = 10, 4.6 Hz, 1H), 4.08 (dd, *J* = 10, 5.3 Hz, 1H), 2.7 – 2.48 (m, 2H), 2.15 – 1.77 (m, 4H) and ^{13}C NMR (Chloroform-*d*) δ (ppm): 129.83, 121.56, 114.77, 77.26, 69.61, 29.93, 24.98.

2.2.8 Polymerization materials and methods

Vials and magnetic stir bars used for polymerization reactions were dried in a 100 °C oven overnight before use. DPP catalyst and PDHL monomer were dried for 24 h before use in the room

temperature vacuum oven. TBD was dried overnight in the antechamber of a nitrogen glovebox and kept in the glovebox under nitrogen after received. Vials, caps, syringes, spatulas and all other materials used to set up polymerization reactions were dried in the antechamber of the glovebox overnight before use.

2.2.9 General polymerization procedure for PDHL

Polymerization of phenoxy-δ-hexalactone (PDHL) proceeded as follows. Two different stock solutions of initiator and catalyst were prepared by adding 15 μL benzyl alcohol in 300 μL 1,4-dioxane and 3 mg TBD in 300 μL 1,4-dioxane separately in an N_2 filled glovebox. First, the stock solution of benzyl alcohol (5 μL, 0.0024 mmol) and then the stock solution of TBD (10 μL, 0.00072 mmol) were added using glass syringes to PDHL monomer (50 mg, 0.24 mmol) dissolved in dioxane solvent (155 μL) already in 2 mL vial with a septum. The homogenous mixture was stirred for the desired reaction time at ambient temperature. The polymerization was quenched by adding excess benzoic acid (1.76 mg, 0.014 mmol). A typical polymerization led to ca. 69% conversion of PDHL. The inactive catalyst was removed by precipitation of the pure polymer into methanol.

2.2.10 Polymerization kinetics experiments

Polymerization kinetics experiments were carried out at ambient temperature for PDHL monomer. The experiment was conducted using benzyl alcohol (BnOH) as an initiator and TBD as catalyst. For measurement of the PDHL polymerization kinetics, the stock solution of benzyl alcohol (5 μL, 0.0024 mmol) and the stock solution of TBD (10 μL, 0.00072 mmol) were added using glass syringes to PDHL monomer (50 mg, 0.24 mmol) dissolved in 1,4-dioxane solvent (155 μL) in 2

mL vial with a septum. The homogenous mixture was stirred until the polymerization reached equilibrium and aliquots were collected throughout the polymerization. The aliquots were quenched by adding 30 molar excess benzoic acid and monomer conversions were determined using ^{1}H NMR spectroscopy.

For the polymerization kinetics experiments, the $[Monomer]_0$:[Initiator] and $[Monomer]_0$:[Catalyst] ratios were fixed. The polymerizations appeared to reach equilibrium, as indicated by a plateau in monomer conversion as a function of time. Equilibrium polymerization behavior was verified by fitting the kinetics data to Equation 1,[57] which describes monomer concentration as a function of time for an equilibrium polymerization:

$$\mathrm{In}\left(\frac{[\mathrm{M}]_0-[\mathrm{M}]_{\mathrm{eq}}}{[\mathrm{M}]_0-[\mathrm{M}]_{\mathrm{t}}}\right)=\mathrm{k}_{\mathrm{app}}\mathrm{t} \qquad \text{(Equation 2.1)}$$

where $[M]_{eq}$ is the equilibrium monomer concentration, $[M]_0$ is the initial monomer concentration, $[M]_t$ is the monomer concentration at given a time, and k_{app} is the apparent rate constant.

2.2.10. Polymerization thermodynamics experiments

For the polymerization thermodynamics experiments, the setup was the same as for the kinetics experiments, but the polymerizations were stirred in an oil bath at a range of temperatures. The temperature range was from 22.5 to 55 °C for PDHL. The polymerizations achieved different equilibrium monomer concentrations ($[M]_{eq}$) at different temperatures. Aliquots were collected after sufficient reaction time to reach equilibrium (168 h for PDHL) and quenched with 15 molar excess benzoic acid. The polymerization progress was tracked using ^{1}H NMR spectroscopy. To ensure the polymerizations reached equilibrium, the reactions were kept running for at least another 48 h after reaching equilibrium. To estimate enthalpy (ΔH_p) and entropy (ΔS_p) for the

polymerization, the equilibrium monomer concentration was plotted as a function of inverse temperature and fit using a van 't Hoff analysis:

$$\ln\left(\frac{[M]_{eq}}{[M]_{ss}}\right) = \frac{\Delta H_p}{RT} - \frac{\Delta S_p}{R} \qquad \text{(Equation 2.2)}$$

where T is the polymerization temperature, R is the ideal gas constant, and $[M]_{eq}$ is a standard state monomer concentration that was set to 1 M.

2.2.11 Analysis of polymer products

^{1}H NMR and ^{13}C NMR spectra were obtained either using Varian Inova 400 MHz and Bruker Avance NEO 500 MHz NMR spectrometers using $CDCl_3$ as a solvent. Size exclusion chromatography (SEC) was conducted in dimethylformamide (DMF) containing 0.5 wt% LiBr as the mobile phase with a flow rate of 1 mL min^{-1} at 70 °C. SEC analysis was performed by three Phenogel columns (Phenomenex) in series with different pore sizes (50, 10^3, and 10^6 Å), using a refractive index detector (35 °C) and calibration curves from linear polystyrene standards.

The crude polymer was dissolved in THF and precipitated in cold methanol (1:10). The T_g of different polymers was measured using a differential scanning calorimeter (DSC, TA Instruments DSC2500) at a rate of 10 °C min^{-1} over a range from -65 to 80 °C using ~1.5 mg sample in a heat/cool/heat experiment under an N_2 atmosphere. The T_g were reported from the second heating cycle and analyzed with TA TRIOS software (v5.0.0).

2.3. Results and discussion

To protect the carbonyl group of the methyl cyclopentanone-2-carboxylate cyclic acetal group was introduced by reacting with ethylene glycol in the presence of p-toluene sulfonic acid. When an

aldehyde or ketone reacts with a large excess of alcohol in the presence of a trace of strong acid, an acetal is formed. Since acetal formation is a reversible reaction, there was the possibility of the reactant not full conversion to the product if water was present in the reaction medium. Molecular sieves (3Å) were used to absorb water in the reaction mixture which provide high conversion. The appearance of multiplets at 3.9 ppm and 4.01 ppm confirmed the acetal group formation (Figure 2.3).

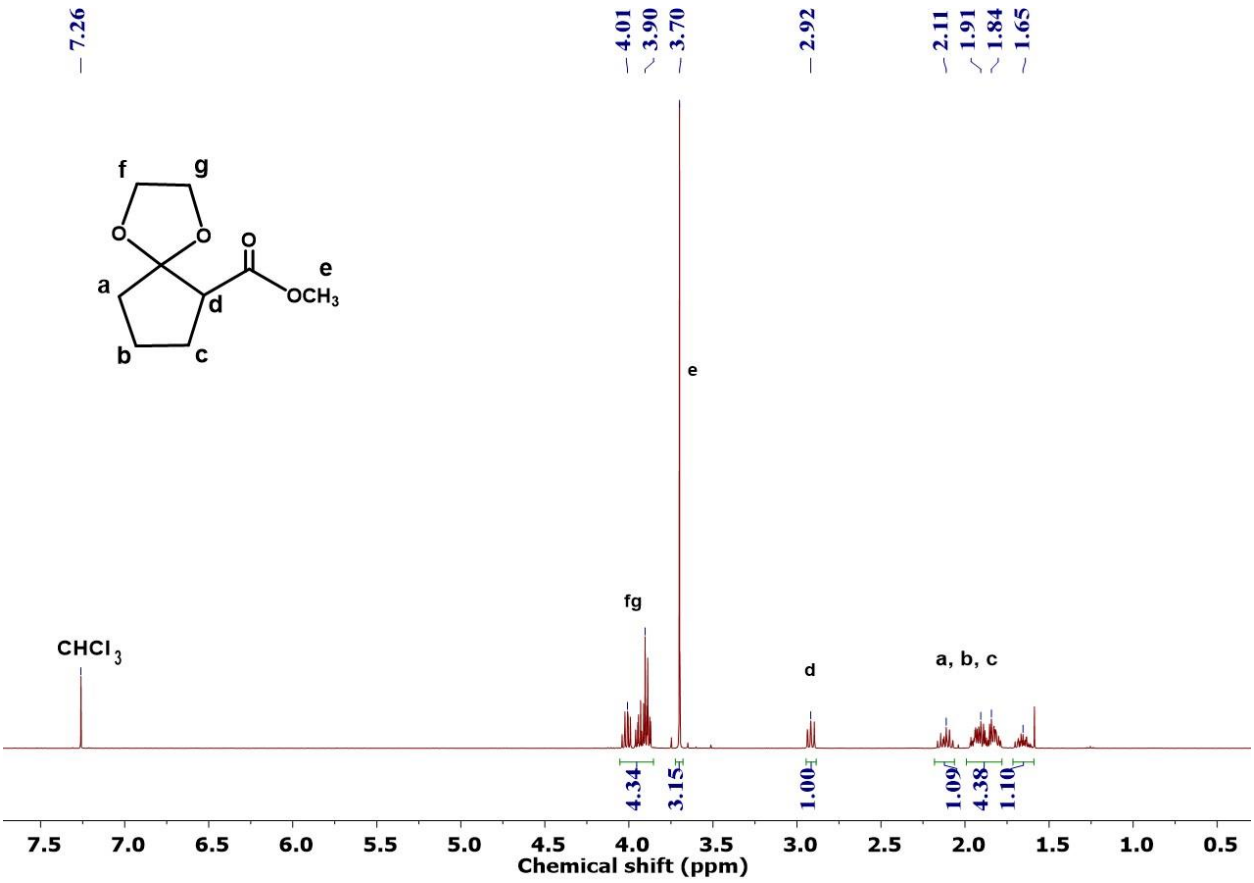

Figure 2.3. ^{1}H NMR spectrum of methyl 1,4-dioxaspiro[4.4]nonane-6-carboxylate (1)

The ester group end of the methyl 1,4-dioxaspiro[4.4]nonane-6-carboxylate (**1**) was converted to alcohol using a strong $LiAlH_4$ reducing agent. This step involved the nucleophilic attack by the

hydride at the electrophilic carbon of the ester group, further nucleophilic attack by the hydride anion after the removal of alcohol group as a leaving group in the form of alkoxide anion (RO^-) from the ester and finally reduction of the aldehyde. The successful conversion of alcohol from ester was indicated by the disappearance of singlet at 3.7 ppm and appearance of multiplets at 3.62 ppm in the ^1H NMR spectrum (Figure 2.4).

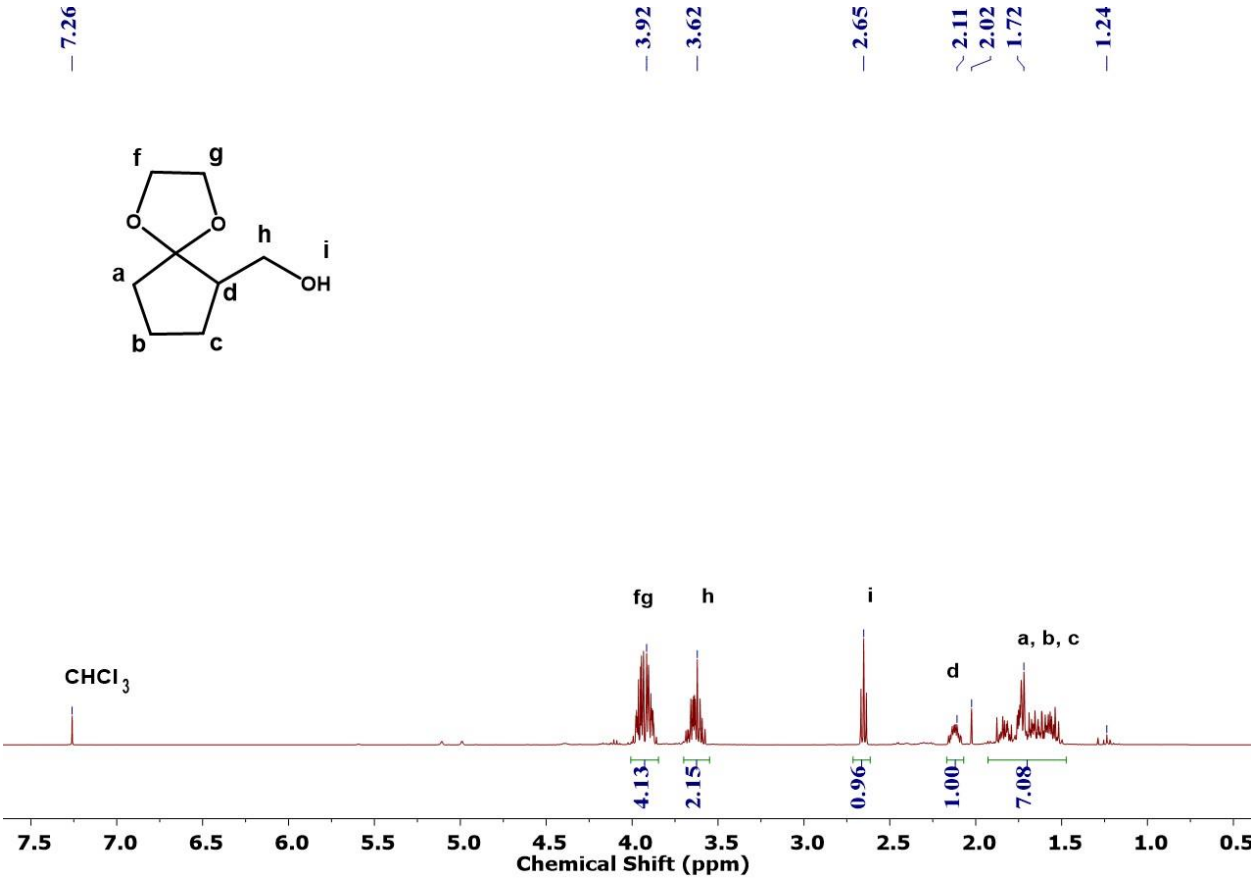

Figure 2.4. ^1H NMR spectrum of 1,4-dioxaspiro[4.4]non-6-ylmethanol (2).

Mesylate groups are considered excellent leaving groups in nucleophilic substitution reactions. Mesylate esters are a group of organic compounds that share a common functional group with the general structure $CH_3SO_2O–R$, abbreviated as MsO–R, where R is an organic substituent. Mesylate groups were introduced by reacting mesyl chloride (MsCl) with 1,4-dioxaspiro[4.4]non-

6-ylmethanol (2) in the presence of pyridine in DCM. The appearance of a singlet at 3 ppm in ^{1}H NMR spectrum confirmed the successful introduction of mesylate group at the end as a leaving group for Williamson ether synthesis reaction in the next step (Figure 2.5).

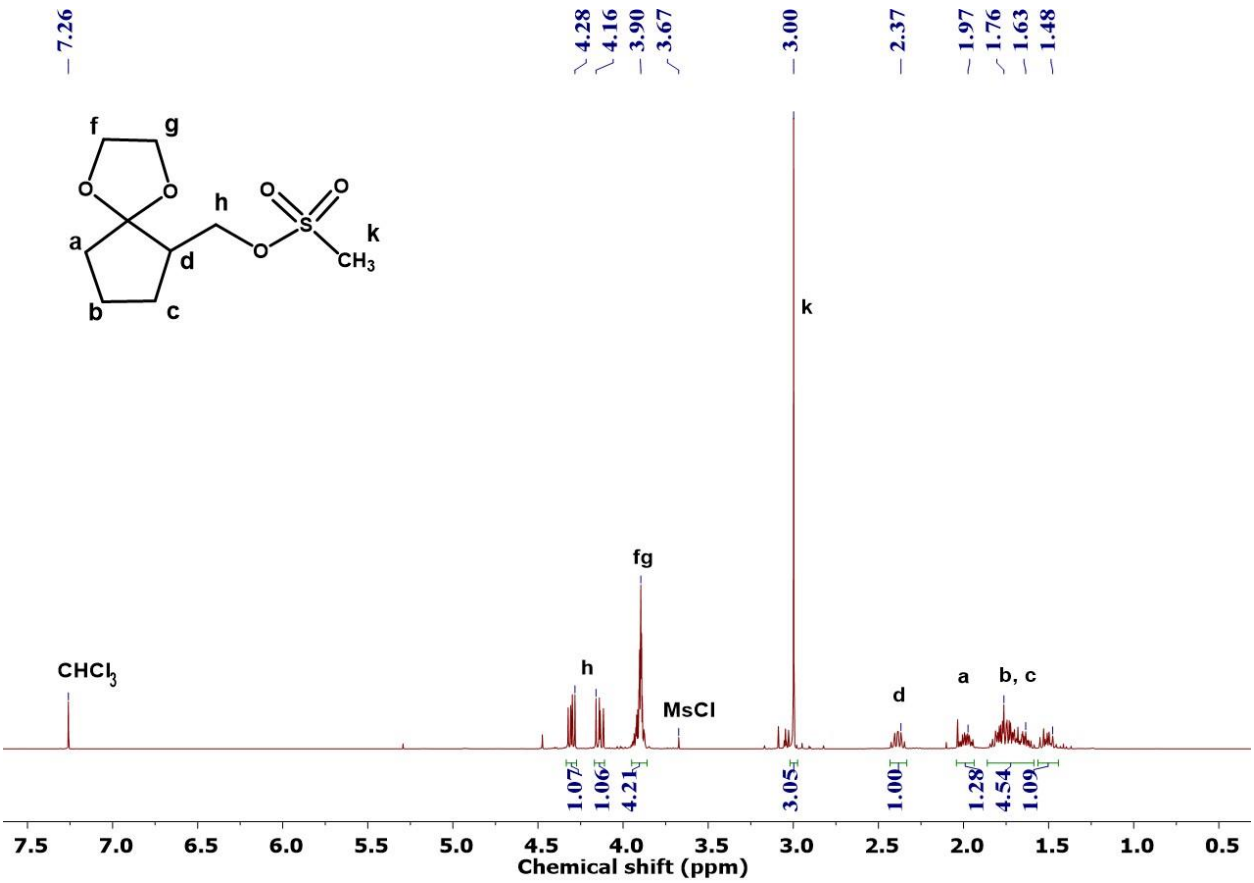

Figure 2.5. ^{1}H NMR spectrum of 1,4-dioxaspiro[4.4]non-6-ylmethyl methanesulfonate (3)

In the next step, powerful base sodium hydride (NaH) was used to deprotonate the phenol in DMF solvent. The phenoxide anion was stable and worked as a nucleophile in the presence of the mesylate leaving group. Successful etherification was confirmed by the disappearance of the mesylate methyl singlet at 3 ppm. The protons next to the ether linkage were shielded more which

confirmed further successful etherification (Figure 2.6). Excess phenol was removed by washing with 5 M KOH solution.

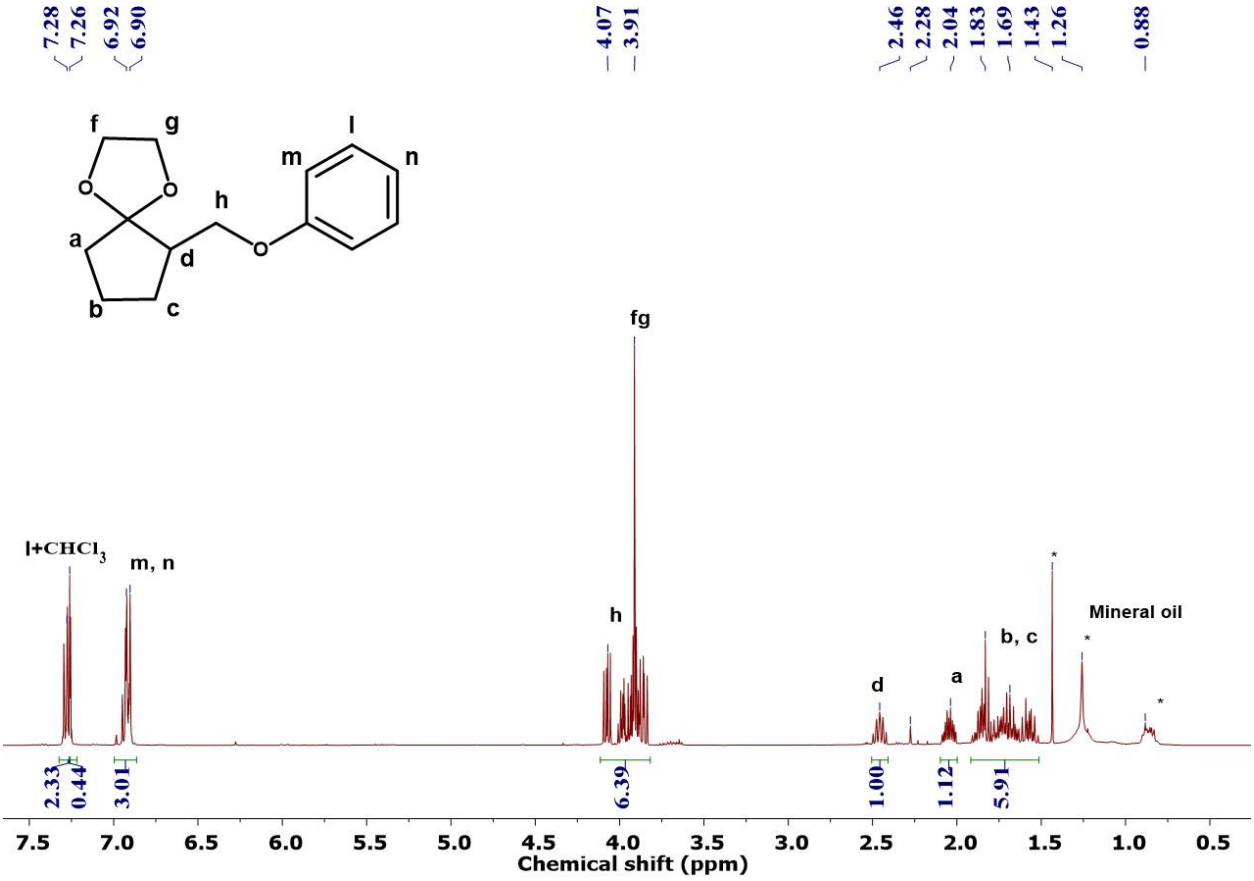

Figure 2.6. ^{1}H NMR spectrum of 6-(phenoxymethyl)-1,4-dioxaspiro[4.4]nonane (4). *Mineral oil from NaH washing step

The protecting acetal group was removed in the next step in the presence of an acidic solution. Sulfuric acid (1 M) was used to remove the acetal group. The removal of the acetal group was confirmed by the disappearance of peaks at 3.91 ppm (Figure 2.7). The protons next to ether linkage were affected mostly due to the removal of the acetal group and those protons showed a de-shielding effect (4.1 ppm and 4.19 ppm) in the ^{1}H NMR spectrum.

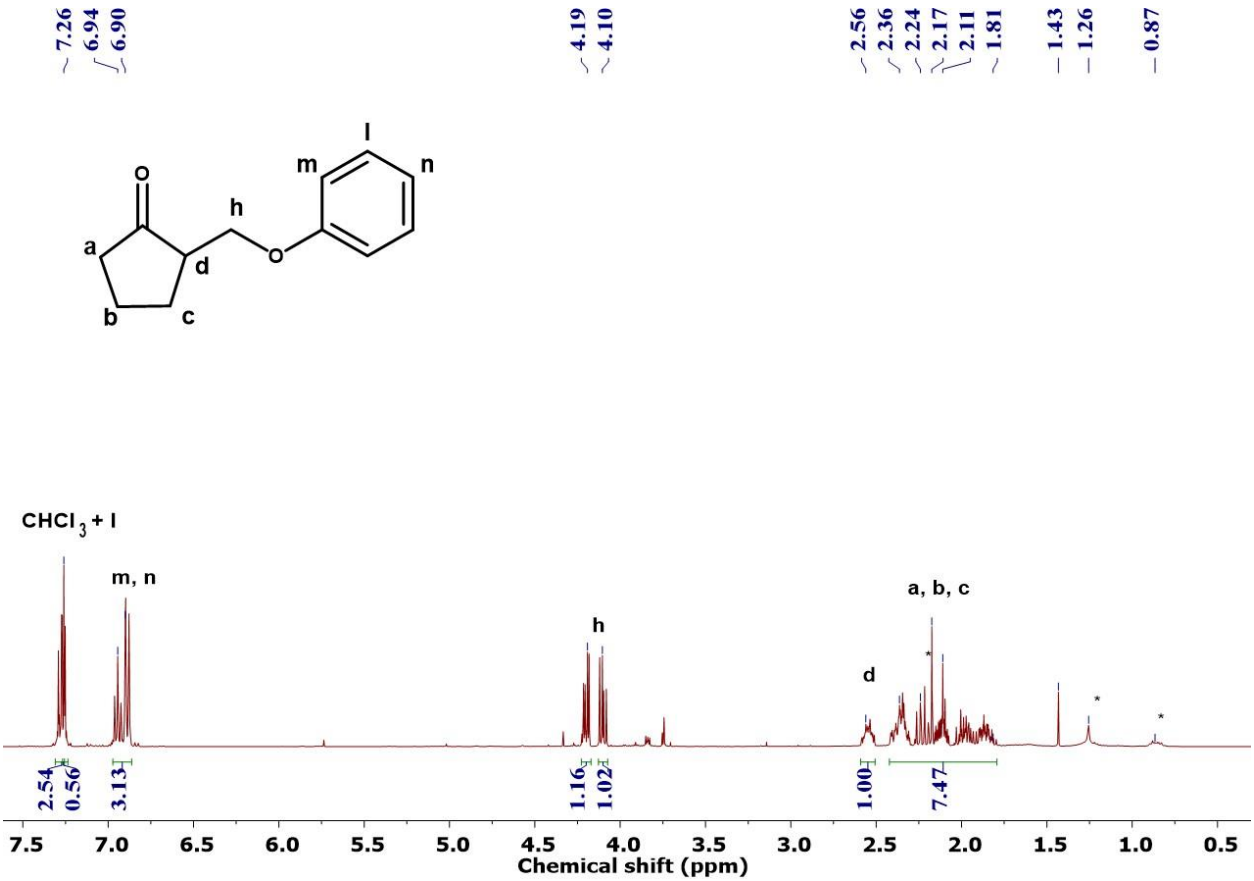

Figure 2.7. ^{1}H NMR spectrum of 2-(phenoxymethyl)cyclopentanone (5). *Acetone solvent and mineral oil

Baeyer-Villiger oxidation is an organic reaction that forms an ester from a ketone or a lactone from a cyclic ketone, using peroxyacids or peroxides as the oxidant. The Baeyer-Villiger oxidation reaction was used to synthesize six membered lactones from the five-membered cyclic ketones. 3-Chloroperoxybenzoic acid (mCPBA) was used as a peroxyacid source. Both α-substituted and δ-substituted products were observed in the ^{1}H NMR spectrum due to the unsymmetrical cyclic ketone. The δ-substituted product (93.5%) was the major product in the synthesis due to the higher migratory aptitude of the tertiary alkyl group over the secondary alkyl group. The peak of protons next to the ester group confirmed the successful six-membered lactone synthesis at 4.68 ppm for the major product (Figure 2.8). After this step, a mixture of major and minor products was obtained

in the presence of 3-chlorobenzoic acid as a by-product. Flash column chromatography was used to separate the pure PDHL monomer. Pure PDHL was separated successfully by using more non-polar hexane solvent. A 70:30 hexane and ethyl acetate mixture was used as a mobile phase. The products were tracked by thin layer chromatography (R_f = 0.33 for δ-substituted product and R_f = 0.42 for α-substituted product). The pure PDHL was confirmed by both ^{1}H and ^{13}C NMR spectroscopy (Figure 2.9-2.10).

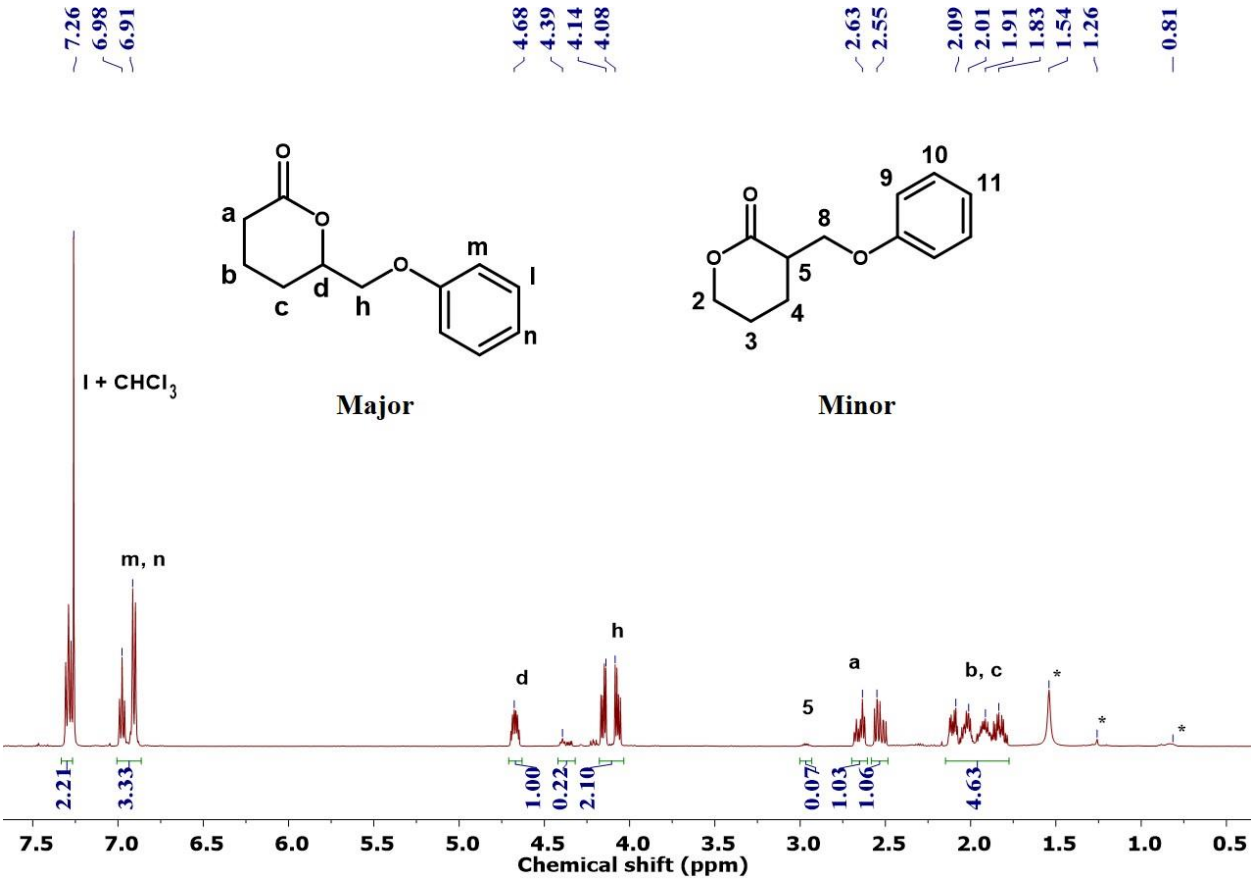

Figure 2.8. ^{1}H NMR spectrum of a crude mixture of 6-(phenoxymethyl)oxan-2-one (6)

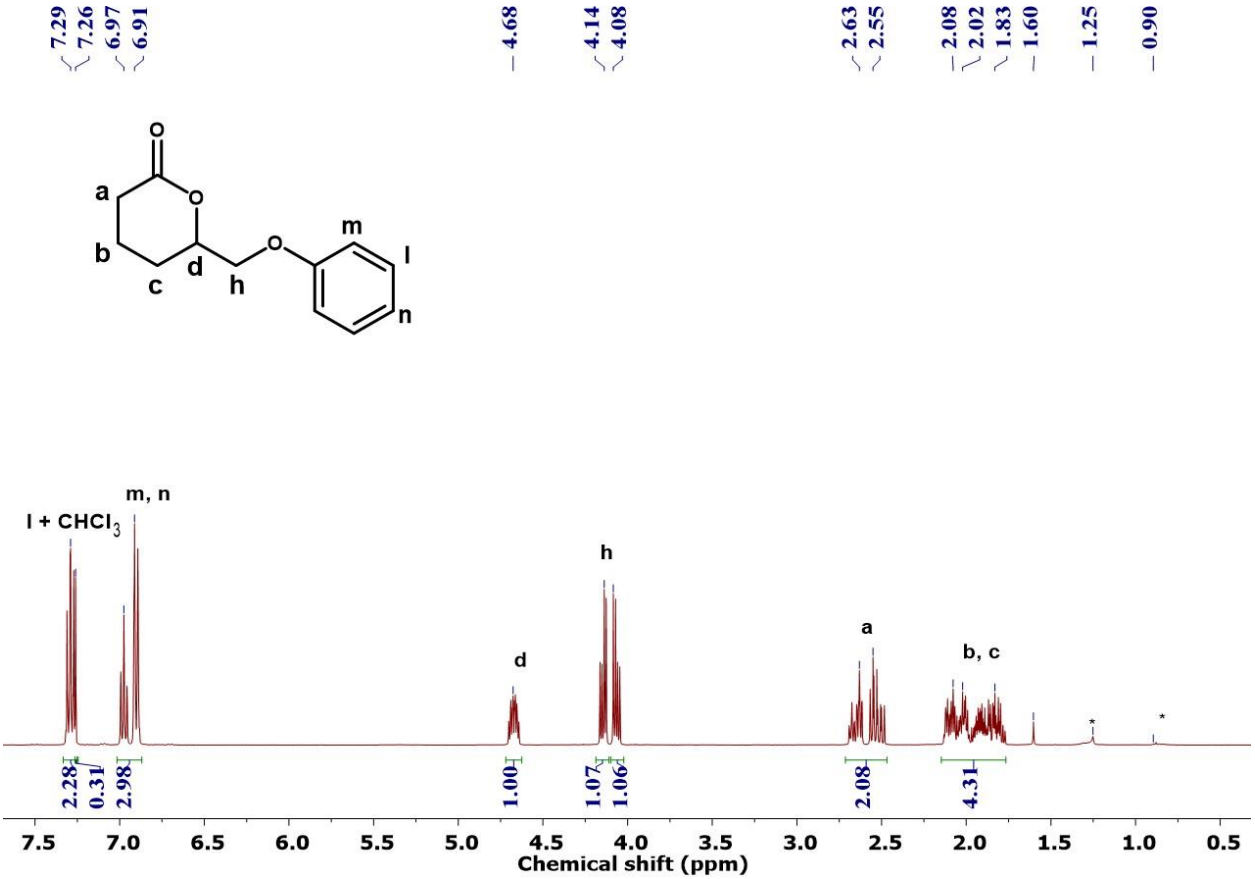

Figure 2.9. ^{1}H NMR spectrum of pure PDHL monomer (6), collected after flash column chromatography.

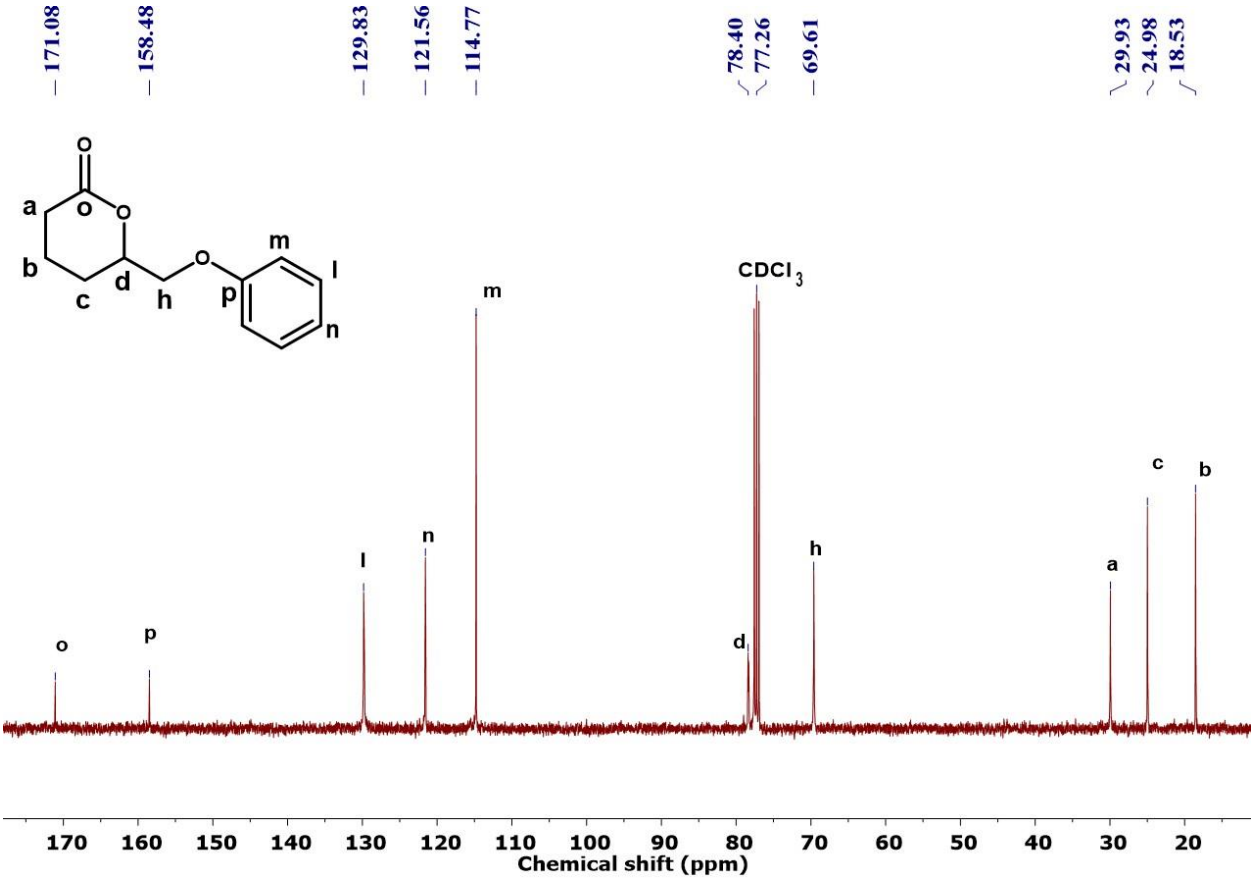

Figure 2.10. ^{13}C NMR spectrum of pure PDHL monomer (6)

2.3.1. Ring-opening polymerization of PDHL lactone

For the ROP of PDHL monomer (solid), 1,4-dioxane solvent was used to dissolve the monomer. PDHL monomer was not soluble in non-polar hexane but highly soluble in 1,4-dioxane. Diphenyl phosphate (DPP)[59], thiourea[75] (Schreiner′s thiourea), thiourea (1,3-diisopropyl-2-thiourea) with IMes (1,3-Dimesitylimidazol-2-ylidene) cocatalyst[76], urea[77,78] (*N*-(2-aminoethyl)-*N*-(3,5-bis(trifluoromethyl)phenyl)urea), 1,5,7-triazabicyclo[4.4.0]dec-5-ene[60,61,62] (TBD), phosphazene[79] base t-BuP_4 (Figure 1.4) are the common organocatalyst systems reported in the literature for ROP of unsubstituted δ-valerolactone (DVL) as mentioned in Chapter 1. The general polymerization scheme for PDHL monomer shown in Figure 2.11 below.

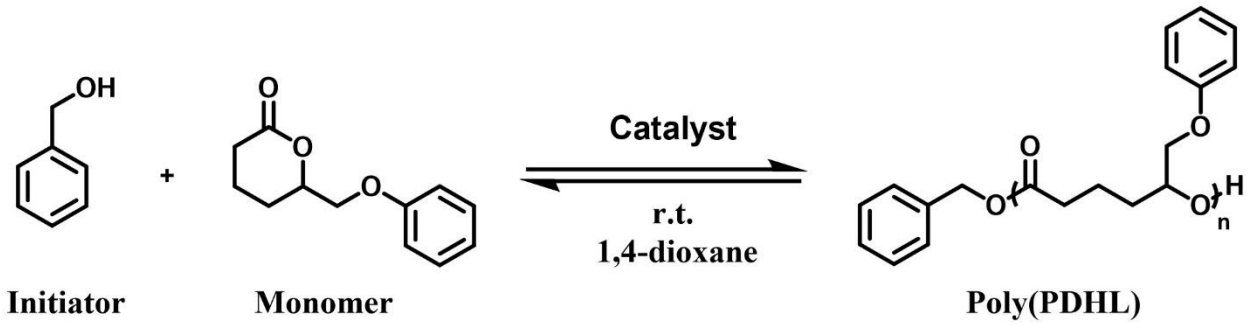

Figure 2.11. Polymerization scheme for ring opening polymerization of PDHL

To polymerize PDHL monomer in a controlled manner, different acidic to basic catalysts as mentioned above were screened first (Figure 2.12). In the catalyst screening process, PDHL monomer was polymerized at ambient temperature using benzyl alcohol (BnOH) as the initiator in 1,4-dioxane. First acidic DPP was tested as a catalyst and it polymerized PDHL monomer successfully. The methylene protons of the BnOH initiator shifted from 4.7 to 5.13 ppm, confirming that polymerization was initiated by BnOH in the ^{1}H NMR spectrum. The methine protons of PDHL (4.68 ppm) shifted to 5.2 ppm corresponding to the lactone ring opening and the successful polymerization for PDHL monomer. The further shifting of methylene protons of the BnOH initiator from 5.15 ppm to 5.1 ppm confirmed the propagation of polymerization. Thiourea and urea catalysts system initiated the polymerization, but no propagation was observed in the presence of co-catalyst MTBD. However, propagation and polymerization was observed while carbene (IMes) co-catalyst was used instead of MTBD. More basic TBD catalyst polymerized the PDHL monomer in low amount. Super basic phosphazene could initiate and propagate the polymerization but full propagation was not observed from ^{1}H NMR spectrum as both initiation peak (denoted by 1) and propagation peak (denoted by 2) were present (Figure 2.12). So, DPP,

thiourea/IMes and TBD were the catalysts system that polymerized the PDHL monomer successfully.

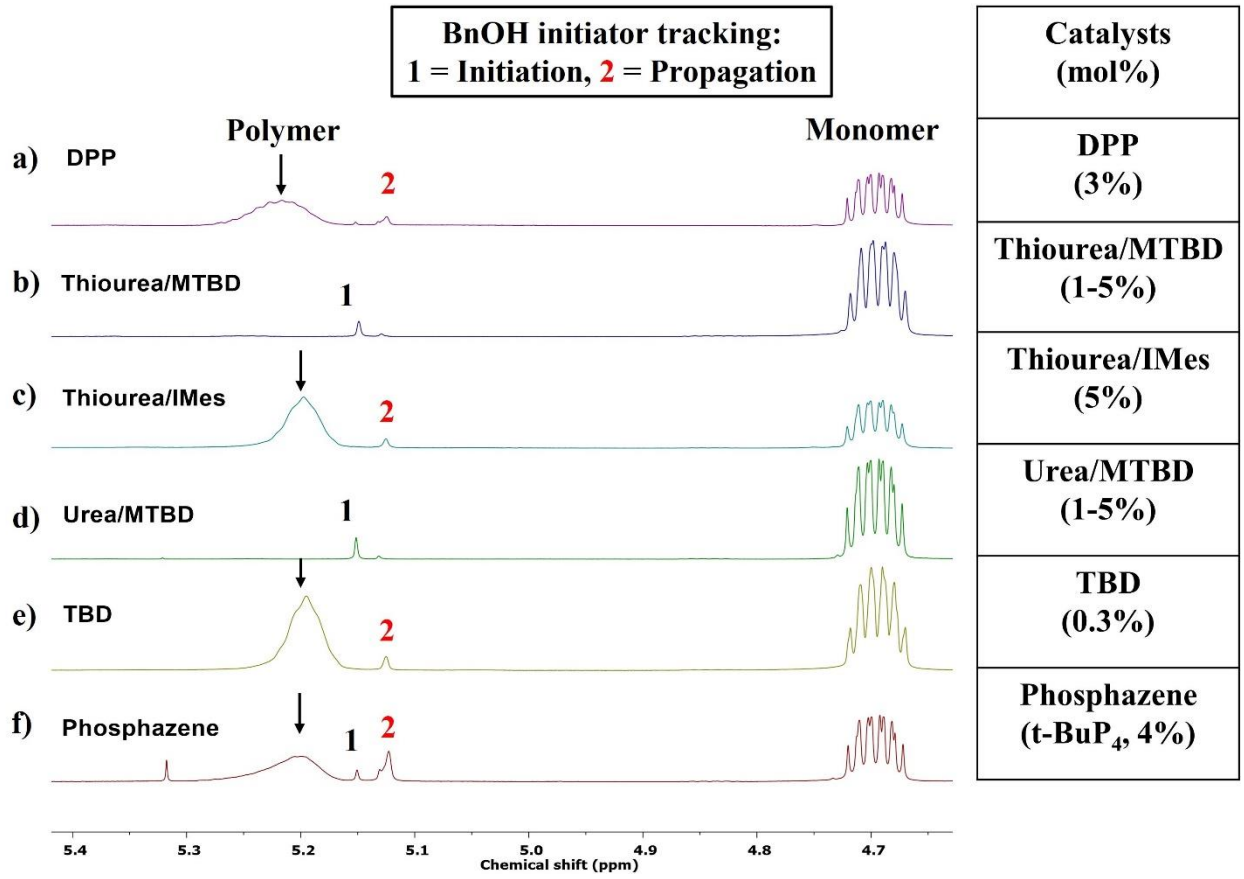

Figure 2.12. ^{1}H NMR spectrum of ring-opening polymerization of PDHL monomer using different acidic to basic organocatalysts (left). Catalysts loading ranges used to polymerize PDHL monomer (right).

2.3.2 Controlling the molecular weight of poly(PDHL)

As mentioned above PDHL monomer was polymerized at room temperature using benzyl alcohol (BnOH) as the initiator and diphenyl phosphate (DPP) as a catalyst. DPP has previously been reported to be active as an acidic organocatalyst for ROP of both unsubstituted (DVL)[59] and substituted (n-alkyl-DVL)[48] six-membered lactones. The conversion of PDHL monomers was

tracked by taking aliquots from the polymerization and analyzing them using ^{1}H NMR spectroscopy. The monomer conversion of PDHL was 73% after 9 days (Table 3, Entry 1), which indicates a slower polymerization rate than unsubstituted DVL[80,59] due to steric hindrance or a decrease in ring strain by the substituents on the lactone monomers.[81,82] The number average molecular weight ($M_{n,SEC}$) of polyPDHL measured by size exclusion chromatography was 2.2 kg mol^{-1}, lower than the expected value ($M_{n,expected}$) based off monomer conversion. The $M_{n,SEC}$ of polyPDHLs with higher $[M]_0/[I]$ values changed little and remained low when the polymer size was expected to increase (Table 2.1, Entries 1-3). This behavior suggests that either backbiting or other side reactions played a vital role in shortening the growing polymer chains. Polymerizations of PDHL without initiator yielded higher molecular weight polymers (Table 2.1, entry 4), indicating that adventitious initiation likely occurred. Similar molecular weight observations have been made for structurally similar hemiacetal cyclic monomers where the polymerization proceeded by both activated-monomer (AM) and active-chain-end (ACE) mechanisms while catalyzed by DPP.[83] Further studies are needed to understand the origin of low molecular weight polyPDHLs catalyzed by DPP for future use.

Table 2.1. Results for acidic DPP catalyzed ROP of PDHL monomer

Entry	**$[M]_0/[I]/[C]$**	**Time (days)**	**Conv. [a] (%)**	**$M_{n,\ expected}$[b] (kg/ mol)**	**$M_{n,\ SEC}$[c] (kg/ mol)**	**Đ[c]**
1	50/1/1.5	9	73	7.5	2.2	1.2
2	50/1/3	9	75	7.7	1.2	2.14
3	100/1/6	9	69	14.2	1.3	1.5
4	50/0/1	6	57	-	3.5	1.8

[a]Conversion measured by ^{1}H NMR spectroscopy. [b]Calculated from $[M]_0/[I]$ × monomer conversion × MW of PDHL. [c]Measured by SEC in THF as the mobile phase, using linear polystyrene standards with a refractive index detector.

To address the low molecular weights obtained using DPP, we screened TBD[64] as a catalyst using BnOH as an initiator in 1,4-dioxane at room temperature. The equilibrium monomer conversion of PDHL was 70% (Figure 2.13) and the $M_{n,SEC}$ of polyPDHL closed with the expected value (Table 2.2, entry 1). The $M_{n,SEC}$ values could be increased by increasing $[M]_0/[I]$ for polyPDHL (Table 2.2, entries 2-3). The molar mass distributions were unimodal for all polymers (Figure 2.14), which indicated limited backbiting occurred prior to equilibrium. Lower catalyst loadings reduced the polymer dispersity (Table 2.3, runs 1-8). Simon and Goodman reported that the TBD-catalyzed ROP proceeds by either a nucleophilic or acid-base catalytic mechanism, where the nucleophilic catalytic mechanism predominates when the alcohol concentration is low compared to the catalyst loading.[65] Higher catalyst loadings relative to the alcohol may favor reaching equilibrium monomer concentration faster or the polymerization propagation through the nucleophilic mechanism instead of the acid-base mechanism, which led to the higher dispersity observed.

Table 2.2**.** Results for basic TBD catalyzed ROP of PDHL monomer

Monomer	**Catalyst**	**Entry**	**$[M]_0/[I]/[C]$**	**Time (days)**	**Conv.[b] (%)**	**$M_{n,\ expected}$[c] (kg/ mol)**	**$M_{n,\ SEC}$[d] (kg/ mol)**	**Đ[d]**
PDHL[a]	TBD	1	50/1/0.15	7	0.70	7.2	10.5	1.64
		2	100/1/0.3	10	0.67	14.0	22.0	1.49
		3	300/1/0.9	10	0.50	31.0	30.0	1.59

[a]1,4-dioxane as solvent, $[M]_0 = 1.1$ M; where $[M]_0$ = Initial monomer concentration. [b]Conversion measured by ^{1}H NMR spectroscopy. [c]Calculated from $[M]_0/[I]$ × monomer conversion × MW of MDHL or PDHL. [d]Measured by SEC in DMF with 0.5 wt% LiBr as the mobile, using linear polystyrene standards with a refractive index detector.

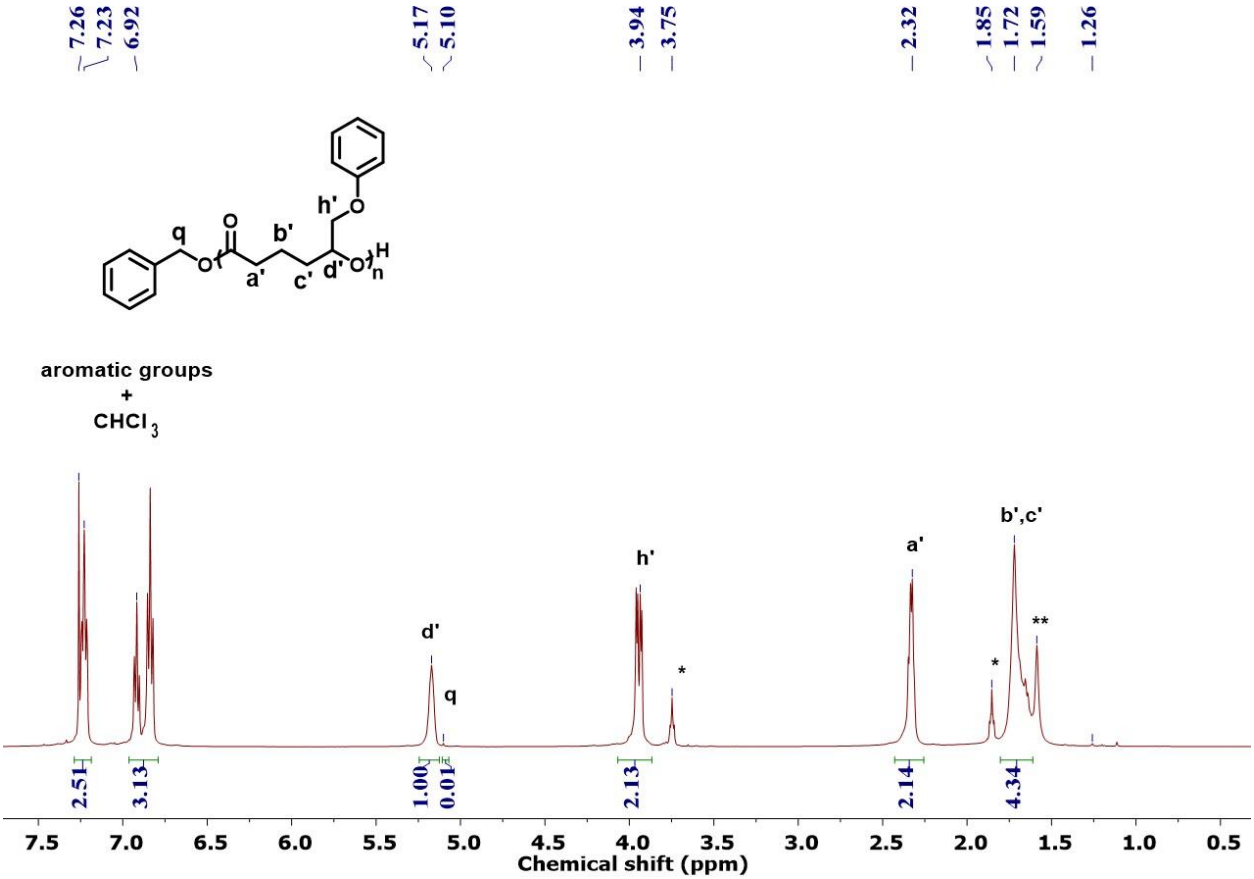

Figure 2.13. ^{1}H NMR spectrum of crude poly(PDHL). ^{1}H NMR spectrum was collected after the polymerization reached equilibrium on day seven. (*THF solvent,**H_2O)

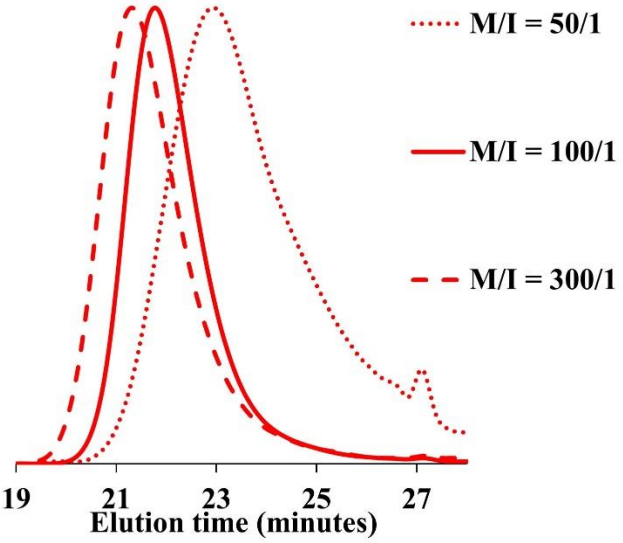

Figure 2.14. SEC elution curves for TBD catalyzed ROP of PDHL after reaching equilibrium conversion at different $[M]_0/[I]$ ratios. Molecular weights ($M_{n,\ SEC}$) and dispersity are in the Table 2.2.

Table 2.3: Results for ROP of PDHL monomer with different TBD catalyst loading after 48 hours

Run	**$[M]_0/[I]$**	**Catalyst (mole%)**	**% Conversion**	**Đ**
1	50/1	9%	50%	2.08
2	100/1	3%	48%	1.9
3	50/1	2%	49%	2.1
4	50/1	1.5%	48%	2.1
5	100/1	0.7%	47%	1.6
6	100/1	0.5%	48%	1.6
7	100/1	0.3%	45%	1.4

Table 2.3: Continued

8	100/1	0.1%	5%	1.2

2.3.3 Glass transition temperature (Tg) of poly(PDHL)

The T_g was measured by DSC from the second heating cycle (Figure 2.15). The T_g for polyPDHL (M_n = 22 kg mol^{-1}) was 6 °C, which is higher than that of unsubstituted six-membered poly(δ-valerolactone) (ca. -65 °C)[84,85] and seven-membered poly(ε-caprolactone) (-60 °C)[86]. This T_g is higher than those of all alkyl-substituted poly(δ-valerolactone)s (-52 °C to -50 °C) and 3-mercaptovalerolactones (-14 °C),[87] and is the highest reported for substituted VL to the best of our knowledge.[87,48,88] The polymers did not crystallize above its T_g because of the racemic mixture and the catalysts afforded no stereochemical preference. Because the T_g increases rapidly with increasing molecular weight and plateaus at higher values,[89] we analyzed a lower molecular weight and no difference was observed in the T_g of polyPDHL with lower molecular weight (M_n = 7 kg mol^{-1}) (Figure 2.15), indicating that the T_g for polyPDHL had plateaued as a function of molecular weight.

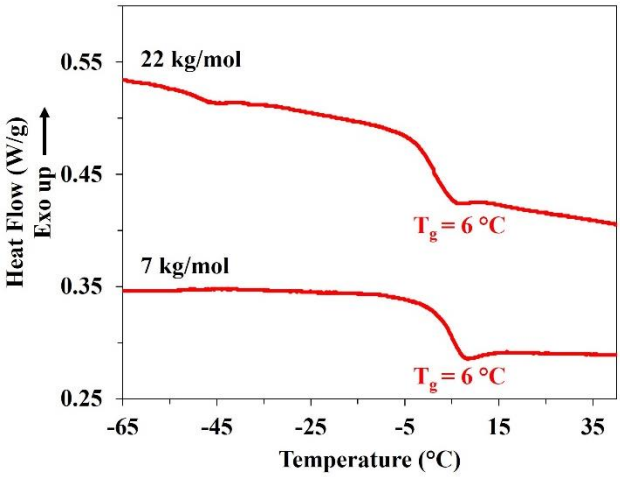

Figure 2.15. DSC thermograms of polyPDHL. Curves are shifted vertically to provide clarity.

2.3.4 Thermodynamics of polymerization

The thermodynamics of the ROP were examined by polymerizing PDHL (solution, TBD catalyst) over a range of temperatures and performing a van 't Hoff analysis to calculate the entropy and enthalpy of polymerization (Figure 2.16). Table 2.4 shows the $[M]_{eq}$ values obtained by running the polymerization at different temperatures.

Table 2.4. Observed equilibrium monomer concentration ($[M]_{eq}$) at different temperatures

Temperature (°C)	**$[M]_{eq}$ (M)**
22.5	0.526
35	0.611
45	0.707
55	0.759

The enthalpy of polymerization (ΔH_P^o) was -9.4 ± 0.7 kJ mol^{-1} for PDHL, which is close to the values reported for DVL (ca. -10 kJ mol^{-1}), but slightly lower than the values reported for δ-decalactones (-17.1 ± 0.6 kJ mol^{-1}) and other alkyl-substituted δ-lactones (-13 to -19 kJ mol^{-1}).[48, 59,66] The inclusion of an ether linkage in the pendant group appears to decrease the ring strain as compared to the all-carbon pendant group of alkyl-substituted δ-lactones, which may be due to the increased rotational freedom of the ether group.[48,88] The entropy of polymerization (ΔS_P^o) was -26 ± 2 J mol^{-1} K^{-1} for PDHL, whereas the value reported in the literature for DVL is around -15 J mol^{-1} K^{-1}, which indicates that the PDHL is more entropically disfavored as compared to DVL.[88] However, the entropic penalty for polymerization is less than that of alkyl-substituted DVLs (ca. -55 J mol^{-1} K^{-1}),[48] which enables the significant conversions observed in spite of the lower ΔH_P^o. The addition of a pendant group likely decreases the internal rotational freedom of a polymer chain relative to its unsubstituted parent, DVL,[48] which leads to the higher entropic penalty observed for substituted DVL monomers. However, for the ether-substituted monomer PDHL, this entropic penalty is not as significant as for alkyl-substituted DVL monomers, presumably due to the extra degrees of freedom possible from the more freely rotating ether group. The measured thermodynamic parameters indicate that PDHL can be polymerized at room temperature and higher, achieving useful monomer conversions (i.e., >50%).

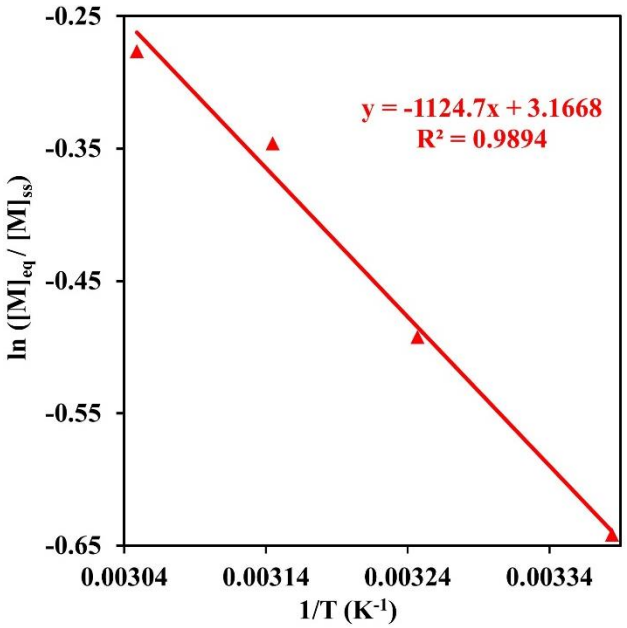

Figure 2.16. Van't Hoff analysis for poly(PDHL) (red triangle).

2.3.5. Kinetics of polymerization

The polymerization kinetics were analyzed for PDHL monomer under optimal catalyst and polymerization conditions determined above, which demonstrated equilibrium polymerization as evidenced by plateauing conversion (Figure 2.17a). Schneiderman et al. found six-membered lactone followed pseudo zero-order kinetics when conducted in the bulk,[48] and followed first-order kinetics while conducted in dilute conditions.[48,59,66] A semilogarithmic plot of monomer conversion as a function of reaction time for PDHL was linear, which indicates PDHL polymerization is first-order with respect to monomer concentration (Figure 2.17b). Martello et al. also reported that similar TBD-catalyzed δ-decalactone polymerization followed first order kinetics.[88]

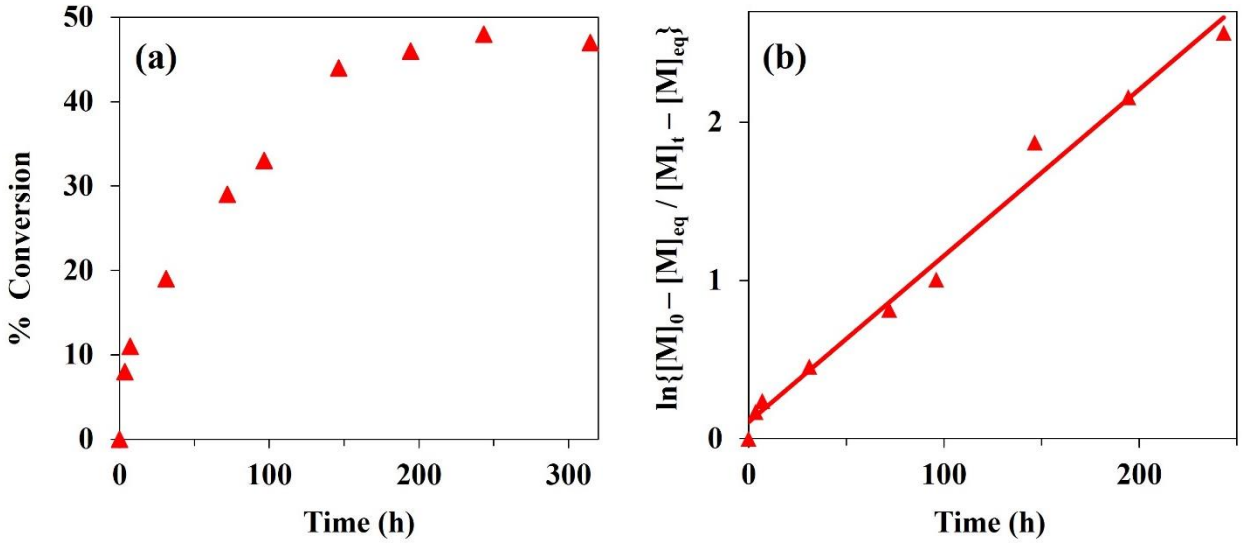

Figure 2.17. a) Monomer conversion as a function of time for poly(PDHL); b) Linearized kinetics behavior for ROP of PDHL (red triangle) before reaching equilibrium, where $[M]_{eq}$ is the equilibrium monomer concentration, $[M]_0$ is the initial monomer concentration, $[M]_t$ is the monomer concentration at given a time.

The molecular weight of polyPDHL linearly increased as a function of monomer conversion and the dispersity values ranged from 1.19 to 1.6, respectively (Figure 2.18). This behavior is expected for controlled ROP where all chains are initiated at the same time and then propagate simultaneously. The polymerization kinetics and time-dependent evolution of molecular weight for PDHL indicate that it follows controlled polymerization behavior under these conditions.

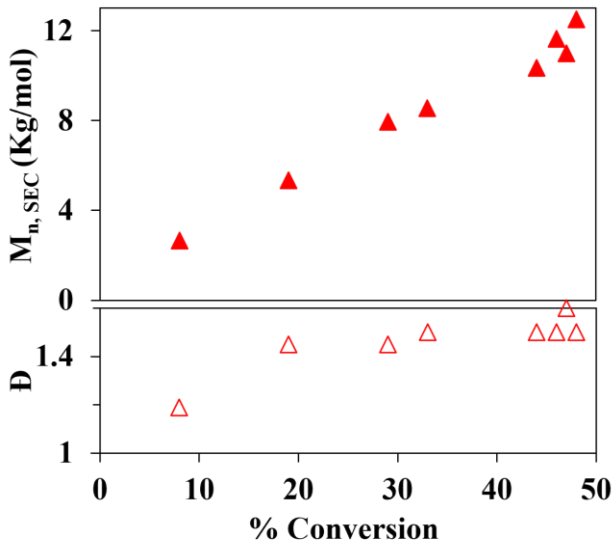

Figure 2.18. Number average molecular weight (M_n) and dispersity (Đ) as a function of monomer conversion for poly(PDHL). Both M_n and Đ measured by SEC. Ratios of $[M]_0/[I]$ = 100/1 for poly(PDHL) used throughout this study.

2.4 Conclusions

The phenoxy-functionalized δ-hexalactone monomer (PDHL) has sufficient thermodynamic driving force to polymerize in the presence of different organo-catalysts at room temperature. A basic organo-catalyst system was needed for the successful ROP of PDHL and activation of both monomer and initiator was necessary. The dual activation mechanism of TBD had the advantage for ring-opening polymerization of the PDHL lactone monomer with high molecular weight and low dispersity polyesters. The molecular weight of PDHL can be controlled by varying the monomer-to-initiator ratio. The introduction of a bulkier pendant group significantly increased the glass transition temperature relative the parent unsubstituted valerolactone (from -65 °C to +6 °C) and to a value near room temperature, yielding the highest reported T_g at this time for a substituted δ-valerolactone.

CHAPTER 3

SYNTHESIS AND RING-OPENING POLYMERIZATION OF 6-((2-PHENYLPHENOXY)METHYL)OXAN-2-ONE (2-PHPDHL)

3.1 Introduction

In our previous study, we successfully synthesized a six-membered lactone monomer bearing a phenol group (PDHL) at the δ-position and showed the conditions for polymerizing this new monomer. We hypothesized that incorporating lignin-derived aromatic molecules (e.g., phenol) as a pendant group in aliphatic polyesters would increase the glass transition temperature (T_g) of polyesters. We found an increase in T_g from -65 to +6 °C for polyPDHL compared to its unsubstituted six-membered polyDVL. The result we found was promising and the polymerization was well controlled. The robust synthetic route we developed to synthesize PDHL monomer suggests adding bulkier group at the δ-position is possible and we can synthesize a library of pendant diverse lactone monomers. The motivation to add a bulkier group at the pendant position is to get higher T_g aliphatic polyester polymers as well as to tune other properties like toughness, moisture resistance, etc. By adding one phenol group at the pendant position, we increased the T_g around 70 °C. So, it was hypothesized that another additional phenol ring would increase the T_g to room temperature or more due to the steric hindrance as mentioned in Chapter 1. Two aromatic rings were introduced (2-phenylphenol) at the δ-position position by synthesizing a new 2-PhPDHL monomer (Figure 3.1) and then its polymerization conditions were figured out. Finally, thermodynamics and kinetics studies were conducted for the new monomer and polymeric system.

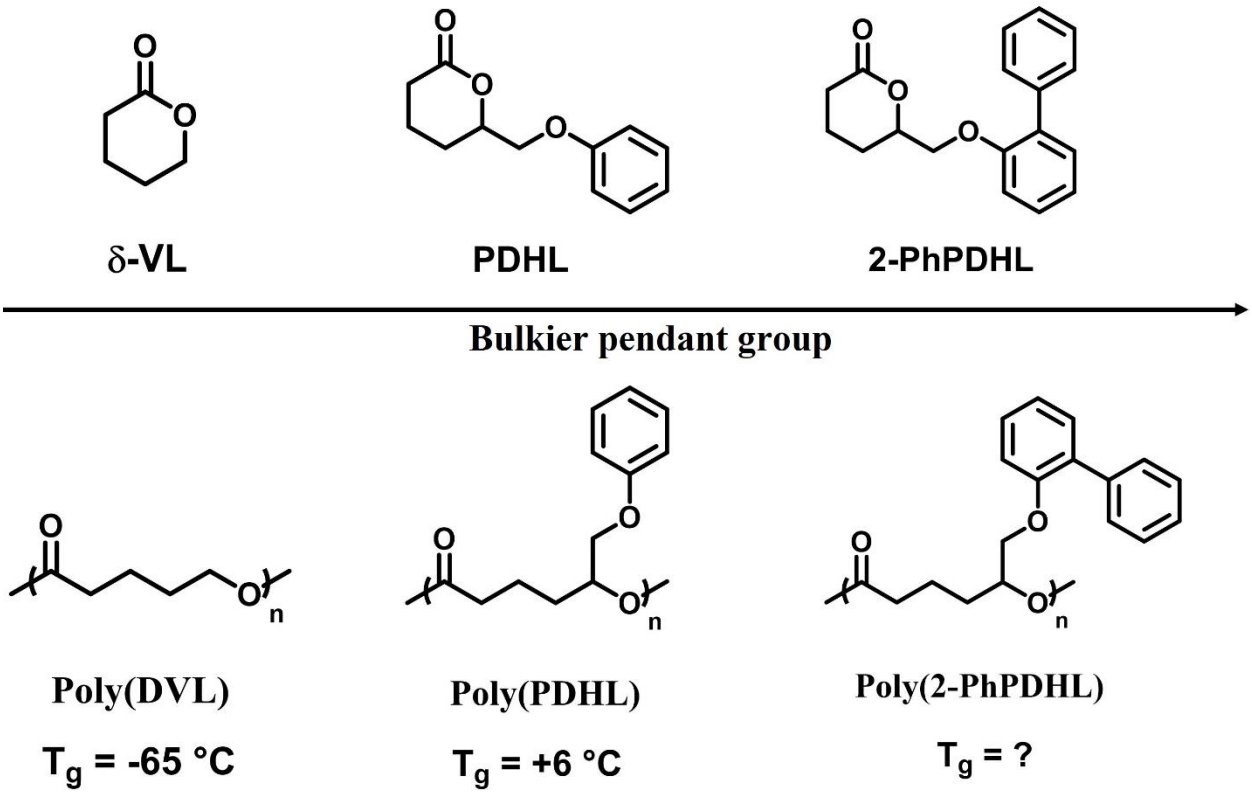

Figure 3.1. Introducing bulkier pendant group at the δ-position of the six-membered lactone monomers to get higher T_g polyesters

A six-membered lactone monomer bearing a phenolic group (PDHL) at pendant position was synthesized from commercially available methyl cyclopentanone-2-carboxylate previously. As we showed earlier in Chapter 2, the ketone mesylate (3) can be used as an intermediate to attach new bulky pendant groups. Mesylate is working as a leaving group in the Williamson ether synthesis reaction and nucleophilic attack by the deprotonated 2-phenylphenol will yield an ether linkage at the δ-position. By following, deprotection and Baeyer-Villiger oxidation reactions we can get a new six-membered lactone monomer bearing a new phenolic group (2-PhPDHL) (Figure 3.2).

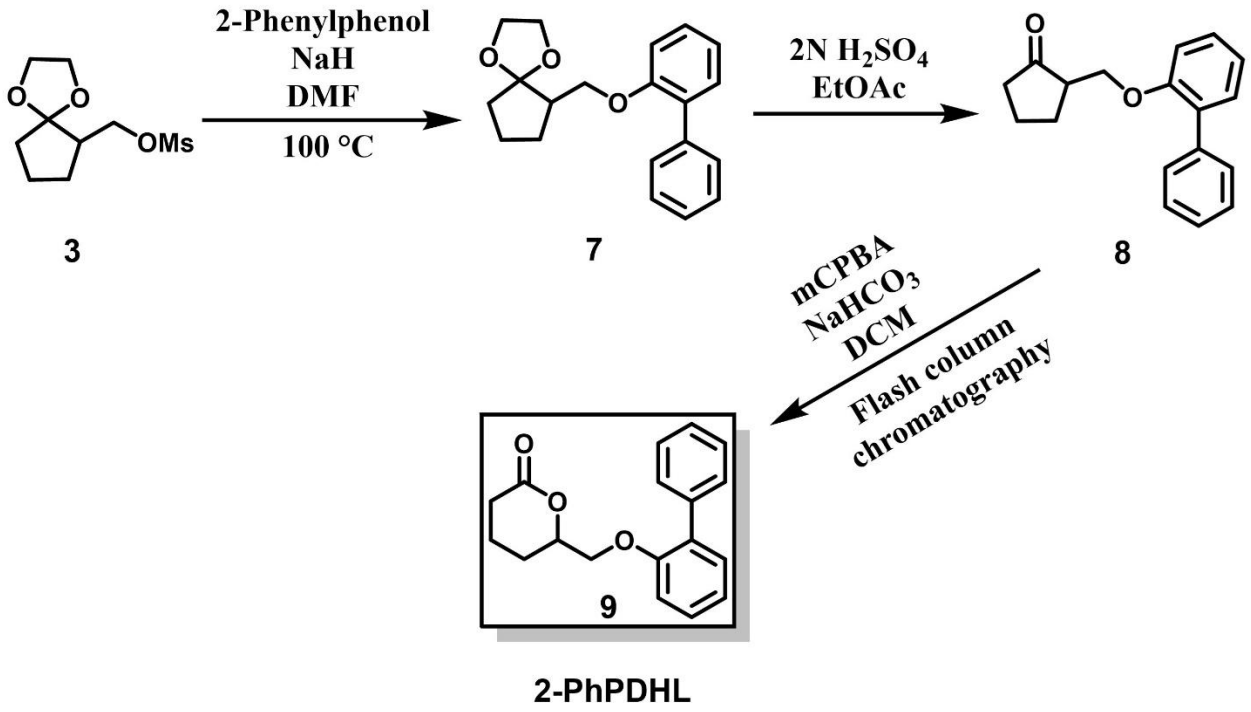

Figure 3.2. Reaction scheme for 2-PhPDHL monomer synthesis

3.2. Materials and methods

Reagents, including methyl cyclopentanone-2-carboxylate (TCI), p-toluenesulfonic acid (Acros), lithium aluminum hydride (Aldrich), potassium sodium tartrate tetrahydrate (Aldrich), sodium hydride (Acros), methanesulfonyl chloride (Fisher), 2-phenylphenol (Aldrich), potassium hydroxide (Aldrich), 3-chloroperoxybenzoic acid (Acros), sodium bicarbonate (Fischer), TBD: 1,5,7-triazabicyclo[4.4.0]dec-5-ene (Fisher), benzyl alcohol (Aldrich), 1,4-dioxane (extra dry) (Acros), dichloromethane (anhydrous) (Acros), and N,N-dimethylformamide (anhydrous) (Aldrich), ketone mesylate (Chapter 2) were used as received. All the other solvents and reagents were used as received from commercial suppliers without further purification unless stated otherwise.

3.2.1 Synthesis of 6-((2-phenylphenoxy)methyl)-1,4-dioxaspiro[4.4]nonane (7)

NaH (3.05 g, 60% dispersion in mineral oil) was washed with THF (3 x 10 mL) in a 500 mL round-bottom flask to remove the mineral oil, and then the NaH was suspended in DMF (20 mL) solvent. 2-Phenylphenol (6.92 g or 0.041 mol in 20 mL DMF) solution was added dropwise into the NaH suspension under an ice bath and stirred for 30 min at room temperature to deprotonate the 2-phenylphenol. After deprotonation, the round-bottom flask was sealed with a septum, flushed with N_2, and connected to a bubbler. **3** (6 g, 0.0254 mol) (Section 2.2.3) was added to the mixture and stirred for 18 h at 100 °C. After the reaction time, the round-bottom flask was removed from the oil bath and excess NaH was quenched by adding deionized water (100 mL). The mixture was extracted with ethyl acetate (3 x 50 mL) and washed with 5 M KOH solution (100 mL). The organic layer was dried over Na_2SO_4 and removed on a rotary evaporator to give **7** (4 g, 51% yield).

^{1}H NMR (Chloroform-*d*) δ (ppm): 7.56 (m, 2H), 7.41 - 7.51 (m, 5H), 7.32 (m, 1H), 7.03 (m, 1H), 3.69-4.06 (m, 6H), 2.41 (m, 1H), 1.96 (m, 1H), 1.5 - 1.96 (m, 6H).

3.2.2 Synthesis of 2-((2-phenylphenoxy)methyl)cyclopentanone (8)

In this synthesis, a 2N H_2SO_4 (35 mL, 0.35 mol) solution was added into a mixture of **7** (4 g**,** 0.0129 mol) in ethyl acetate (35 mL) solvent and stirred overnight at room temperature. Brine solution (50 mL) was poured into the mixture the next morning and extracted with ethyl acetate (3 x 50 mL). The extracted organic layer was dried over Na_2SO_4 and concentrated on a rotary evaporator to give **8** (1.89 g, 55% yield).

^{1}H NMR (Chloroform-*d*) δ (ppm): 7.28 - 7.5 (m, 7H), 6.98 (m, 2H), 4.19 (dd, *J* = 9 Hz, 5.2 Hz, 1H), 4.14 (dd, *J* = 9 Hz, 3.3 Hz, 1H), 2.42 (m, 1H), 2.3 – 1.7 (m, 7H).

3.2.3 Synthesis of 6-((2-phenylphenoxy)methyl)oxan-2-one (9)

In this synthesis, 3-chloroperoxybenzoic acid (mCPBA, 70%) (2.8 g, 0.016 mol) and sodium bicarbonate (1.25 g, 0.015 mol) were added to dichloromethane (100 mL) and stirred for 15 mins at room temperature. **8** (1.89 g, 0.0071 mol) was added into the mixture and stirred overnight. After the reaction time, extra dichloromethane (50 mL) solvent was added to the reaction mixture. The organic layer was washed with saturated Na_2SO_3 (20 mL), saturated $NaHCO_3$ (50 mL), then brine solution (20 mL), and separated. The organic layer was dried over anhydrous Na_2SO_4 and removed on a rotary evaporator to get the crude product (δ-substituted 82% major and α-substituted 18% minor product). The resulting solid was purified via silica gel flash column chromatography using 70:30 hexane:ethyl acetate mobile phase. After running flash column chromatography, 1.3 g of pure 2-PhPDHL (**9**) was collected at a 40% yield.

^{1}H NMR (Chloroform-*d*) δ (ppm): 7.5 (m, 2H), 7.4 - 7.27 (m, 5H), 7.07 (m, 1H), 6.95 (m, 1H), 4.68 (m, 1H), 4.09 (m, 2H), 2.52 (m, 1H), 2.32 (m, 1H), 1.86 – 1.67 (m, 4H) and ^{13}C NMR (Chloroform-*d*) δ (ppm): 171.03, 155.43, 138.47, 129.80, 121.91, 112.98, 78.38, 77.27, 70.25, 29.98, 24.72, 18.52.

3.2.4. Polymerization materials and methods

Vials and magnetic stir bars used for polymerization reactions were dried in an oven at 100 °C overnight before use. The 2-PhPDHL monomer was dried overnight before use in the room temperature vacuum oven. TBD was dried overnight in the antechamber of a nitrogen glovebox

and kept in the glovebox under nitrogen after received. Vials, caps, syringes, spatulas, and all other materials used to set up polymerization reactions were dried in the antechamber of the glovebox overnight before use.

3.2.5. General polymerization procedure for 2-PhPDHL

Polymerization of 2-phenylphenoxy-δ-hexalactone (2-PhPDHL) proceeded as follows. Two different stock solutions of initiator and catalyst were prepared by adding 3 μL benzyl alcohol in 300 μL 1,4-dioxane and 6 mg TBD in 200 μL 1,4-dioxane separately in an N_2 filled glovebox. First, the stock solution of benzyl alcohol (8 μL, 0.0081 mmol) and then the stock solution of TBD (6 μL, 0.00123 mmol) were added using glass syringes to 2-PhPDHL monomer (11.5 mg, 0.041 mmol) dissolved in dioxane solvent (11.5 μL) already in 2 mL vial with a septum. The homogenous mixture was stirred for the desired reaction time at ambient temperature. The polymerization was quenched by adding excess benzoic acid (3 mg, 0.0246 mmol). A typical polymerization led to ca. 60% conversion of 2-PhPDHL. The inactive catalyst was removed by precipitation of the pure polymer into diethyl ether.

3.2.6. Polymerization kinetics experiments

Polymerization kinetics experiments were carried out at ambient temperature for 2-PhPDHL monomers. The experiment was conducted using benzyl alcohol (BnOH) as an initiator and TBD as a catalyst. For measurement of the 2-PhPDHL polymerization kinetics, the stock solution of benzyl alcohol (49 μL, 0.0047 mmol) and the stock solution of TBD (15 μL, 0.007 mmol) were added using glass syringes to 2-PhPDHL monomer (66 mg, 0.234 mmol) dissolved in dioxane solvent (81 μL) in 2 mL vial with a septum. The homogenous mixture was stirred until the

polymerization reached equilibrium and aliquots were collected throughout the polymerization. The aliquots were quenched by adding 30 molar excess benzoic acid and monomer conversions were determined using ^{1}H NMR spectroscopy.

For the polymerization kinetics experiments, the $[Monomer]_0$:[Initiator] and $[Monomer]_0$:[Catalyst] ratios were fixed. The polymerization appeared to reach equilibrium, as indicated by a plateau in monomer conversion as a function of time. Equilibrium polymerization behavior was verified by fitting the kinetics data to Equation 3.1,[90] which describes monomer concentration as a function of time for an equilibrium polymerization:

$$\ln\left(\frac{[M]_0-[M]_{eq}}{[M]_0-[M]_t}\right) = k_{app}t \qquad \text{(Equation 3.1)}$$

where $[M]_{eq}$ is the equilibrium monomer concentration, $[M]_0$ is the initial monomer concentration, $[M]_t$ is the monomer concentration at given a time, and k_{app} is the apparent rate constant.

3.2.7. Polymerization thermodynamics experiments

For the polymerization thermodynamics experiments, the setup was the same as for the kinetics experiments, but the polymerizations were stirred in an oil bath at a range of temperatures. The temperature was varied for 2-PhPDHL from 23 to 55 °C. The polymerizations achieved different equilibrium monomer concentrations ($[M]_{eq}$) at different temperatures. Aliquots were collected after sufficient reaction time to reach equilibrium (typically 48 h for 2-PhPDHL) and quenched with excess benzoic acid. The polymerization progress was tracked using ^{1}H NMR spectroscopy. To ensure the polymerizations reached equilibrium, the reactions were kept running for at least another 48 h after reaching equilibrium. To estimate enthalpy (ΔH_p) and entropy (ΔS_p) for the

polymerization, the equilibrium monomer concentration was plotted as a function of inverse temperature and fit using a van 't Hoff analysis:

$$\ln\left(\frac{[M]_{eq}}{[M]_{ss}}\right) = \frac{\Delta H_p}{RT} - \frac{\Delta S_p}{R} \qquad \text{(Equation 3.2)}$$

where T is the polymerization temperature, R is the ideal gas constant, and $[M]_{ss}$ is a standard state monomer concentration that was set to 1 M.

3.2.8. Analysis of polymer products

^{1}H NMR and ^{13}C NMR spectra were obtained either using Varian Inova 400 MHz and Bruker Avance NEO 500 MHz NMR spectrometers using $CDCl_3$ as a solvent. Size exclusion chromatography (SEC) was conducted in dimethylformamide (DMF) containing 0.5 wt% LiBr as the mobile phase with a flow rate of 1 mL min^{-1} at 70 °C. SEC analysis was performed by three Phenogel columns (Phenomenex) in series with different pore sizes (50, 10^3, and 10^6 Å), using a refractive index detector (35 °C) and calibration curves from linear polystyrene standards.

The crude polymer was dissolved in dichloromethane and precipitated in cold diethyl ether (1:5). The purified polymers were dried in a vacuum oven. The T_g of different polymers was measured using a differential scanning calorimeter (DSC, TA Instruments DSC2500) at a rate of 10 °C min^{-1} over a range from -90 to 100 °C using ~1.5 mg sample in a heat/cool/heat experiment under an N_2 atmosphere. The T_g were reported from the second heating cycle and analyzed with TA TRIOS software (v5.0.0).

3.3 Results and discussion

The powerful base sodium hydride (NaH) was used to deprotonate the 2-phenylphenol in DMF solvent. The phenylphenoxide anion was stable and worked as a nucleophile in the presence of the mesylate leaving group. Successful etherification was confirmed by the disappearance of the mesylate methyl singlet at 3 ppm. The protons next to the ether linkage were shielded more which confirmed further successful etherification (Figure 3.3). Excess 2-phenylphenol was not removed from the reaction medium as more washing was needed which would affect the overall yield. Our previous studies showed excess phenol did not have any impact on the next reaction steps.

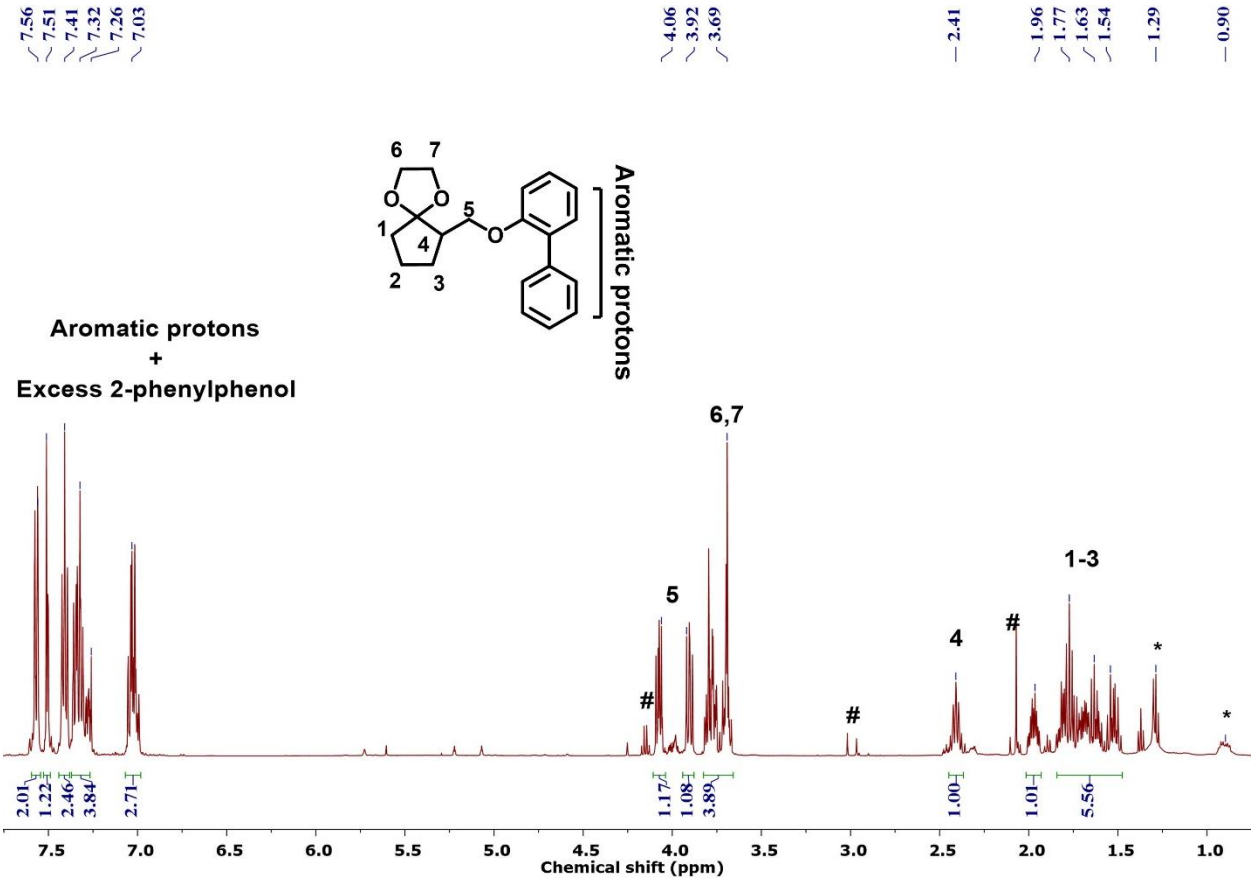

Figure 3.3. ^{1}H NMR spectrum of 6-((2-phenylphenoxy)methyl)-1,4-dioxaspiro[4.4]nonane (7). *Mineral oil from NaH washing step, #DMF, and ethyl acetate solvents

The protecting acetal group was removed in the next step in the presence of an acidic solution. Sulfuric acid (1 M) was used to remove the acetal group. The removal of the acetal group was confirmed by the disappearance of peaks at 3.69 ppm (Figure 3.4). The protons next to the ether linkage were affected mostly due to the removal of the acetal group and those protons showed a de-shielding effect in the ^{1}H NMR spectrum. The removal of the acetal group was a straightforward process in this synthesis step as no elimination product was observed.

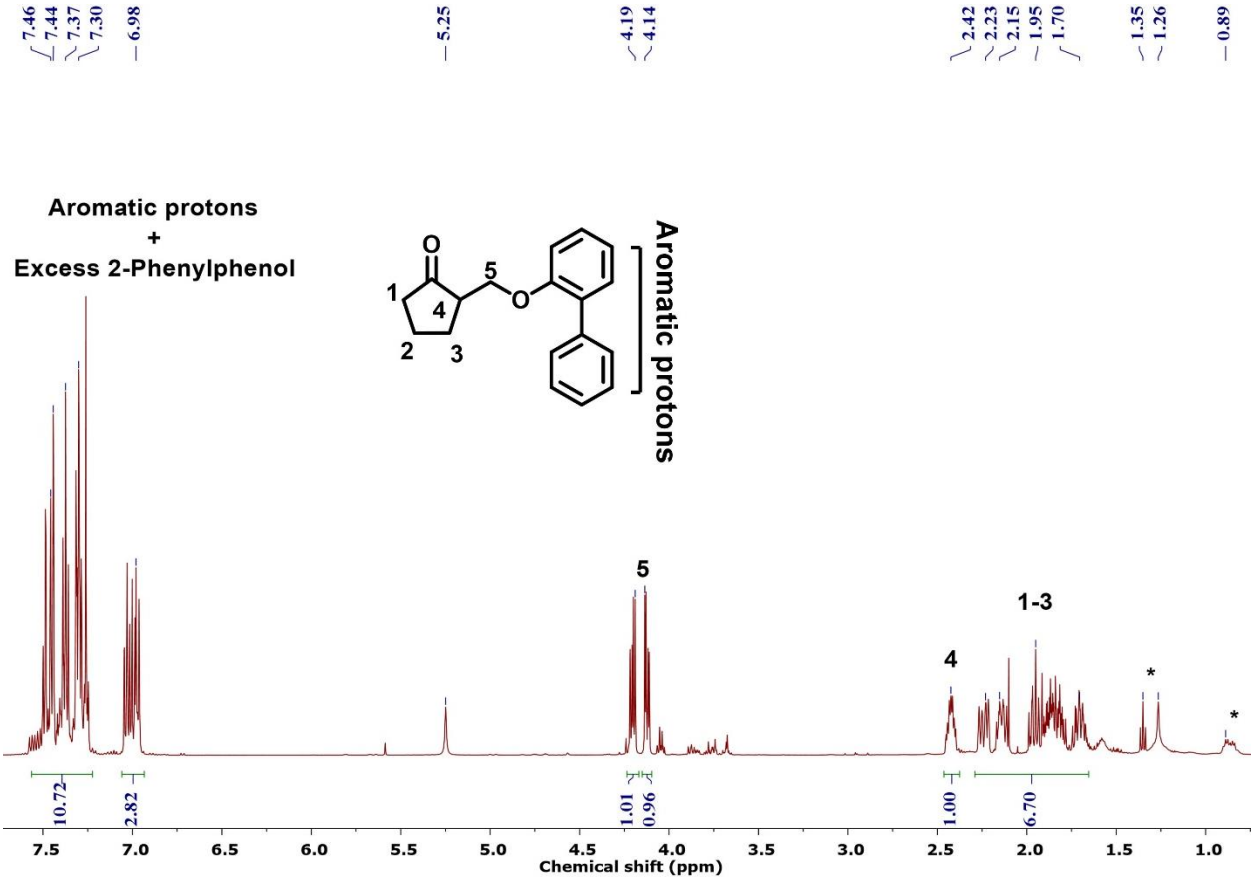

Figure 3.4. ^{1}H NMR spectrum of 2-((2-phenylphenoxy)methyl)cyclopentanone (8). *Mineral oil

A Baeyer-Villiger oxidation reaction was used to synthesize six membered lactones from the five-membered cyclic ketones. 3-Chloroperoxybenzoic acid (mCPBA) was used as a peroxyacid source. Both α-substituted and δ-substituted products were observed in the ^{1}H NMR spectrum due to the unsymmetrical cyclic ketone. The δ-substituted product (82%) was the major product in the synthesis due to the higher migratory aptitude of the tertiary alkyl group over the secondary alkyl group. The peak of protons next to the ester group confirmed the successful six-membered lactone synthesis at 4.57 ppm for the major product (Figure 3.5). After this step, a mixture of major and minor products was obtained in the presence of chlorobenzoic acid as a by-product. For ROP and controlled polymerizations, pure 2-PhPDHL was required. Flash column chromatography was used to separate the pure 2-PhPDHL monomer. Pure 2-PhPDHL was separated successfully by using more non-polar hexane solvent. A 70:30 hexane and ethyl acetate mixture was used as a mobile phase. The products were tracked by thin layer chromatography (R_f = 0.33 for δ-substituted product and R_f = 0.42 for α-substituted product) primarily. The pure 2-PhPDHL was confirmed by both ^{1}H and ^{13}C NMR spectroscopy (Figure 3.6-3.7).

The difficulty of synthesizing 2-PhPDHL was similar to the PDHL monomer. Both behaved in a similar way during the six-step reactions. Separating pure 2-PhPDHL was a little harder than PDHL one during the flash column chromatography technique due to the byproduct 3-chlorobenzoic acid having similar polarity. Washing with excess 10% $NaHCO_3$ made it easier to remove of excess 3-chlorobenzoic acid as byproducts from the reaction mixture before running the column technique.

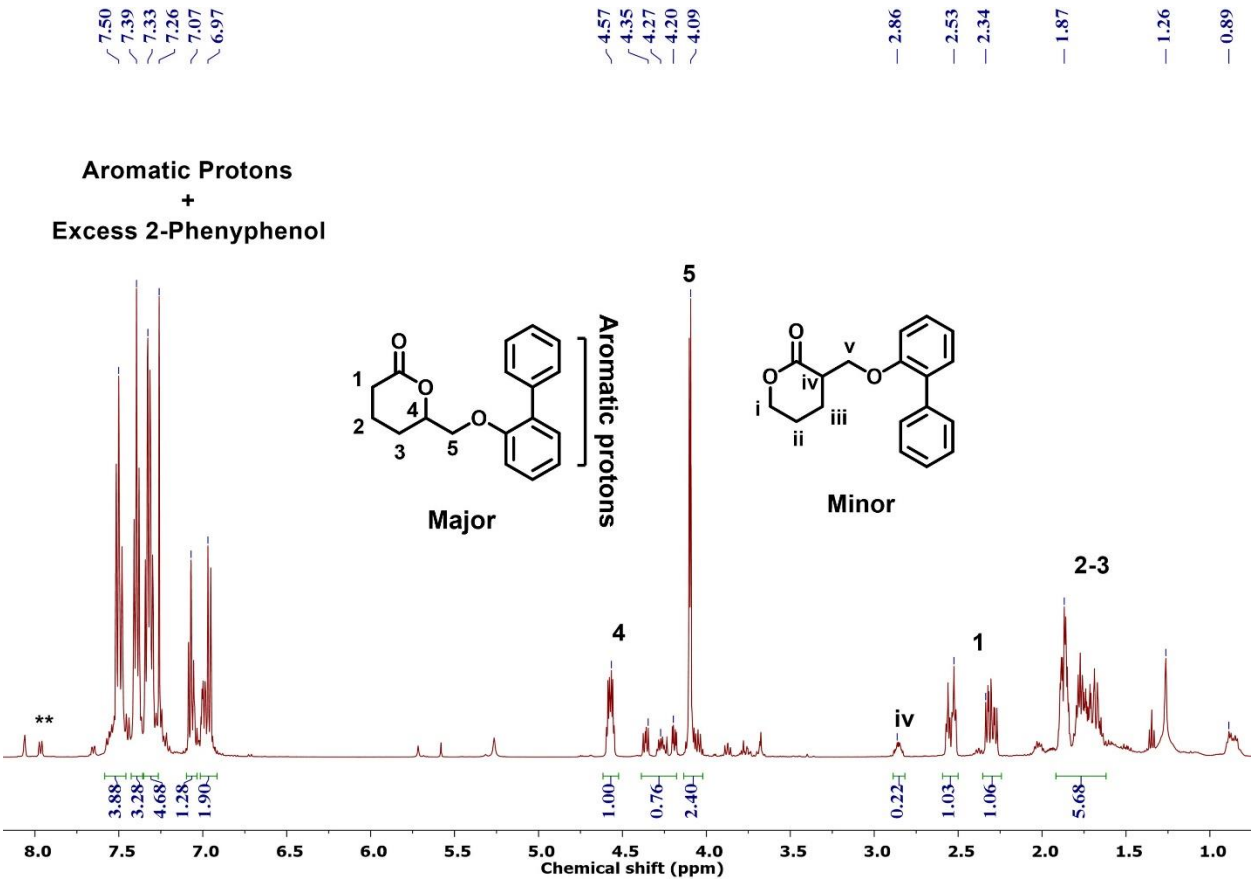

Figure 3.5. ^{1}H NMR spectrum of a crude mixture of 6-((2-phenylphenoxy)methyl)oxan-2-one (9), ** 3-chlorobenzoic acid

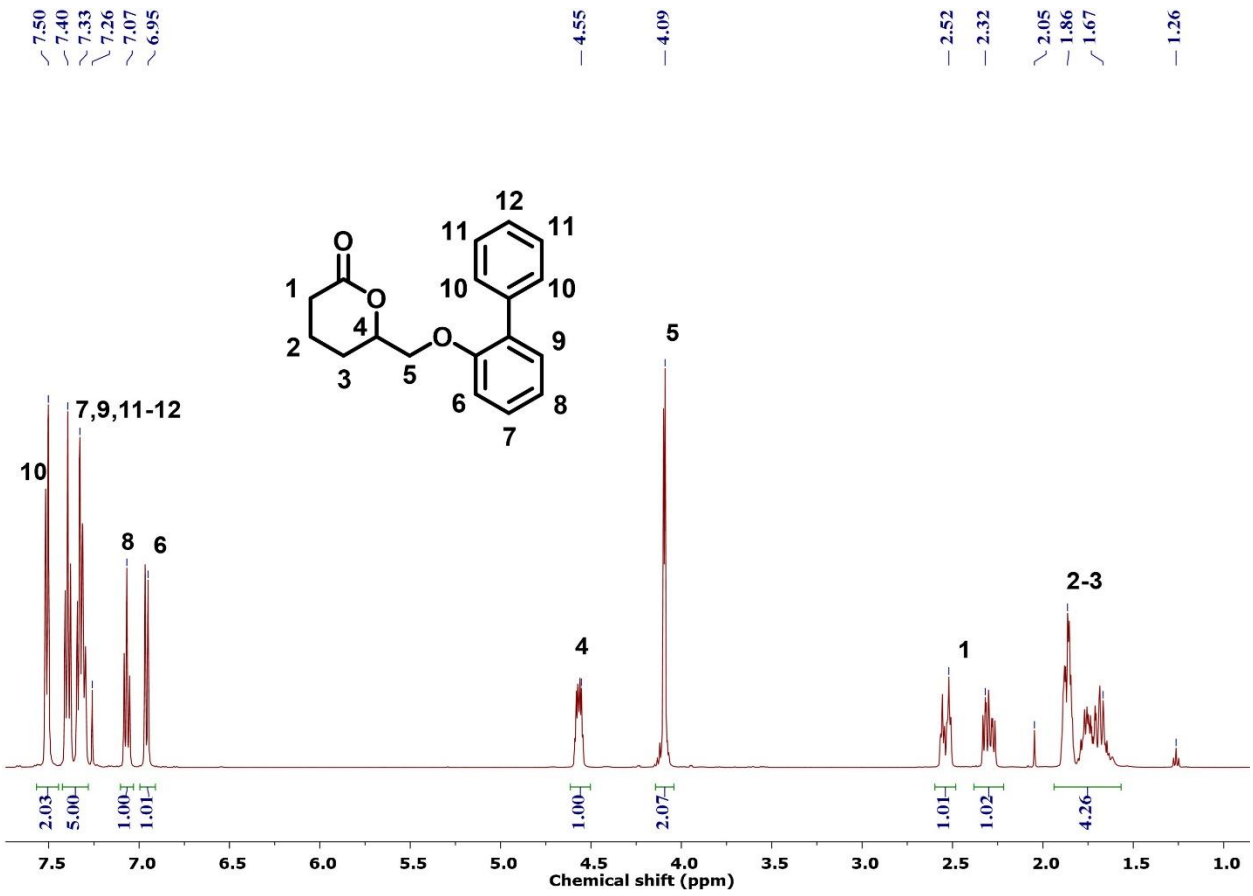

Figure 3.6. ^{1}H NMR spectrum of pure 2-PhPDHL monomer (9), collected after flash column chromatography.

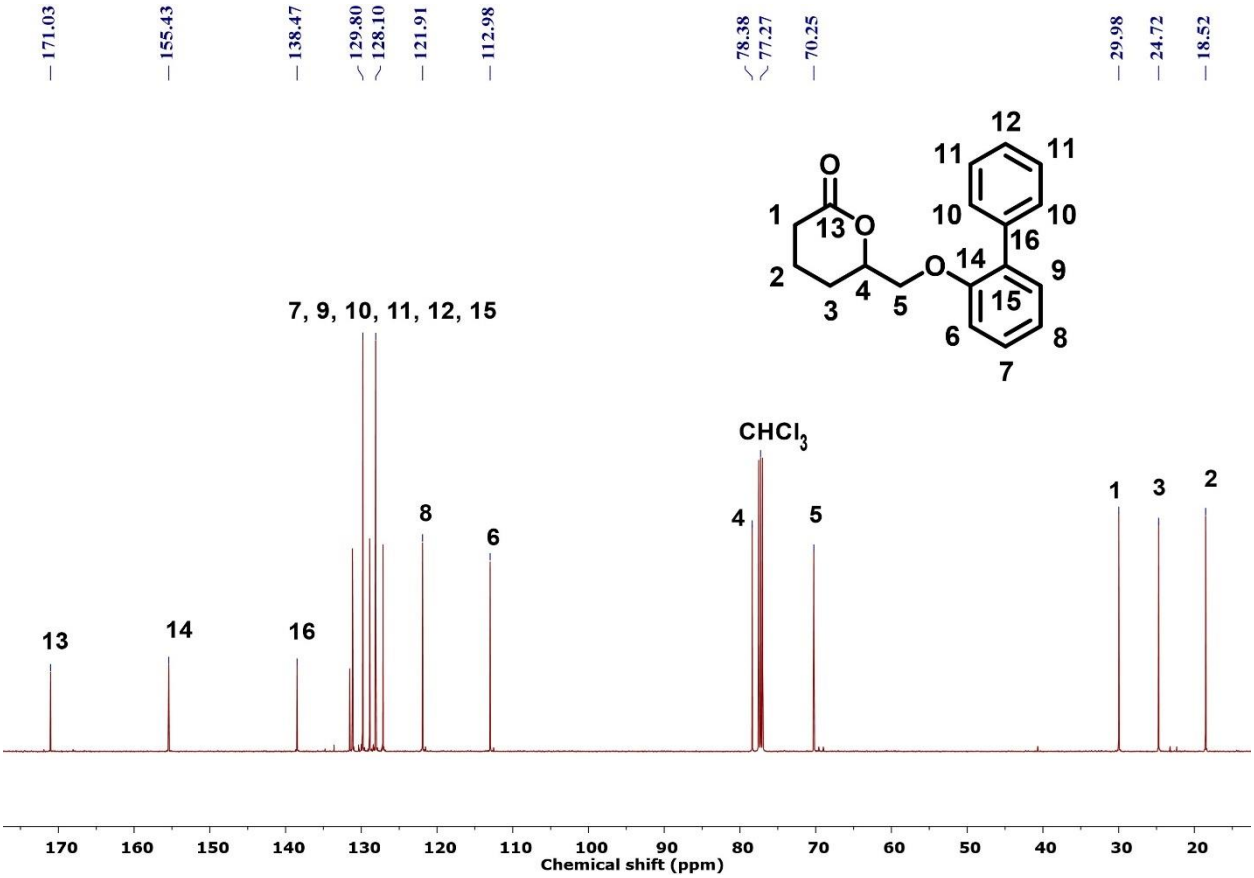

Figure 3.7. ^{13}C NMR spectrum of pure 2-PhPDHL monomer (9).

3.3.1 Ring-opening polymerization of 2-PhPDHL lactone

Finding the optimum conditions for the polymerization reaction are necessary for a new bulkier 2-PhPDHL monomer system. The objectives of the optimization reactions were to obtain a higher conversion, to find a catalytic system for polymerizing the new monomer in a controlled manner, and to get high molecular weight polymers. The general scheme for the ring opening polymerization of 2-PhPDHL is shown in Figure 3.8 below. For ROP, the lower temperature gives higher conversion due to low equilibrium monomer concentration ($[M]_{eq}$) values. However, practically keeping the temperature below room temperature is not feasible and it affects the polymerization rate significantly. Bulk polymerization (no solvent) yielded low molecular weight

polymers because polymers precipitated out from the reaction. Dioxane solvent was used to dissolve the monomer and polymers during the reaction.

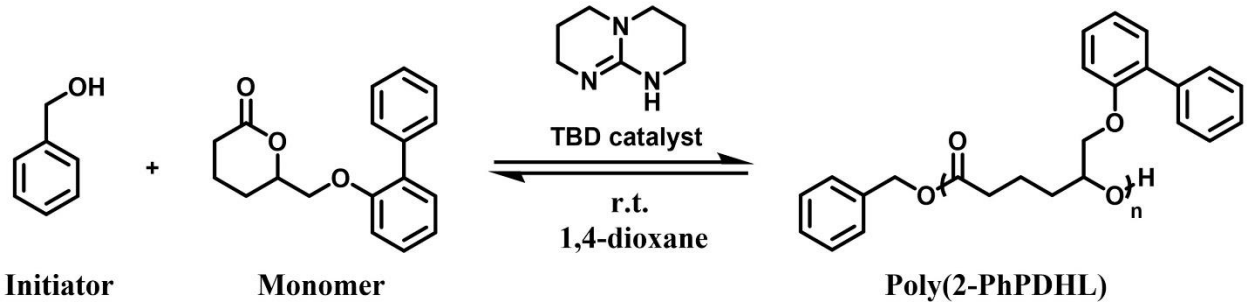

Figure 3.8. Polymerization scheme for the ring opening polymerization of 2-PhPDHL

The 2-PhPDHL monomer was polymerized at room temperature using benzyl alcohol (BnOH) as the initiator and basic TBD (0.3 mol%) as a catalyst as an initial test in 1,4-dioxane while keeping the initial monomer concentration at 1.1 M. But only 5% conversion was found even if the reaction kept running for few weeks (Table 3.1). The initiator initiated the polymerization successfully, but no propagation was observed from the ^{1}H NMR spectroscopic analysis. The conversion was less than 5% until 3 mol% catalyst was used. Minimum 3 mol% (33 mM) TBD was needed to get higher conversion in the polymerization of 2-PhPDHL (Table 3.1). This kind of behavior is reported in the literature. A primary alcohol (like BnOH) can initiate the polymerization instantaneously, but the secondary alcohol of the propagating chain end is a slow initiator for the upcoming monomer (Figure 3.9).[91] So, excess TBD is needed to activate the propagating chain end to push this equilibrium forward. Also, TBD can act as an initiator in addition to the alcohols and excess TBD is needed to make up the TBD that acted as an initiator to proceed the polymerization.[92] Additionally, the basic nature of the solvent (THF, 1,4-dioxane, etc.) can

coordinate with hydroxyl groups of initiator or chain end. Alamri et al. reported the addition of excess catalyst yielded higher conversion of poly(ε-caprolactone) which overcame the competition between the catalyst and the cyclic ethers (THF) in coordination with the hydroxyl initiator/chain end.[91] So, for 2-PhPDHL system, propagation did not observe due to the secondary propagating chain end and higher catalyst loading was necessary to activate this chain end for further polymerization conversion.

Table 3.1. Effect of catalyst loading for ROP of 2-PhPDHL

Catalyst (mol%)[a]	**Catalyst (mM)[b]**	**% Conversion[c]**
0.3	3.3	<5%
0.5	5.5	<5%
1	11	<5%
1.5	16.5	<5%
2	22	<5%
3	33	60%
6	66	60%

[a]Based on monomer moles; [b]Calculated by the moles of the catalyst over total volume; [c]Conversion measured by ^{1}H NMR spectroscopy. Ratios of $[M]_0/[I]$ = 50/1 for the polymerization used throughout this study where initial monomer concentration, $[M]_0$ = 1.1 M

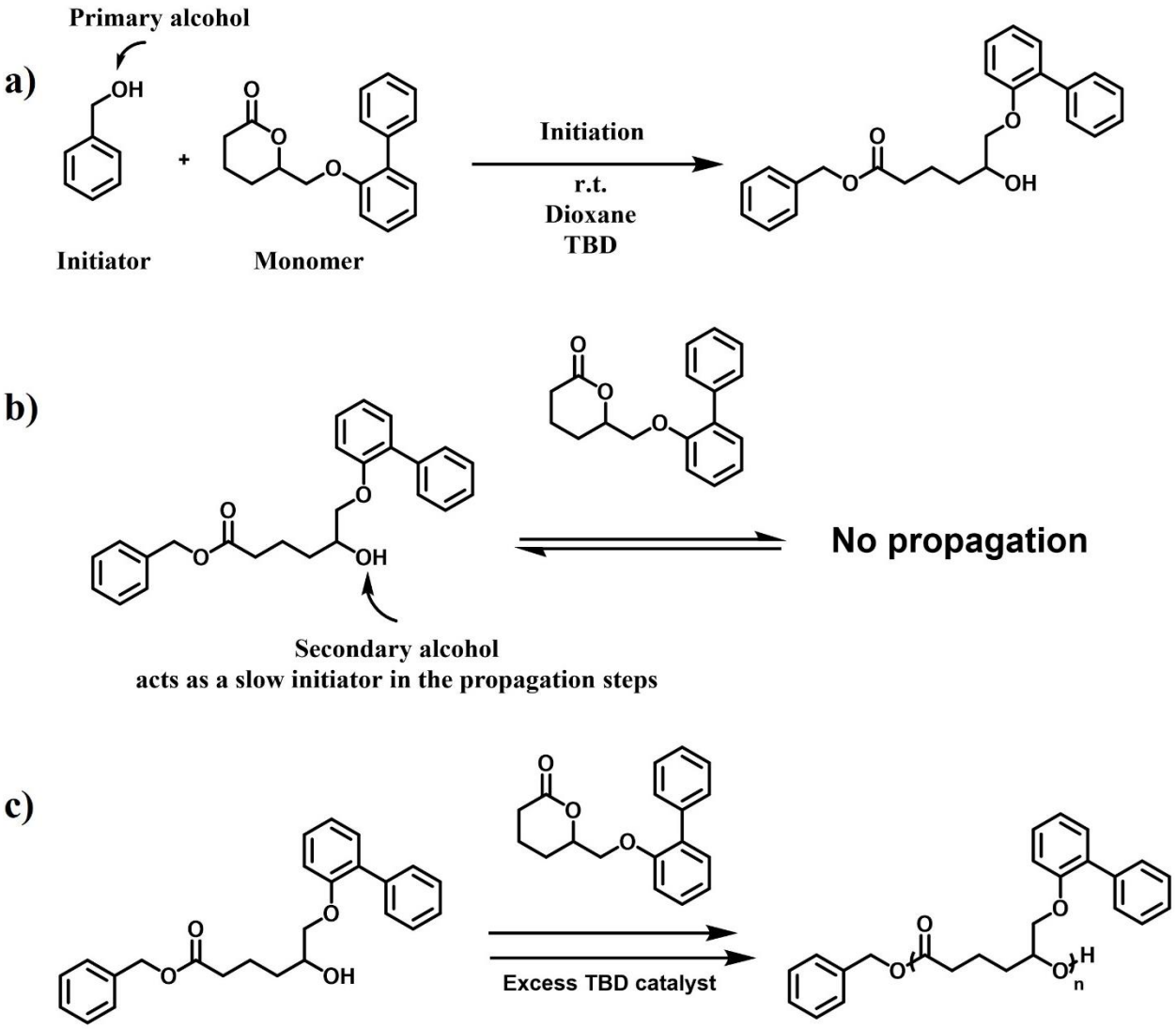

Figure 3.9. a) Primary alcohol from the initiator initiates the polymerization instantaneously. b) Secondary alcohol of the propagating chain end acts as a slow initiator for the upcoming monomer. c) Excess catalysts can activate the secondary alcohol of the propagating chain end and push the reaction forward.

3.3.2 Controlling the molecular weight of poly(2-PhPDHL)

The 2-PhPDHL monomer was polymerized at room temperature (22-25 °C) using benzyl alcohol (BnOH) as the initiator and TBD as a catalyst. The conversion was tracked by taking aliquots from the reaction and analyzing them using ^{1}H NMR spectroscopy (Figure 3.10). The methylene protons of the BnOH initiator shifted from 4.7 to 5.07 ppm, confirming that the monomer was initiated by

BnOH. The methine protons of 2-PhPDHL (4.55 ppm) shifted to 5.03 ppm, corresponding to the lactone ring opening and the successful polymerization.

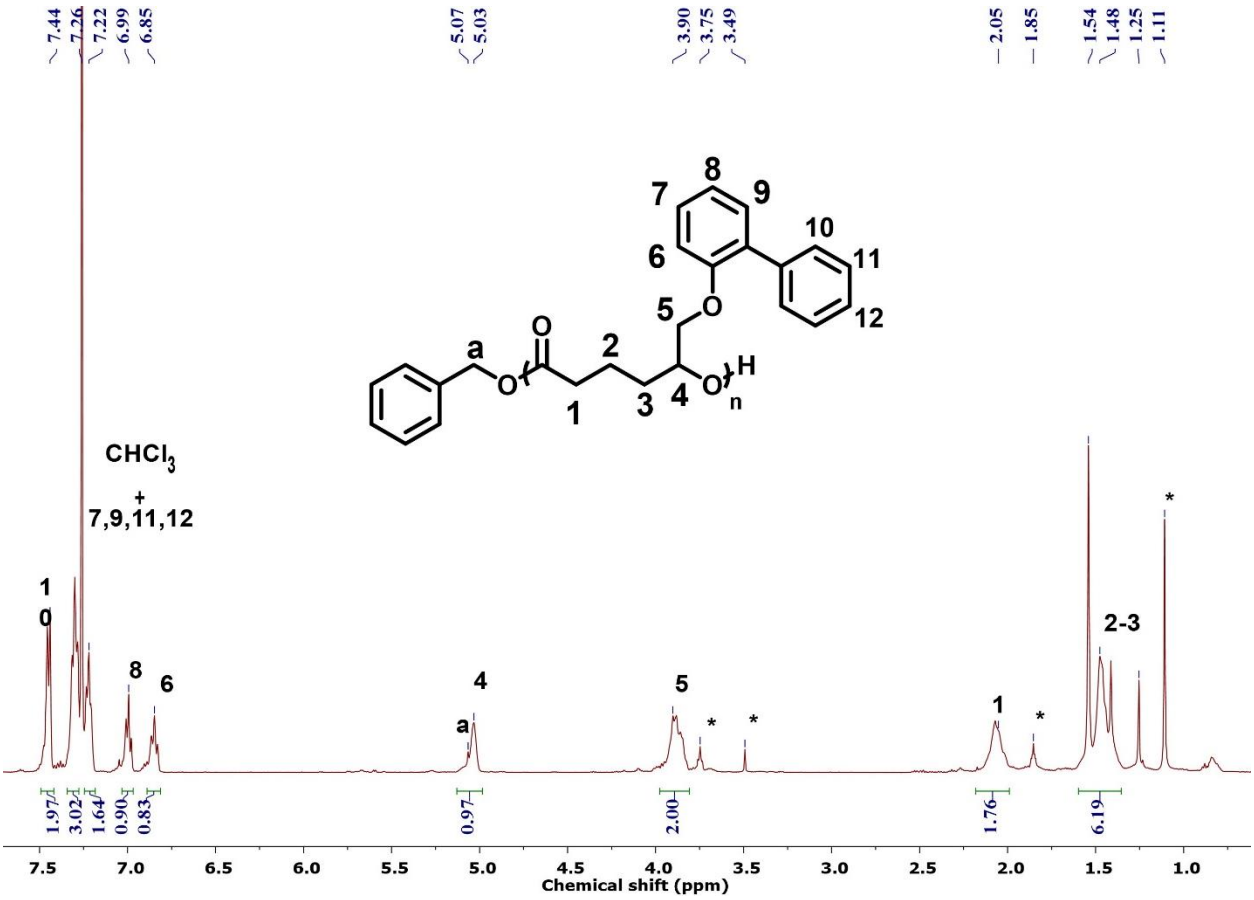

Figure 3.10. ^{1}H NMR spectrum of crude poly(2-PhPDHL). ^{1}H NMR spectrum was collected after the polymerization reached equilibrium on day three. (*THF and methanol solvent)

Table 3.2 summarizes the results obtained from different polymerizations. As mentioned above, the minimum 3 mol% TBD catalyst (33 mM) is needed to get the higher conversion for the polymerization of 2-PhPDHL. The equilibrium monomer conversion of 2-PhPDHL was about 50-60% range. The conversion varied due to the room temperature difference in summer and winter seasons (20-27 °C ranges). The molar mass distributions were unimodal for all the polymers (Figure 3.11), which indicated limited backbiting occurred prior to equilibrium.

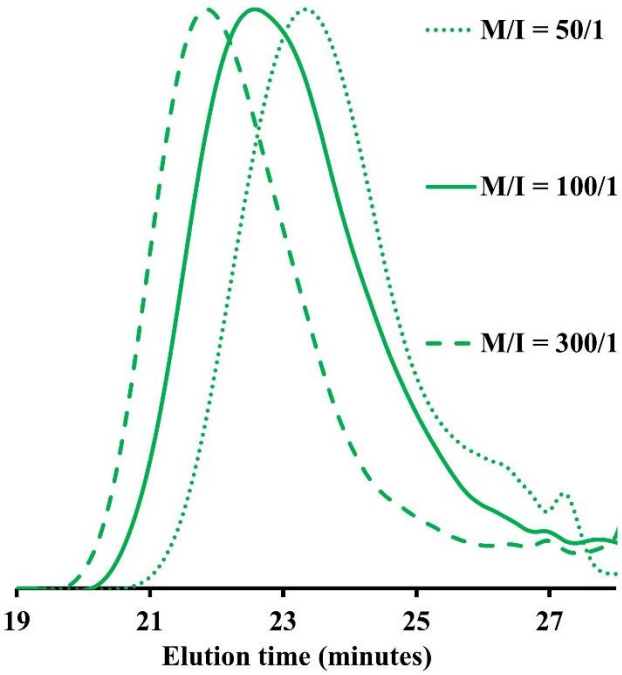

Figure 3.11. SEC elution curves for ROP of 2-PhPDHL after reaching equilibrium conversion at different $[M]_0/[I]$ ratios. Molecular weights ($M_{n,\ SEC}$) and dispersity are in Table 2.

The experimental M_n values from size exclusion chromatography (SEC) differed from the calculated expected values. The $M_{n,SEC}$ of poly(2-PhPDHLs) were still close to the expected values at lower $[M]_0/[I]$ ratios (Table 3.2, entries 1-2). $M_{n,SEC}$ values should increase by increasing $[M]_0/[I]$ for poly(2-PhPDHL), but the $M_{n,SEC}$ value deviated significantly from the $M_{n,\ expected}$ value while we increased the $[M]_0/[I]$ ratio from 100 to 300 (Table 3.2, entry 3). Though size exclusion chromatographic technique cannot deliver actual MW of the polymers due to the calibration of the RI detector with polystyrene (PS) standards, a nearly three-fold increase in the $M_{n,sec}$ values were expected while changing the $[M]_0/[I]$ ratio from 100 to 300. This result suggests a failure in the controlled polymerization. Broader dispersities were expected due to the higher catalyst loading as mentioned in Chapter 2 for PDHL monomer section (Table 3.2, entries 1-3). Higher catalyst

loadings may favor reaching equilibrium monomer concentration faster or nucleophilic mechanism over acid-base mechanism and lead to broader dispersity.[93]

Table 3.2. Results for TBD catalyzed ROP of 2-PhPDHL

Monomer	Entry	$[M]_0/[I]/[C]$	Time (days)	Conv.[b] (%)	$M_{n,\ expected}$[c] (kg/ mol)	$M_{n,\ SEC}$[d] (kg/ mol)	Đ[d]
2-PhPDHL[a]	1	50/1/1.5	3	60	8.5	6.5	1.7
	2	100/1/3	5	51	14.5	10.0	1.75
	3	300/1/9	5	50	42.0	16.0	1.71
	4	20/1/0.6	3	55	3.1	5.5	1.4
	5	20/0/0.6	3	56	-	20.5	1.9

[a]1,4-dioxane as solvent, $[M]_0$ = 1.1 M; where $[M]_0$ = Initial monomer concentration. [b]Fractional conversion measured by ^{1}H NMR spectroscopy. [c]Calculated from $[M]_0/[I]$ × monomer conversion × MW of 2-PhPDHL. [d]Measured by SEC in DMF with 0.5 wt% LiBr as the mobile phase, using linear polystyrene standards with a refractive index detector.

3.3.3 Role of TBD as an initiator in the ROP of 2-PhPDHL

To polymerize both PDHL and 2-PhPDHL, all the variables were kept the same except for TBD catalyst loading. Besides acting as a catalyst, TBD may act as an initiator. Two additional polymerizations were carried out with and without the BnOH initiator for 2-PhPDHL (Table 3.2, entries 4-5). Both polymerizations yielded similar conversion with or without BnOH initiator (Table 3.2, entries 4-5). Only TBD catalyzed polymerization gave the highest $M_{n,\ SEC}$ value in the absence of any initiator (Table 3.2, entry 5). Since polymer formed without any initiator, TBD participates in the polymerization process as a catalyst and competes with BnOH in the initiation process also. Pascual et al. reported the similar initiator role of TBD catalyst in the event of ROP of ethylene brassylate.[92,94] The appearance of proton peaks at 3.27 and 3.22 ppm confirmed the

role of TBD as an initiator for the polymerization of 2-PhPDHL without any BnOH (Figure 3.12). Further end group studies by matrix assisted laser desorption/ionization (MALDI) are needed to confirm the initiation process by TBD.

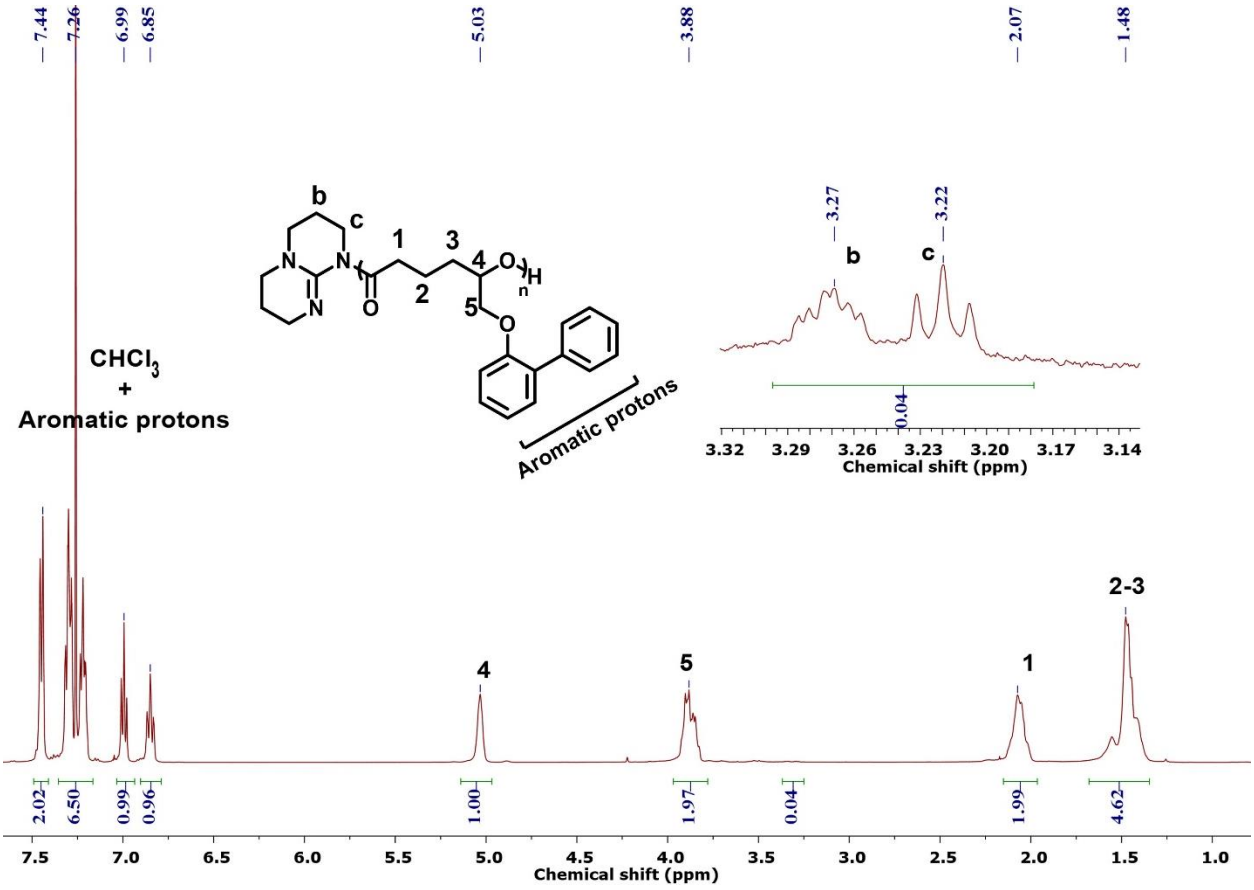

Figure 3.12. ^{1}H NMR spectrum of poly(2-PhPDHL) obtained by TBD catalyzed ROP in the absence of BnOH as an initiator (Table 3.2, entry 5)

3.3.4 Glass transition temperature (T_g) of poly(2-PhPDHL)

Glass transition temperature (T_g) was measured by DSC from the second heating cycle (Figure 3.13). The unsubstituted six-membered poly(δ-valerolactone) has a T_g of -65 °C [95,96] and seven-membered poly(ε-caprolactone) has a T_g of -60 °C reported in the literature.[97] It was hypothesized

that a higher T_g can be achieved by attaching another phenyl at the δ-position due to the presence of bulky aromatic groups. A significant increase in T_g was found for poly(2-PhPDHL) (39.5 °C), which is higher than those of all alkyl-substituted poly(δ-valerolactone)s (-52 °C to -50 °C).[98] Additionally, the poly(2-PhPDHL) did not crystallize above its T_g due to the racemic mixture, and the catalysts afforded no stereochemical preference.

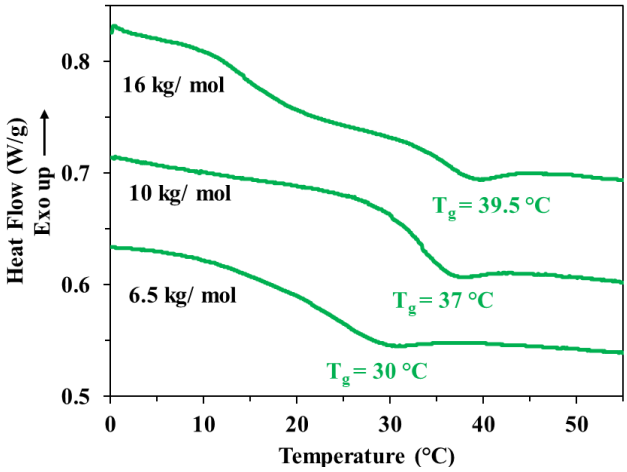

Figure 3.13. DSC thermograms of poly(2-PhPDHL). Curves are shifted vertically to provide clarity.

The T_g of a polymer depends on the molecular weight and it increases rapidly with increasing molecular weight and plateaus at higher values. The T_g kept increasing with the increase of molecular weight of the poly(2-PhPDHL) from 6.5 kg/mol to 16 kg/mol (Figure 3.14). Whether the T_g already hit the plateau for poly(2-PhPDHL) could not be tested due to the unavailability of high molecular weight polymers. T_g for an infinite molecular weight polymer can be estimated by plotting the T_g found as a function of inverse molecular weight in Equation 3.3 below.

$$T_g(M_n) = T_g(M \to \infty) - \frac{A}{M_n} \qquad \text{(Equation 3.3)}$$

In the equation, A is an empirical parameter. After reaching a certain molecular weight, the T_g becomes independent of the M_n values. In Figure 3.13, the intercept of the equation shows the T_g of poly(2-PhPDHL) will hit the plateau at 46.5 °C and become independent of the molecular weight of the polymer.

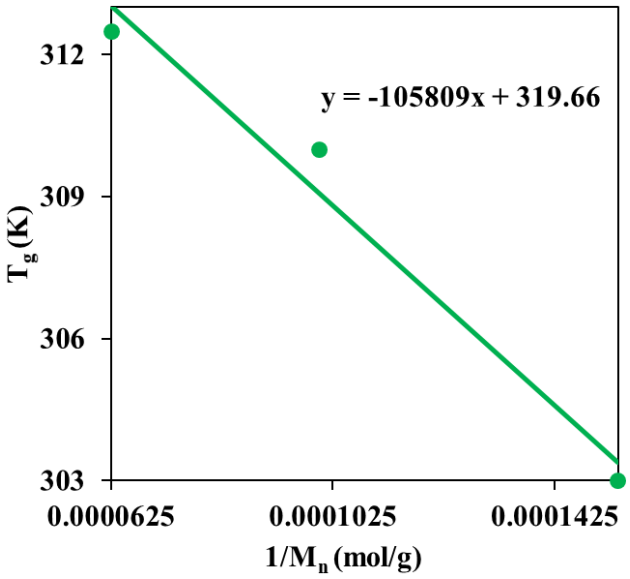

Figure 3.14. Dependence of the glass transition temperature on molecular weight for poly(2-PhPDHL) where plot shows the T_g versus $1/M_n$.

3.3.5 Thermodynamics of polymerization

For a typical ROP, it reaches an equilibrium over time where the rate of polymerization equals the rate of depolymerization. This results in an equilibrium monomer concentration, $[M]_{eq}$. The polymerizations achieved different equilibrium monomer concentrations ($[M]_{eq}$) at different temperatures and should be independent of the catalyst. Table 3.3 shows the $[M]_{eq}$ values obtained by running the polymerization at different temperatures.

Table 3.3. Observed equilibrium monomer concentration ($[M]_{eq}$) at different temperatures

Temperature (°C)	**$[M]_{eq}$ (M)**
23	0.55
35	0.649
45	0.693
55	0.814

The thermodynamics of the ROP was examined by polymerizing 2-PhPDHL over a range of temperatures and performing a van't Hoff analysis to calculate the entropy and enthalpy of polymerization and to learn how monomer structure impacts polymerization thermodynamics (Figure 3.15). The enthalpy of polymerizations (ΔH_P^o) was -9.4 ± 0.9 kJ mol^{-1} and the entropy of polymerizations (ΔS_P^o) was -26 ± 3 J mol^{-1} K^{-1} for 2-PhPDHL. Both values were close to the PDHL monomer (ΔH_P^o = -9.4 ± 0.7 kJ mol^{-1}, ΔS_P^o = -26 ± 2 J mol^{-1} K^{-1}), and it suggests attaching another phenol group at δ-position does not impact polymerization thermodynamics. The negative enthalpy of polymerization of a cyclic monomer results mostly from its ring strain.[99] The enthalpy of 2-PhPDHL is close to the values reported for DVL (ca. -10 kJ mol^{-1}), but slightly lower than the values reported for δ-decalactones (-17.1 ± 0.6 kJ mol^{-1})[100,101] and other alkyl-substituted δ-lactones (-13 to -19 kJ mol^{-1}).[98] The inclusion of an ether linkage in the pendant group appears to decrease the ring strain as compared to the all-carbon pendant group of alkyl-substituted δ-lactones, which may be due to the increased rotational freedom of the ether group. The entropy of 2-PhPDHL indicates that it is entropically disfavored as compared to DVL (-15 J mol^{-1} K^{-1}).

However, the entropic penalty for polymerization is less than that of alkyl-substituted DVLs (ca. -55 J mol^{-1} K^{-1}), which enables the significant conversions observed in spite of the lower ΔH_P^o. The addition of a pendant group likely decreases the internal rotational freedom of a polymer chain relative to its unsubstituted parent, DVL, which leads to the higher entropic penalty observed for substituted DVL monomers. However, for the ether-substituted monomer 2-PhPDHL, this entropic penalty is not as significant as for alkyl-substituted DVL monomers, presumably due to the extra degrees of freedom possible from the more freely rotating ether group. Thermodynamically, both polymers (PDHL and 2-PhPDHL) showed similar enthalpic values (ΔH_P^o) for polymerizations, and their entropic penalty for polymerizations were also very similar. Running ring opening polymerization at room temperature yielded higher conversions and at higher temperatures, both polymers reached equilibrium faster and earlier. So, the additional phenol group hanging at the δ-position (2-PhPDHL) does not affect thermodynamics of polymerizations.

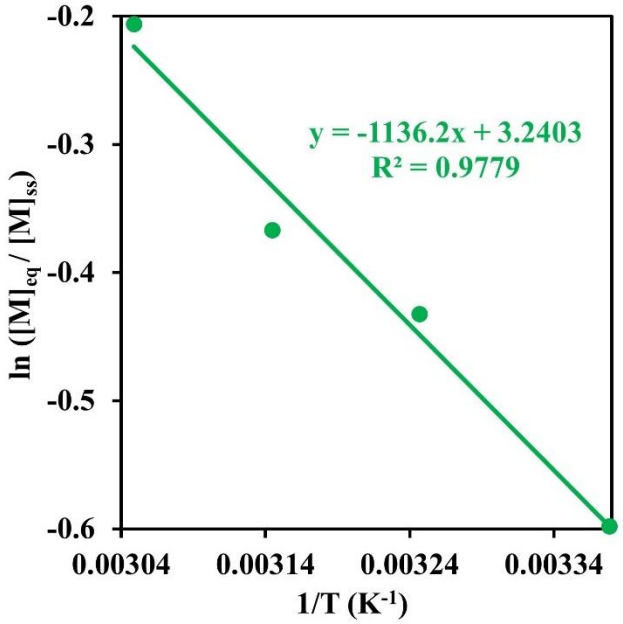

Figure 3.15. Van't Hoff analysis for poly(2-PhPDHL) (green circle).

3.3.6 Kinetics of polymerization

Characteristics of a living chain-growth polymerization include the first-order kinetics in monomer concentration and a linear relationship between molecular weight and monomer conversion.[102] Deviations from the linear dependence are attributed to the presence of slow initiation or side reactions such as chain transfer and termination reactions. The controlled/living characteristic of ROP can be confirmed by the kinetics experiments.

The polymerization kinetics were analyzed for 2-PhPDHL monomer under optimal catalyst loadings and polymerization conditions determined above, which demonstrated equilibrium polymerization as evidenced by plateauing conversion (Figure 3.16a). The polymerization rate is faster than PDHL due to higher catalyst loading but still slower than unsubstituted DVL[48] due to steric hindrance or a decrease in ring strain by the substituents on the lactone monomers.

Schneiderman et al. found six-membered lactone polymerization followed pseudo zero-order kinetics when conducted in the bulk[98] and followed first-order kinetics while conducted in dilute conditions.[98,101,100] A semilogarithmic plot of monomer conversion as a function of reaction time for 2-PhPDHL was linear. It indicates 2-PhPDHL polymerization is first-order with respect to monomer concentration (Figure 3.16b). Martello et al. also reported that similar TBD-catalyzed δ-decalactone polymerization followed first order kinetics.[103] The inclusion of another aromatic group at δ-position does not affect the rate law of polymerization.[104]

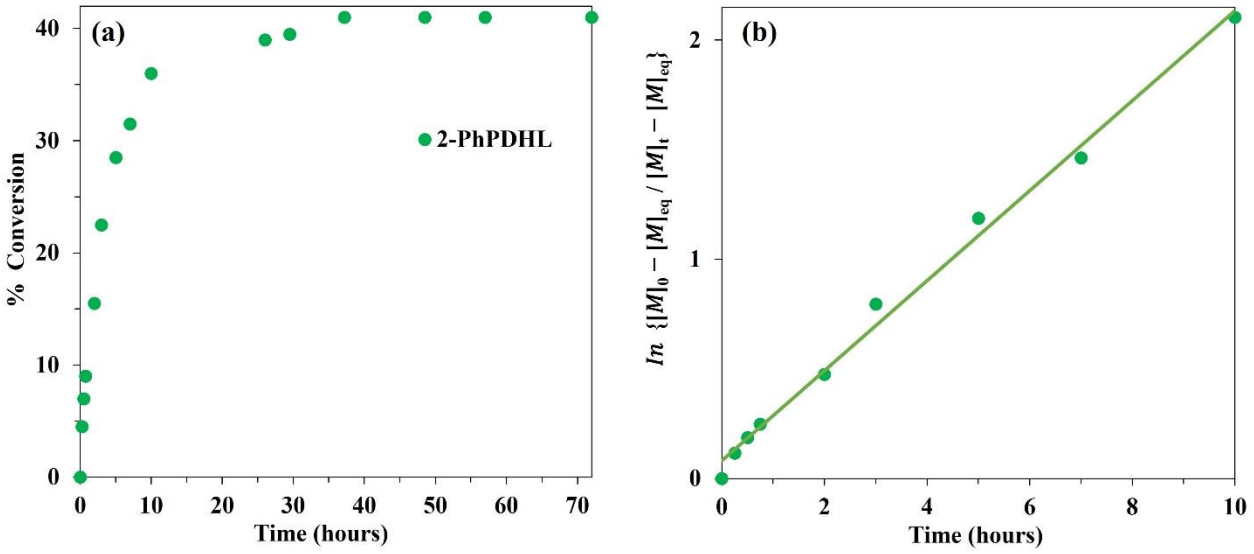

Figure 3.16. a) Monomer conversion as a function of time for poly(2-PhPDHL); b) Linearized kinetics behavior for ROP of 2-PhPDHL (green circle) before reaching equilibrium where $[M]_{eq}$ is the equilibrium monomer concentration, $[M]_0$ is the initial monomer concentration, $[M]_t$ is the monomer concentration at given a time.

A controlled polymerization reaction would show a linear increase of molecular weight throughout the polymerization reaction until it reaches equilibrium. The molecular weight of poly(2-PhPDHL) linearly increased as a function of monomer conversion and the dispersity values ranged from 1.1

to 1.42 (Figure 3.17). This behavior is expected for controlled ROP where all chains are initiated at the same time and then propagate simultaneously. The polymerization kinetics and time-dependent evolution of molecular weight for 2-PhPDHL indicate that it follows controlled polymerization behavior under these conditions.

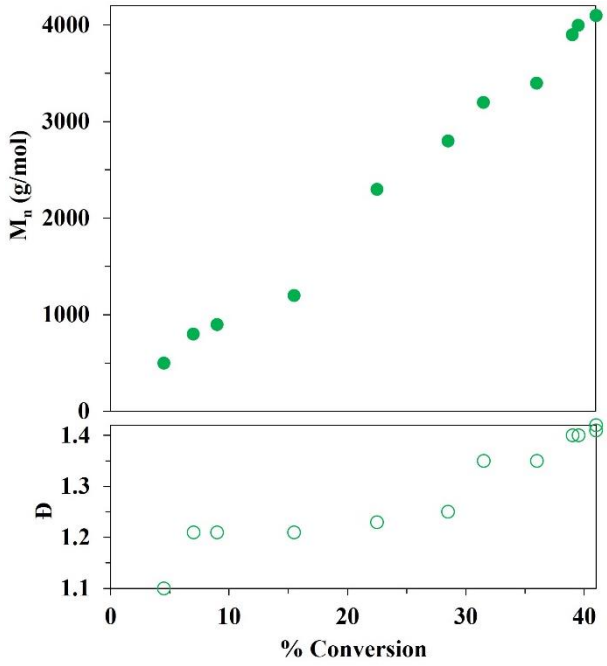

Figure 3.17. Number average molecular weight (M_n) and dispersity (Đ) as a function of monomer conversion for poly(2-PhPDHL). Both M_n and Đ measured by SEC. Ratios of $[M]_0/[I] = 50/1$ for poly(2-PhPDHL) used throughout this study.

3.4 Conclusions

The optimum conditions for the polymerization of 2-PhPDHL showed a higher catalyst loading was necessary for the polymerization as compared to PDHL. Higher (10 times higher than PDHL: 3 mol% or 33 mM minimum at the same conditions and monomer concentration) TBD catalyst loading was needed to get higher conversion in the polymerization reaction due to more sterically

hindered pendant group and the slower secondary alcohol propagating chain end. TBD catalyst can act as an initiator to initiate and propagate the polymerization.

At lower $[M]_0/[I]$ ratios, the polymerizations of 2-PhPDHL delivered the expected molecular weight of polymers. But at higher $[M]_0/[I]$ ratios, lower MW polymers than expected was found due to the role of the TBD catalyst as an initiator. Similar behavior was not observed for PDHL monomer due to the low catalyst loading was needed for the polymerization. Like PDHL monomer, 2-PhPDHL polymerization follows first-order kinetics with respect to monomer concentration and showed a linear increase of molecular weight throughout the polymerization reaction until reached equilibrium.

The most significant change we observed by moving from one phenol group (PDHL) to two phenyl groups (2-PhPDHL) monomeric system is in their glass transition temperature (T_g). A significant increase in T_g was observed for poly(2-PhPDHL) due to the presence of a bulkier pendant group than poly(PDHL). We improved the T_g from +6 °C to 39.5 ˚C by introducing an additional phenyl group at the pendant position. Further increase in T_g (up to 46.5 ˚C) is possible by getting higher MW poly(2-PhPDHL).

CHAPTER 4

SYNTHESIS AND RING OPENING POLYMERIZATION OF 6-((NAPHTHALEN-1-YLOXY)METHYL)OXAN-2-ONE (NDHL)

4.1 Introduction

In the previous studies in chapters 2 and 3, six-membered lactone monomers bearing one (PDHL) and two phenyl (2-PhPDHL) groups at the δ-position were synthesized and their polymerization conditions were described. The glass transition temperatures (T_gs) were increased from -65 to +39.5 °C by introducing these aromatic rings compared to its unsubstituted six-membered polyDVL. For the 2-PhPDHL monomer, two aromatic rings were attached by a C-C bond at the δ-pendant position. More sterically hindered two fused aromatic rings as a pendant group of the polymer can be introduced (Figure 1). Zuniga et al. estimated two fused aromatic rings like 1-naphthol would increase the T_g close to the value of 60 °C by introducing it as a pendant group of the polymer.[105] Two-fused aromatic naphthyl rings was introduced at the δ-position by synthesizing a new NDHL monomer (Figure 4.1) and it was polymerized using ROP technique. Finally, full thermodynamics and kinetics studies were conducted for the new monomer and polymeric system.

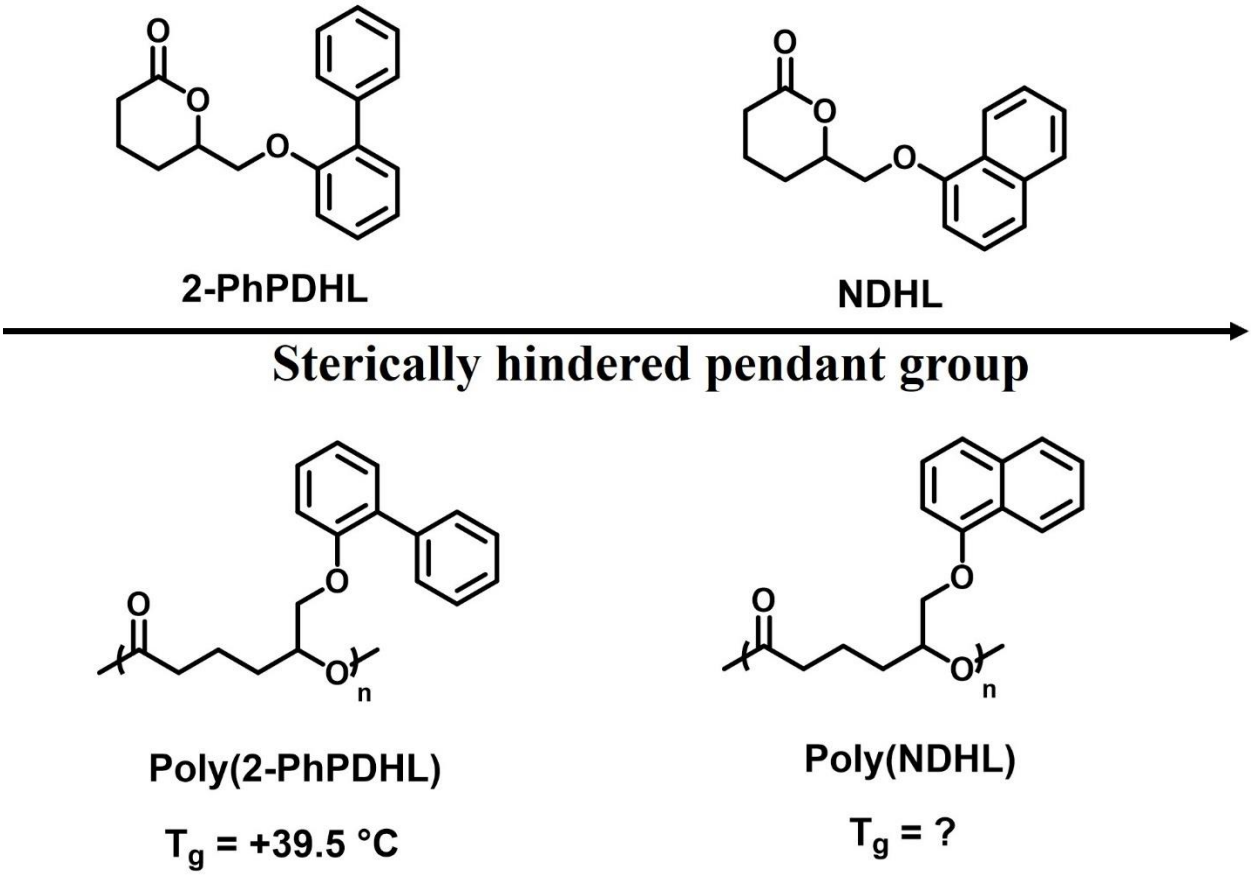

Figure 4.1. Introducing more sterically hindered pendant group at δ-position of the six-membered lactone monomers to get higher T_g polyesters

Two six-membered lactone monomers bearing different phenolic groups (PDHL and 2-PhPDHL) at δ-position were synthesized from commercially available methyl cyclopentanone-2-carboxylate in the previous chapters. As we showed earlier, ketone mesylate (3) worked as an intermediate to attach new bulky pendant groups. Mesylate acts as a leaving group in the Williamson ether synthesis reaction and nucleophilic attack by the deprotonated 1-naphthol will yield an ether linkage at the δ-position. A new six-membered lactone monomer bearing naphthol group (NDHL) was synthesized by following deprotection and Baeyer-Villiger oxidation reactions in the next

steps (Figure 4.2). The NDHL monomer was successfully polymerized using basic TBD catalyst system in the presence of BnOH as initiator in 1,4-dioxene solvent.

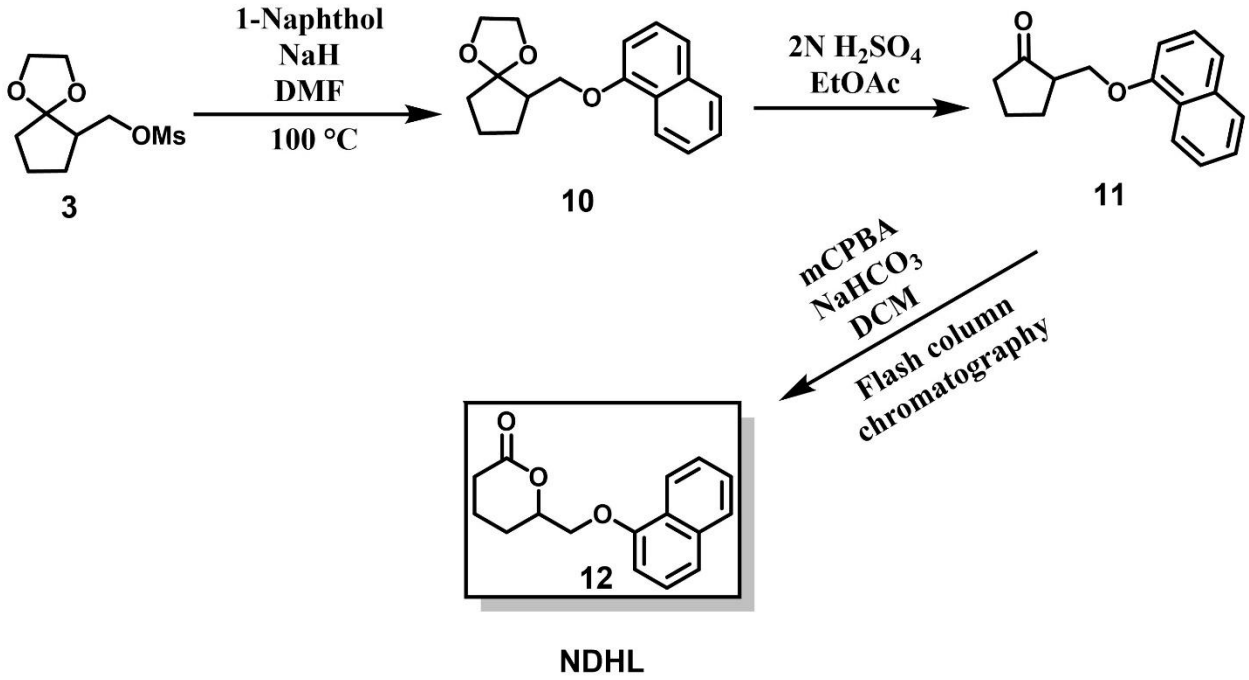

Figure 4.2. Reaction scheme for NDHL monomer synthesis

4.2 Materials and methods

Reagents, including methyl cyclopentanone-2-carboxylate (TCI), p-toluenesulfonic acid (Acros), lithium aluminum hydride (Aldrich), potassium sodium tartrate tetrahydrate (Aldrich), sodium hydride (Acros), methanesulfonyl chloride (Fisher), 1-naphthol (Aldrich), potassium hydroxide (Aldrich), 3-chloroperoxybenzoic acid (Acros), sodium bicarbonate (Fischer), TBD: 1,5,7-triazabicyclo[4.4.0]dec-5-ene (Fisher), benzyl alcohol (Aldrich), 1,4-dioxane (extra dry) (Acros), dichloromethane (anhydrous) (Acros), and N,N-dimethylformamide (anhydrous) (Aldrich) were used as received. All the other solvents and reagents were used as received from commercial suppliers without further purification unless stated otherwise.

4.2.1 Synthesis of 6-((naphthalen-1-yloxy)methyl)-1,4-dioxaspiro[4.4]nonane (10)

NaH (3.45 g, 60% dispersion in mineral oil) was washed with THF (3 x 10 mL) in a 500 mL round-bottom flask to remove the mineral oil, and then the NaH was suspended in DMF (20 mL) solvent. 1-Naphthol (6.64 g or 0.046 mol in 20 mL DMF) solution was added dropwise into the NaH suspension under an ice bath and stirred for 30 min at room temperature to deprotonate the 1-naphthol. After deprotonation, the round-bottom flask was sealed with a septum, flushed with N_2, and connected to a bubbler. **3** (6.8 g, 0.0288 mol) was added to the mixture using a plastic syringe and placed in a 100 °C preheated oil bath and stirred for 20 h. After the reaction time, the round-bottom flask was removed from the oil bath and excess NaH was quenched by adding deionized water (100 mL). The mixture was extracted with ethyl acetate (3 x 50 mL) and washed with 5 M KOH solution two times (2 x 100 mL). The organic layer was dried over Na_2SO_4 and removed on a rotary evaporator to give **7** (4.1 g, 50% yield).

^{1}H NMR (Chloroform-*d*) δ (ppm): 8.27 (m, 1H), 7.79 (m, 1H), 7.41 - 7.27 (m, 4H), 6.84 (m, 1H), 4.27 (m, 1H), 4.06 – 3.92 (m, 5H), 2.66 (m, 1H), 2.15 (m, 1H), 1.93 - 1.67 (m, 5H).

4.2.2 Synthesis of 2-((naphthalen-1-yloxy)methyl)cyclopentanone (11)

In this synthesis, a 2N H_2SO_4 (40 mL, 0.4 mol) solution was added into a mixture of **10** (4.1 g**,** 0.0144 mol) in ethyl acetate (40 mL) solvent and stirred overnight at room temperature. Brine solution (50 mL) was poured into the mixture the next morning and extracted with ethyl acetate (3 x 50 mL). The extracted organic layer was dried over Na_2SO_4 and removed on a rotary evaporator to give **11** (2.25 g, 65% yield).

^{1}H NMR (Chloroform-*d*) δ (ppm): 8.16 (m, 1H), 7.8 (m, 1H), 7.5 - 7.27 (m, 4H), 6.85 (m, 1H), 4.37 (dd, *J* = 9.25 Hz, 3.75 Hz, 1H), 4.33 (dd, *J* = 9.25 Hz, 6.2 Hz, 1H), 2.69 (m, 1H), 2.44 (m, 2H), 2.31 - 1.94 (m, 4H).

4.2.3 Synthesis of 6-((naphthalen-1-yloxy)methyl)oxan-2-one (12)

In this synthesis, 3-chloroperoxybenzoic acid (mCPBA, 70%) (10.4 g, 0.06 mol) and sodium bicarbonate (3.54 g, 0.042 mol) were added to dichloromethane (150 mL) and stirred for 15 mins at room temperature. **11** (2.25 g, 0.0094 mol) was added into the mixture and stirred overnight. After the reaction time, extra dichloromethane (50 mL) solvent was added to the reaction mixture. The organic layer was washed with saturated Na_2SO_3 (20 mL), saturated $NaHCO_3$ (50 mL), then brine solution (20 mL), and separated. The organic layer was dried over anhydrous Na_2SO_4 and removed on a rotary evaporator to get the crude product (δ-substituted 84% major and α-substituted 16% minor product). The resulting solid was purified via silica gel flash column chromatography using 70:30 hexane:ethyl acetate mobile phase. After running flash column chromatography, 1.3 g of pure NDHL (**12**) was collected at a 40% yield.

^{1}H NMR (Chloroform-*d*) δ (ppm): 8.22 (m, 1H), 7.81 (m, 1H), 7.47 - 7.37 (m, 4H), 6.8 (m, 1H), 4.8 (m, 1H) 4.31 (dd, *J* = 9.9 Hz, 4.55 Hz, 1H), 4.26 (dd, *J* = 9.9 Hz, 5.35 Hz, 1H), 2.68 (m, 1H), 2.6 (m, 1H), 2.2 - 1.94 (m, 4H). ^{13}C NMR (Chloroform-*d*) δ (ppm): 169.81, 152.94, 133.52, 126.5, 125.53, 124.36, 120.82, 119.99, 103.9, 77.16, 68.61, 28.77, 24.02, 17.37.

4.2.4 Polymerization materials and methods

Vials and magnetic stir bars used for polymerization reactions were dried in an oven at 100 °C overnight before use. The NDHL monomer was dried overnight before use in the room temperature

vacuum oven. TBD was dried overnight in the antechamber of a nitrogen glovebox and kept in the glovebox under nitrogen after received. Vials, caps, syringes, spatulas and all other materials used to set up polymerization reactions were dried in the antechamber of the glovebox overnight before use.

4.2.5 General polymerization procedure for NDHL

Polymerization of NDHL proceeded as follows. Two different stock solutions of initiator and catalyst were prepared by adding 3 μL benzyl alcohol in 300 μL 1,4-dioxane and 6 mg TBD in 100 μL 1,4-dioxane separately in an N_2 filled glovebox. First, the stock solution of benzyl alcohol (27.5 μL, 0.00394 mmol) and then the stock solution of TBD (91.5 μL, 0.0394 mmol) were added using glass syringes to NDHL monomer (50.5 mg, 0.197 mmol) dissolved in dioxane solvent (5 μL) already in 2 mL vial with a septum. The homogenous mixture was stirred for the desired reaction time at ambient temperature. The polymerization was quenched by adding excess benzoic acid (9 mg, 0.0738 mmol). A typical polymerization led to ca. 65% conversion of NDHL. The inactive catalyst was removed by precipitation of the pure polymer into diethyl ether.

4.2.6 Polymerization kinetics experiments

Polymerization kinetics experiments were carried out at ambient temperature for NDHL monomers. The experiment was conducted using benzyl alcohol (BnOH) as an initiator and TBD as a catalyst. For measurement of the NDHL polymerization kinetics, the stock solution of benzyl alcohol (27.5 μL, 0.00394 mmol) and the stock solution of TBD (91.5 μL, 0.0394 mmol) were added using glass syringes to NDHL monomer (50.5 mg, 0.197 mmol) dissolved in dioxane solvent (5 μL) in 2 mL vial with a septum. The homogenous mixture was stirred until the

polymerization reached equilibrium and aliquots were collected throughout the polymerization. The aliquots were quenched by adding 30 molar excess benzoic acid and monomer conversions were determined using ^{1}H NMR spectroscopy.

For the polymerization kinetics experiments, the $[Monomer]_0$:[Initiator] and $[Monomer]_0$:[Catalyst] ratios were fixed. The polymerization appeared to reach equilibrium, as indicated by a plateau in monomer conversion as a function of time. Pseudo first-order behavior was verified by fitting the kinetics data to Equation 4.1,[106] which describes monomer concentration as a function of time for an equilibrium polymerization:

$$\ln\left(\frac{[M]_0-[M]_{eq}}{[M]_0-[M]_t}\right) = k_{app}t \qquad \text{(Equation 4.1)}$$

where $[M]_{eq}$ is the equilibrium monomer concentration, $[M]_0$ is the initial monomer concentration, $[M]_t$ is the monomer concentration at given a time, and k_{app} is the apparent rate constant.

4.2.7 Polymerization thermodynamics experiments

For the polymerization thermodynamics experiments, the setup was the same as for the kinetics experiments, but the polymerizations were stirred in an oil bath at a range of temperatures. The temperature was varied for NDHL from 20 to 57.5 °C. The polymerizations achieved different equilibrium monomer concentrations ($[M]_{eq}$) at different temperatures. Aliquots were collected after sufficient reaction time to reach equilibrium (typically 12 h for NDHL) and quenched with excess benzoic acid. The polymerization progress was tracked using ^{1}H NMR spectroscopy. To ensure the polymerizations reached equilibrium, the reactions were kept running for at least another 12 h after reaching equilibrium. To estimate enthalpy (ΔH_p) and entropy (ΔS_p) for the

polymerization, the equilibrium monomer concentration was plotted as a function of inverse temperature and fit using a van 't Hoff analysis:

$$\ln\left(\frac{[M]_{eq}}{[M]_{ss}}\right) = \frac{\Delta H_p}{RT} - \frac{\Delta S_p}{R} \qquad \text{(Equation 4.2)}$$

where T is the polymerization temperature, R is the ideal gas constant, and $[M]_{ss}$ is a standard state monomer concentration that was set to 1 M.

4.2.8 Analysis of polymer products

^{1}H NMR and ^{13}C NMR spectra were obtained either using Varian Inova 400 MHz and Bruker Avance NEO 500 MHz NMR spectrometers using $CDCl_3$ as a solvent. Size exclusion chromatography (SEC) was conducted in dimethylformamide (DMF) containing 0.5 wt% LiBr as the mobile phase with a flow rate of 1 mL min^{-1} at 70 °C. SEC analysis was performed by three Phenogel columns (Phenomenex) in series with different pore sizes (50, 10^3, and 10^6 Å), using a refractive index detector and calibration curves from linear polystyrene standards.

The crude polymer was dissolved in dichloromethane and precipitated in cold diethyl ether (1:5). The purified polymers were dried in a vacuum oven. The T_g of different polymers was measured using a differential scanning calorimeter (DSC, TA Instruments DSC2500) at a rate of 10 °C min^{-1} over a range from -90 to 100 °C using ~1.5 mg sample in a heat/cool/heat experiment under an N_2 atmosphere. The T_g were reported from the second heating cycle and analyzed with TA TRIOS software (v5.0.0).

4.3 Results and discussion

The powerful base sodium hydride (NaH) was used to deprotonate the 1-naphthol in DMF solvent. The naphthalen-1-olate anion was stable and worked as a nucleophile in the presence of the mesylate leaving group. Successful etherification was confirmed by the disappearance of the mesylate methyl singlet at 3 ppm. The protons next to the ether linkage were shielded more which confirmed further successful etherification (Figure 4.3). Excess 1-naphthol was removed from the reaction medium by washing with 5M KOH solution.

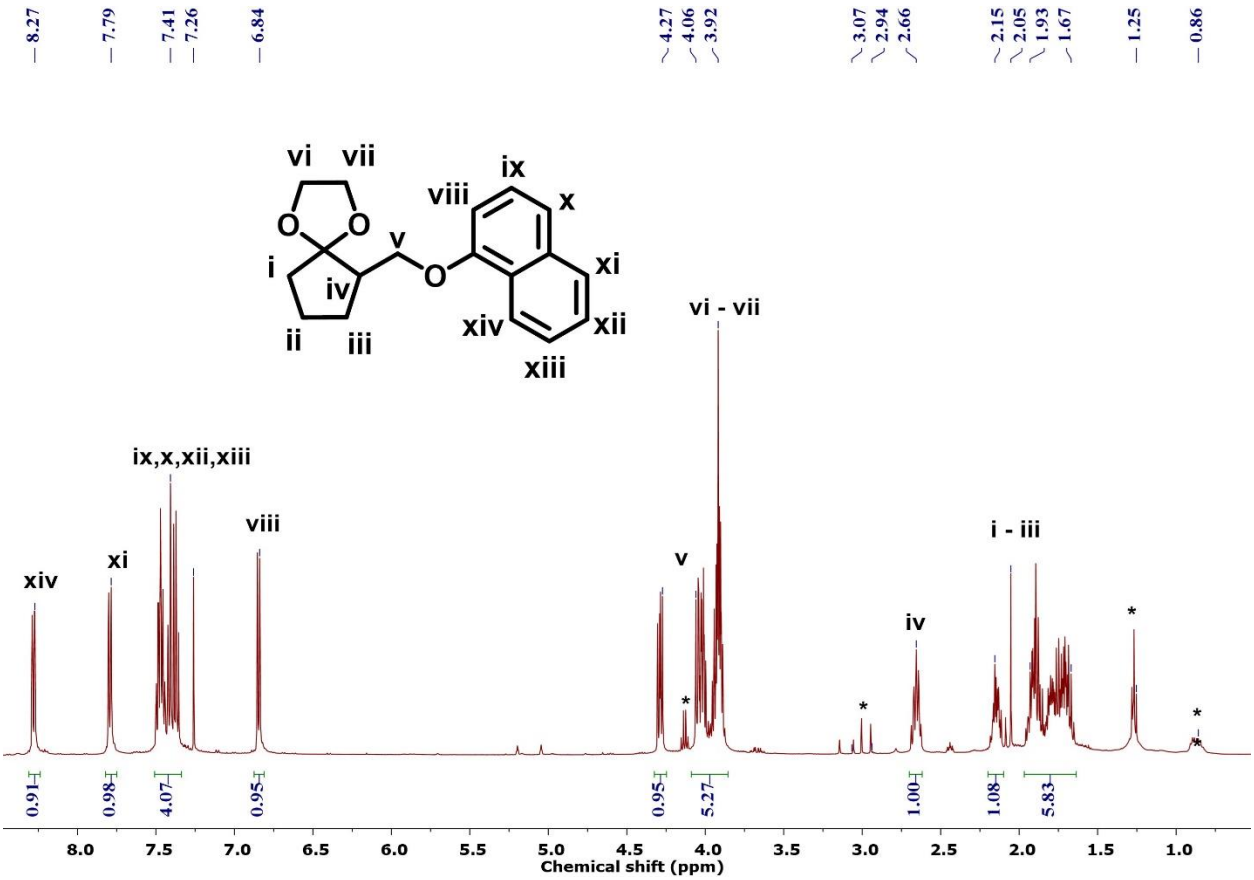

Figure 4.3. ^{1}H NMR spectrum of 6-((naphthalen-1-yloxy)methyl)-1,4-dioxaspiro[4.4]nonane (10). *Mineral oil from NaH washing step, DMF, and ethyl acetate solvents

Removal of acid-labile acetal protecting group was done once the nucleophilic substitution was completed. The protecting acetal group was removed in the next step in the presence of an acidic solution. Sulfuric acid (1 M) was used to remove the acetal group. The removal of the acetal group was confirmed by the disappearance of peaks at 3.92 ppm (Figure 4.4). The protons next to ether linkage were affected mostly due to the removal of the acetal group and those protons showed a de-shielding effect in the ^{1}H NMR spectrum (shifted from 4.06 and 4.27 ppm to 4.33 and 4.37 ppm, respectively).

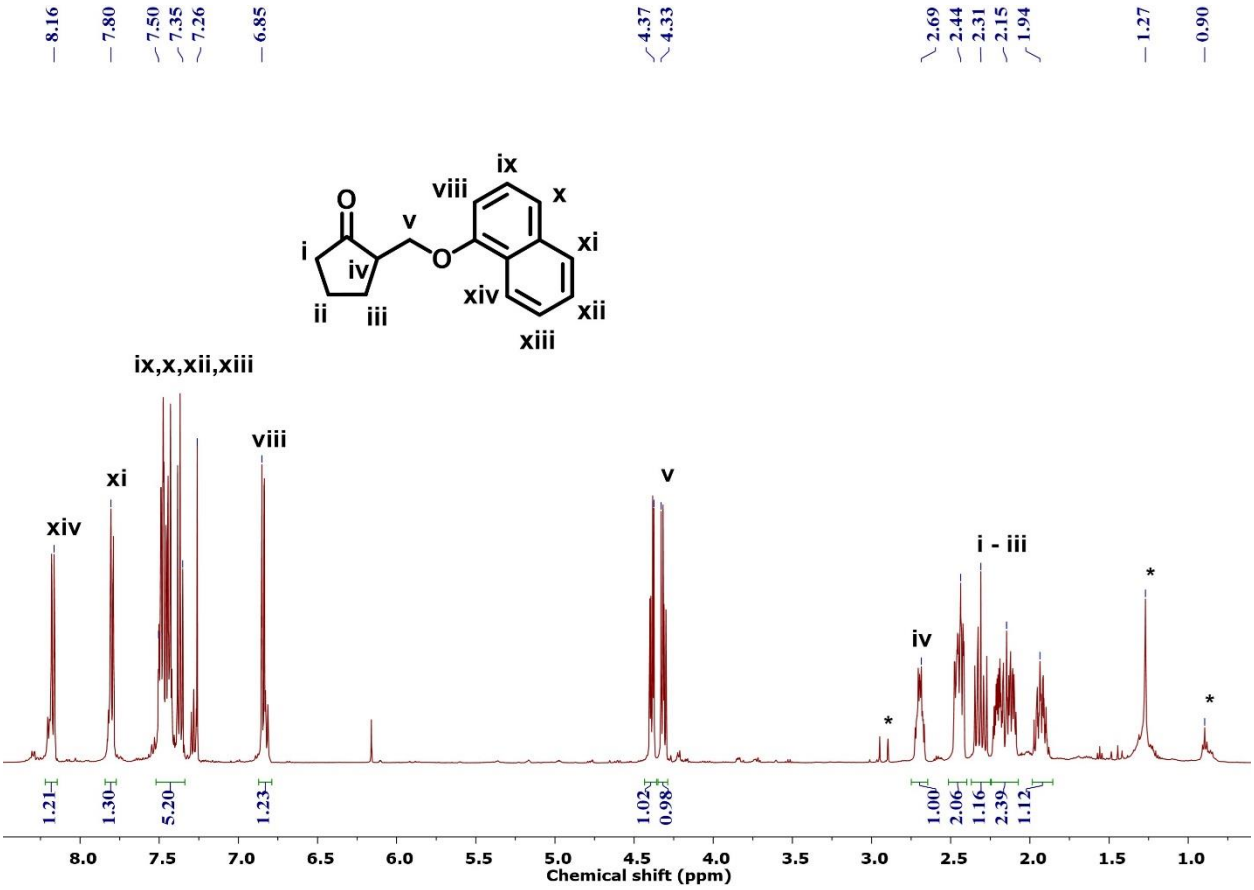

Figure 4.4. ^{1}H NMR spectrum of 2-((naphthalen-1-yloxy)methyl)cyclopentanone (11)

. *Mineral oil and DMF solvent

A Baeyer-Villiger oxidation reaction was used to synthesize six membered lactones from the five-membered cyclic ketones. 3-Chloroperoxybenzoic acid (mCPBA) was used as a peroxyacid source. Excess mCPBA was needed to get full conversion due to the presence of more sterically hindered naphthol group (Table 4.1). Both α-substituted and δ-substituted products were observed in the ^{1}H NMR spectrum due to the unsymmetrical cyclic ketone. The δ-substituted product (84%) was the major product in the synthesis due to the higher migratory aptitude of the tertiary alkyl group over the secondary alkyl group. The peak of protons next to the ester group confirmed the successful six-membered lactone synthesis at 4.79 ppm for the major product (Figure 4.5). After this step, a mixture of major and minor products was obtained in the presence of 3-chlorobenzoic acid as a by-product. For ROP and controlled polymerizations, pure NDHL was separated. Flash column chromatography was used to separate the pure NDHL monomer. Pure NDHL was separated successfully by using more non-polar hexane solvent. A 70:30 hexane and ethyl acetate mixture was used as a mobile phase. The products were tracked by thin layer chromatography (R_f = 0.31 for δ-substituted product and R_f = 0.47 for α-substituted product) primarily. The pure NDHL was confirmed by both ^{1}H and ^{13}C NMR spectroscopy (Figure 4.6-4.7).

Table 4.1. Amounts of 3-chloroperoxybenzoic acid (mCPBA) needed for successful (100% conversion) Baeyer-Villiger oxidation reaction

Monomers	**mCPBA (molar excess)**
PDHL	1.5
2-PhPDHL	1.5
NDHL	4.5

It was difficult to synthesize NDHL monomer as compared to the 2-PhPDHL monomer due to the presence of a more reactive hydroxyl group. Removing excess 1-naphthol from the Williamson ether synthesis reaction step was necessary to get full conversion in the next step. Separating pure NDHL was similar to 2-PhPDHL during the flash column chromatography. Excess 10% $NaHCO_3$ solution was used to get rid of excess 3-chlorobenzoic acid by-products from the reaction mixture before running the column..

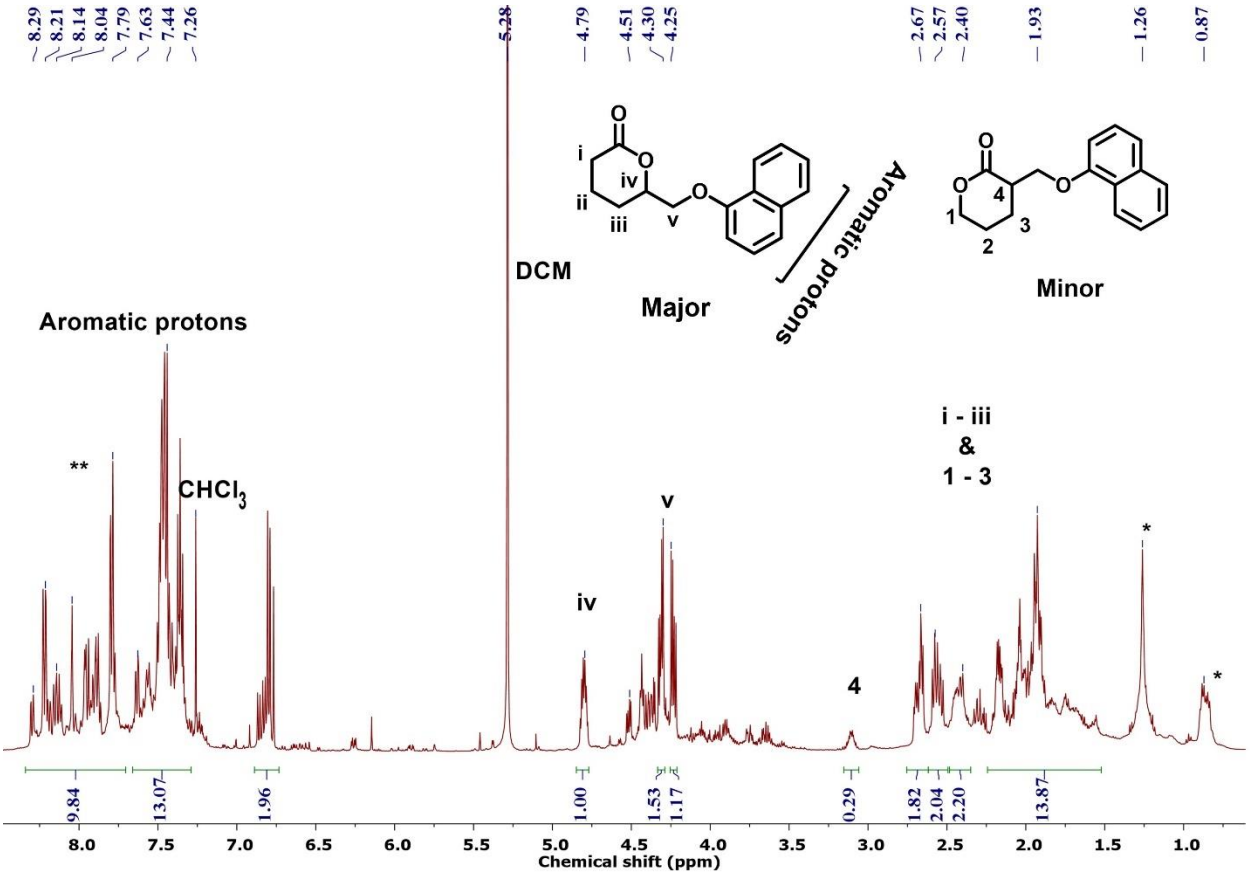

Figure 4.5. ^{1}H NMR spectrum of a crude mixture of 6-((naphthalen-1-yloxy)methyl)oxan-2-one (12), *Mineral oils, **3-Chlorobenzoic acid.

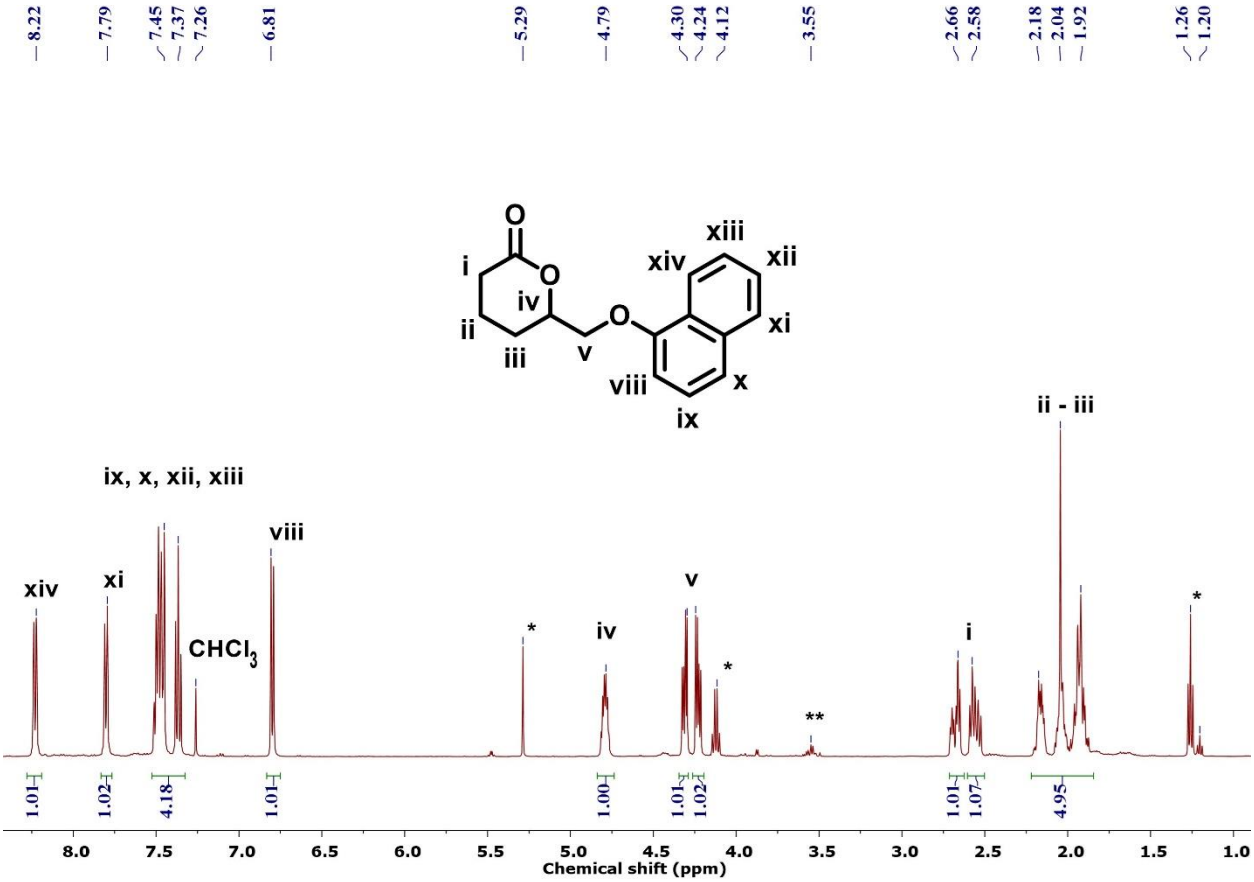

Figure 4.6. ^{1}H NMR spectrum of pure 6-((naphthalen-1-yloxy)methyl)oxan-2-one (12), collected after flash column chromatography. *Ethyl acetate and DCM solvents, **impurities

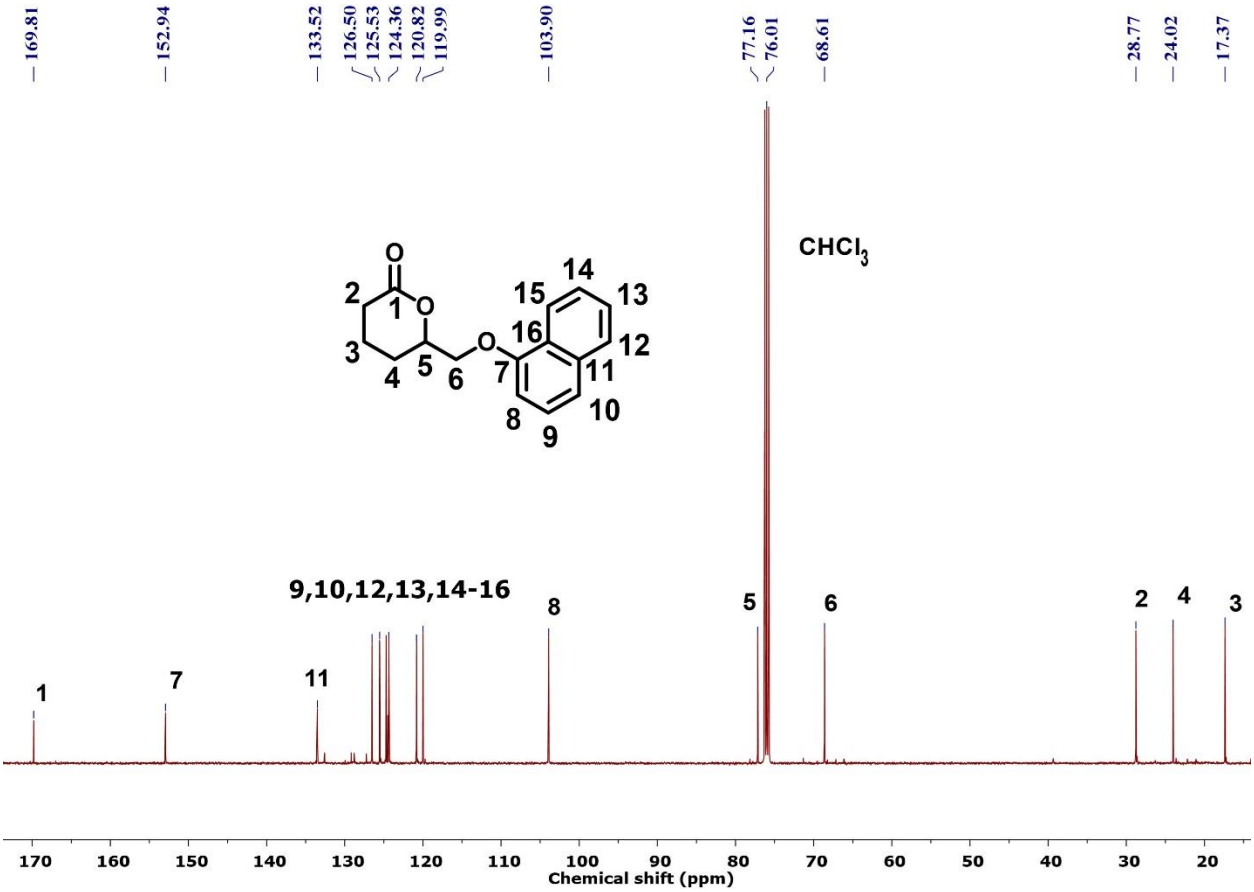

Figure 4.7. ^{13}C NMR spectrum of pure 6-((naphthalen-1-yloxy)methyl)oxan-2-one (12).

4.3.1 Ring-opening polymerization of NDHL lactone

Finding the optimum conditions for the polymerization reaction are necessary for the new bulkier NDHL monomeric system. The objectives of the optimization reactions were to obtain a higher conversion, to find a catalytic system for polymerizing the new monomer in a controlled manner, and to get high molecular weight polymers. The general scheme for the ring opening polymerization of 2-PhPDHL is shown in Figure 4.8 below.

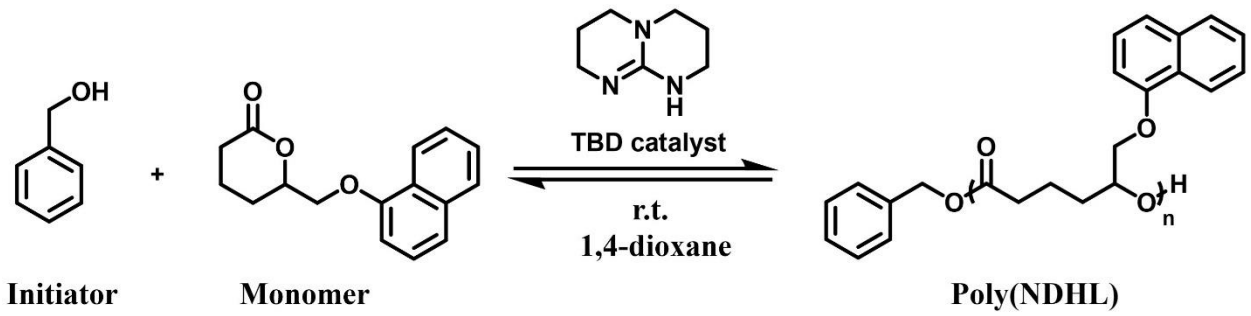

Figure 4.8. Polymerization scheme for the ring-opening polymerization of NDHL

Initially, the NDHL monomer was polymerized at room temperature using benzyl alcohol (BnOH) as the initiator and basic TBD (3 mol%) as a catalyst in 1,4-dioxane while keeping the initial monomer concentration at $[M]_0$ = 1.1 M. The initiator initiated the polymerization successfully, but no propagation was observed in the ^{1}H NMR spectrum. The conversion was less than 5% until 20 mol% catalyst (based on monomer moles) was used. A minimum of 20 mol% (220 mM) TBD was needed to achieve higher conversion in the polymerization of NDHL (Table 4.2). Similar behavior was found for polymerizing 2-PhPDHL also in Chapter 3 using TBD as a catalyst but higher catalyst loading was necessary for NDHL monomer due to the presence of more sterically hindered naphthol group at δ-position and trace amount of impurities still present after purification. A primary alcohol (like BnOH) can initiate the polymerization instantaneously, but the secondary alcohol of propagating chain end is a slow initiator for the upcoming monomer.[107] So, excess TBD is needed to activate the monomer to push the propagation reaction forward as similar behavior was observed for 2-PhPDHL monomer in Chapter 3. Higher catalyst loadings may favor reaching equilibrium monomer concentration faster or nucleophilic mechanism over acid-base mechanism and lead to broader dispersity.[108]

Table 4.2. Effect of TBD catalyst loadings for ROP of NDHL

Catalyst (mol%)[a]	**Catalyst (mM)[b]**	**%Conversion[c]**
3	33	<5%
5	55	<5%
10	110	<5%
15	165	<5%
20	220	65%

[a]Based-on monomer moles; [b]Calculated by the moles of the catalyst over total volume; [c]Conversion measured by ^{1}H NMR spectroscopy. Ratios of $[M]_0/[I]$ = 50/1 for the polymerization used throughout this study where initial monomer concentration, $[M]_0$ = 1.1 M

4.3.2 Controlling the molecular weight of poly(NDHL)

The NDHL monomer was polymerized at room temperature using benzyl alcohol (BnOH) as the initiator and TBD as a catalyst. The conversion was tracked by taking aliquots from the reaction and analyzing them using ^{1}H NMR spectroscopy (Figure 4.9). The methylene protons of the BnOH initiator shifted from 4.7 to 5.09 ppm, confirming that the monomer was initiated by BnOH. The methine protons of NDHL (4.55 ppm) shifted to 5.27 ppm, corresponding to the lactone ring opening and the successful polymerization.

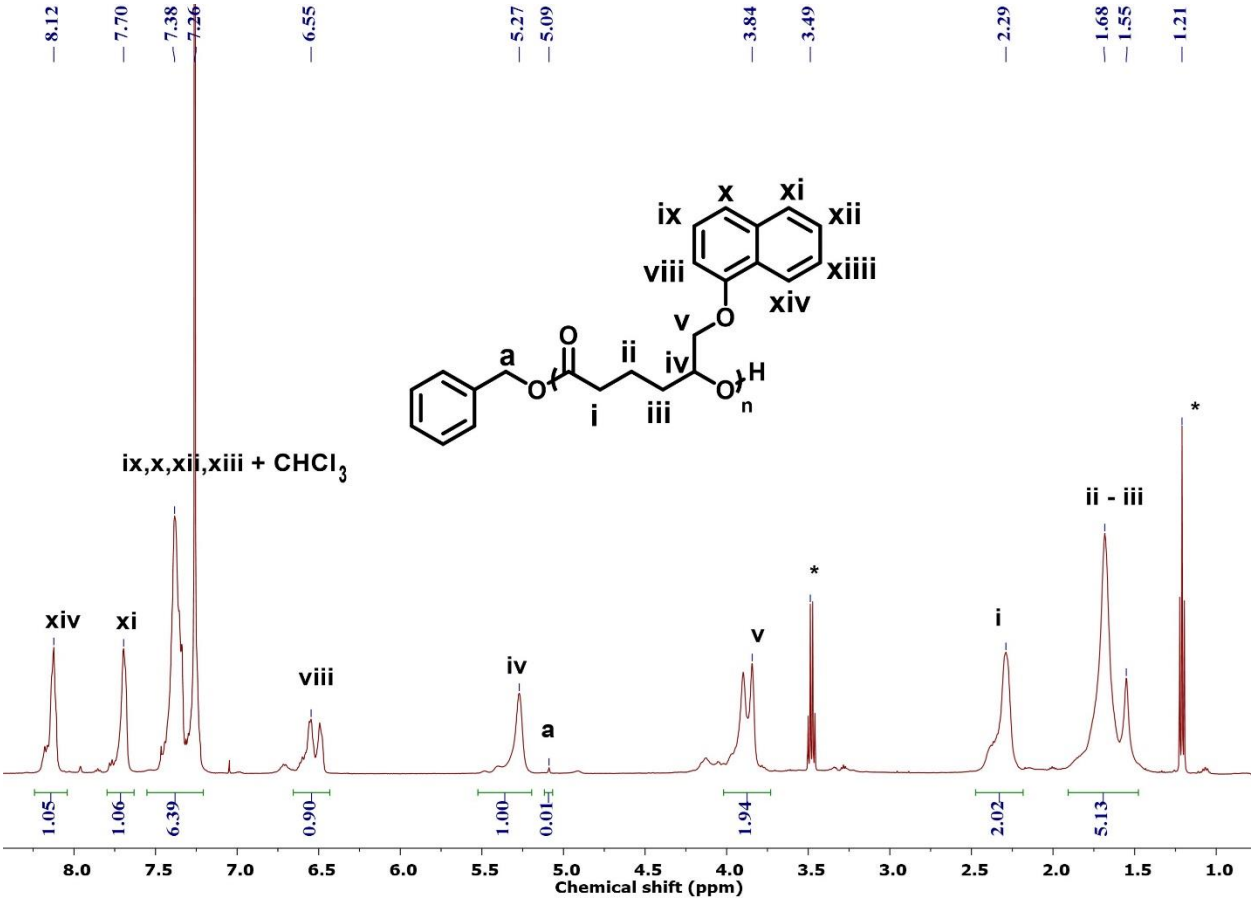

Figure 4.9. ^{1}H NMR spectrum of precipitated poly(NDHL). ^{1}H NMR spectrum was collected after the polymerization reached equilibrium on day three. (*Diethyl ether solvent)

Table 4.3 summarizes the results obtained from different polymerizations. As mentioned above, the minimum 20 mol% TBD catalyst (220 mM) was needed to get the higher conversion for the polymerization of NDHL. The equilibrium monomer conversion of NDHL was about 65%. The molar mass distributions were unimodal for all the polymers (Figure 4.10), which indicated limited backbiting occurred prior to equilibrium.

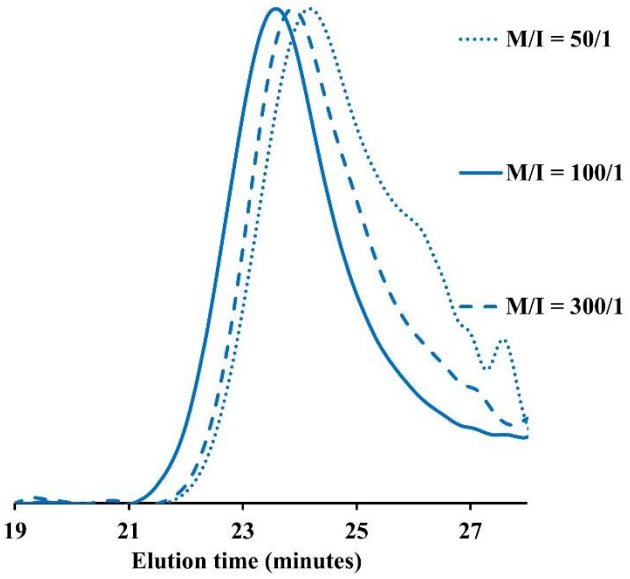

Figure 4.10. SEC elution curves for ROP of NDHL after reaching equilibrium conversion at different $[M]_0/[I]$ ratios. Molecular weights ($M_{n,\ SEC}$) and dispersity are in Table 4.3.

The experimental M_n values from size exclusion chromatography (SEC) differed from the calculated expected values. Unlike 2-PhPDHL, the $M_{n,SEC}$ of poly(NDHLs) differed from the expected values at lower $[M]_0/[I]$ ratios as well (Table 4.3, entries 1-2). The $M_{n,SEC}$ values should increase by increasing $[M]_0/[I]$ for poly(NDHL). However, the $M_{n,SEC}$ value still deviated significantly from the $M_{n,\ expected}$ value while we increased the $[M]_0/[I]$ ratio from 100 to 300 (Table 4.3, entry 3). Though size exclusion chromatographic technique cannot deliver actual MW of the polymers due to the calibration of the RI detector with polystyrene (PS) standards, a nearly three-fold increase in the $M_{n,sec}$ values were expected while changing the $[M]_0/[I]$ ratio from 100 to 300. It suggests a failure in the controlled polymerization. Broader dispersities were expected due to the higher catalyst loading as we mentioned in the 2-PhPDHL monomer section in Chapter 3 (Table 4.3, entries 1-3). Besides acting as a catalyst, TBD can initiate ROP process as shown in Chapter 3 for 2-PhPDHL monomer. It can be hypothesized that TBD initiated the polymerization

of NDHL with the BnOH at the same time (TBD initiation peaks were observed in Figure 4.9) and yielded low molecular weight polymers . One additional polymerization was carried out without the BnOH initiator, and NDHL monomer was polymerized successfully by only TBD catalyst (Table 4.3, entry 4). The proton peaks at 3.25 ppm and 3.32 ppm confirmed that TBD initiated the polymerization (Figure 4.11). The origin of low molecular weight was investigated further by the end group analysis. The end group analysis was done by using ^{1}H NMR spectrum of precipitated polyNDHL. Table 4.4 showed two different expected molecular weight values based on BnOH and TBD initiated polymerization. For $[M]/[I]_0$ ratio of 300/1 experiment, both BnOH and TBD initiation peaks were observed (Figure 4.9). The $M_{n,\,SEC}$ value did not match with the BnOH initiated $M_{n,\,BnOH}$ or TBD initiated $M_{n,\,TBD}$ values (Table 4.4, entry 1). Both initiated the polymerization and lowered the average molecular weight of polymer but further end group studies by matrix assisted laser desorption/ionization (MALDI) are needed to confirm the origin of this low molecular weight. For $[M]/[I]_0$ ratio of 100/0 experiment (without any BnOH initiator), only TBD initiation peaks were observed (Figure 4.11). The $M_{n,\,SEC}$ value closely matched with the TBD initiated $M_{n,\,TBD}$ value (Table 4.4, entry 2). So, TBD initiated the polymerization without any BnOH initiator and delivered the expected molecular weight polymer. No other initiation (self-initiation) mechanism was involved during this polymerization.

Table 4.3. Results for TBD catalyzed ROP of NDHL

Monomer	Entry	$[M]_0/[I]/[C]$	Time (days)	Conv.[b] (%)	$M_{n,\ expected}$[c] (kg/ mol)	$M_{n,\ SEC}$[d] (kg/ mol)	Đ[d]
NDHL[a]	1	50/1/10	3	65	8.5	4.0	1.65
	2	100/1/20	3	65	17.0	3.5	1.75
	3	300/1/60	3	63	48.5	2.1	1.9
	4	100/0/20	3	59	-	1.2	2.0

[a]1,4-dioxane as solvent, $[M]_0$ = 1.1 M; where $[M]_0$ = Initial monomer concentration. [b]Fractional conversion measured by ^{1}H NMR spectroscopy. [c]Calculated from $[M]_0/[I]$ × monomer conversion × MW of NDHL. [d]Measured by SEC in DMF with 0.5 wt% LiBr as the mobile phase, using linear polystyrene standards with a refractive index detector.

Table 4.4. Different molecular weights for poly(NDHL) obtained from ^{1}H NMR spectroscopy and SEC technique

Entry	$[M]_0/[I]/[C]$	$M_{n,\ expected}$[a] (kg/ mol)	$M_{n,BnOH}$[b] (kg/ mol)	$M_{n,TBD}$[b] (kg/ mol)	$M_{n,SEC}$[c] (kg/mol)
1	300/1/60	1.2	34.5	9.5	2.1
2	100/0/20	1.2	-	1.5	1.2

[a]Expected molecular weight if only all the TBD catalyst initiated the polymerization. [b]Measured by ^{1}H NMR spectroscopy. [c]Measured by SEC in DMF with 0.5 wt% LiBr as the mobile phase, using linear polystyrene standards with a refractive index detector.

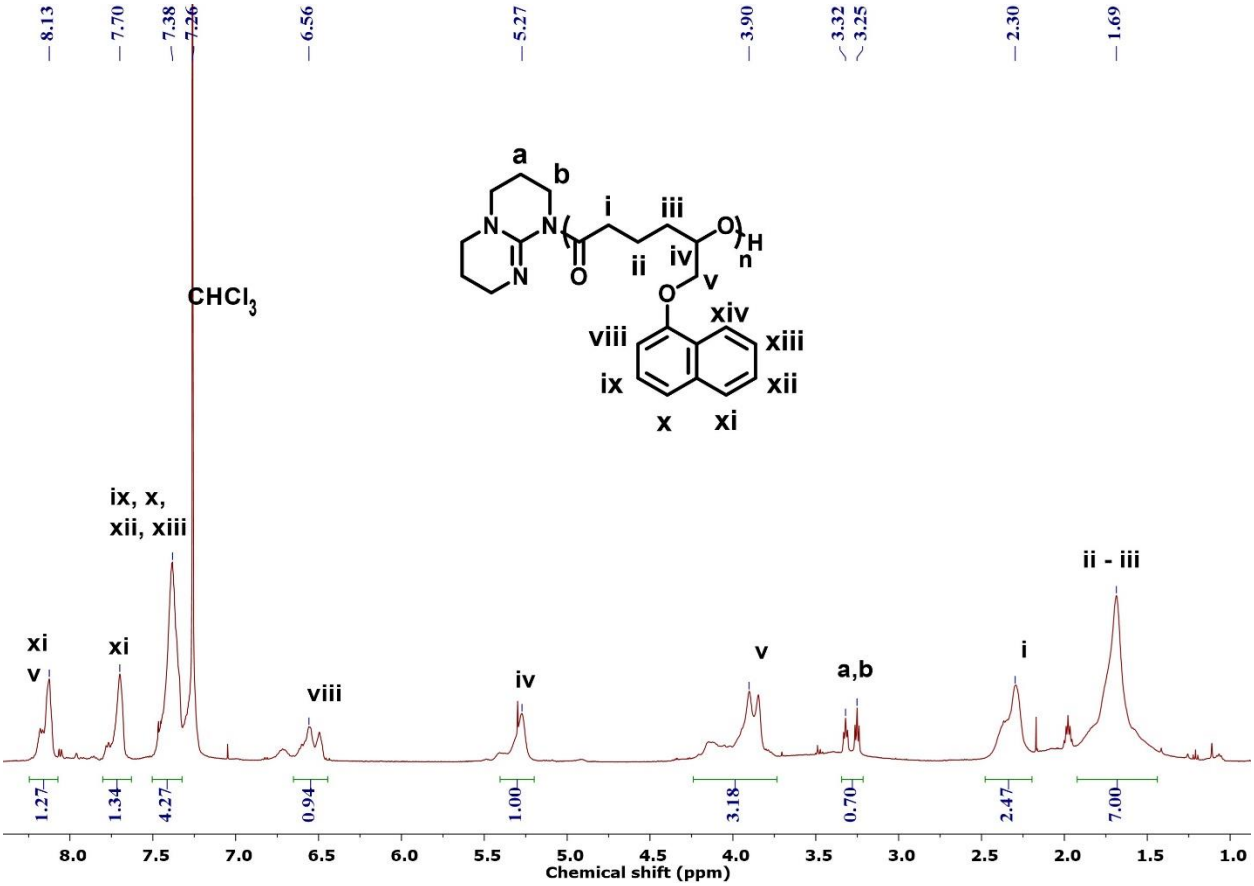

Figure 4.11. ^{1}H NMR spectrum of poly(NDHL) obtained by TBD catalyzed ROP in the absence of BnOH as an initiator (Table 4.3, entry 4)

To overcome the challenges of getting higher MW polymers, super basic phosphazene-based t-BuP_4 was screened as a catalyst to polymerize the NDHL (Figure 4.12). Phosphazene successfully polymerized the PDHL monomer as shown in Chapter 2 in the presence of BnOH initiator. ROP of ε-caprolactone and δ-valerolactone monomers using t-BuP_4 was reported in the literature.[79] For NDHL, t-BuP_4 successfully initiated the polymerization, but no propagation was achieved even at high catalyst loadings (Table 4.5). Steric hindrance of bulky t-BuP_4 might not activate the monomer for further propagation. Less steric t-BuP_2 can be investigated in future for the polymerization of NDHL.[109,110]

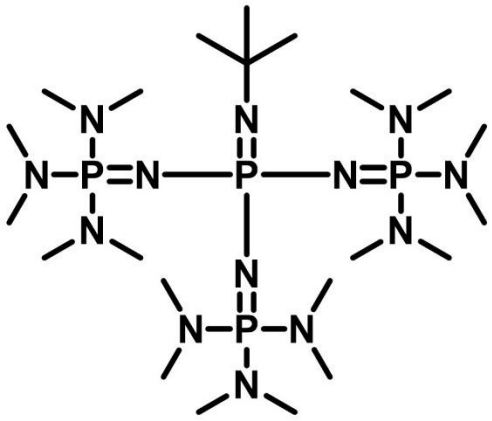

Figure 4.12. t-BuP$_4$ organocatalyst for ROP of lactones

Table 4.5. Effect of t-BuP$_4$ catalyst loadings for ROP of NDHL

Catalyst (mol%)[a]	**%Conversion[c]**
4	<5%
10	<5%
15	<5%
20	<5%

[a]Based-on monomer moles; [c]Conversion measured by ^{1}H NMR spectroscopy. Ratios of $[M]_0/[I]$ = 50/1 for the polymerization used throughout this study where initial monomer concentration, $[M]_0$ = 1.1 M

4.3.3 Glass transition temperature (T_g) of poly(NDHL)

The glass transition temperature (T_g) was measured by DSC from the second heating cycle (Figure 4.13). The unsubstituted six-membered poly(δ-valerolactone) has a T_g of -65 °C [111,112] and seven-membered poly(ε-caprolactone) has a T_g of -60 °C reported in the literature.[113] Introducing one phenol (polyPDHL, 6 °C) and two phenol groups (poly(2-PhPDHL), 39.5 °C) at the δ-position

increased the T_g significantly (Chapter 2 and 3). However, the bulky naphthyl group at the δ-position showed a similar T_g (37 °C) to the poly(2-PhPDHL). The T_g of a polymer depends on the molecular weight and it increases rapidly with increasing molecular weight and plateaus at higher values. The T_g kept increasing with the increase of molecular weight of the poly(NDHL) from 1.0 kg/mol to 3.5 kg/mol (Figure 4.13). Whether the T_g already hit the plateau for polyNDHL could not be tested due to the unavailability of high molecular weight polymers. The T_g was higher comparing to those of all alkyl-substituted poly(δ-valerolactone)s (-52 °C to -50 °C).[114] Additionally, the poly(NDHL) did not crystallize above its T_g due to the racemic mixture, and the catalysts afforded no stereochemical preference.

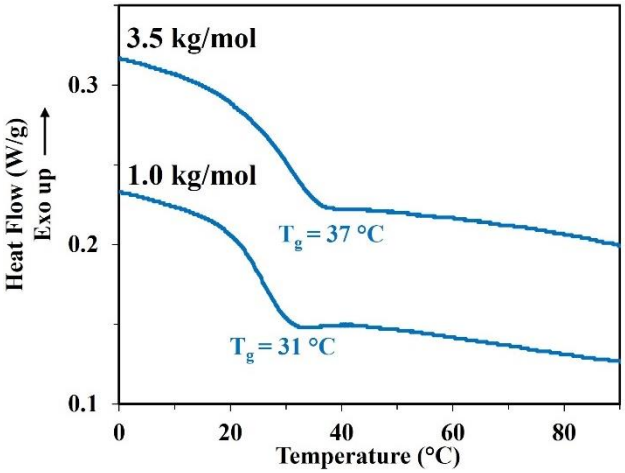

Figure 4.13. DSC thermograms of poly(NDHL). Curves are shifted vertically to provide clarity.

4.3.4 Thermodynamics of polymerization

The polymerizations achieved different equilibrium monomer concentrations ($[M]_{eq}$) at different temperatures and should be independent of the catalyst. Table 4.6 shows the $[M]_{eq}$ values obtained by running the polymerization at different temperatures. The thermodynamics of the ROP was

examined by polymerizing NDHL over a range of temperatures and performing a van't Hoff analysis to calculate the entropy and enthalpy of polymerization and to learn how monomer structure impacts polymerization thermodynamics (Figure 4.14). The enthalpy of polymerization (ΔH_P^o) was -9.8 ± 1.0 kJ mol^{-1} and the entropy of polymerization (ΔS_P^o) was -26 ± 4 J mol^{-1} K^{-1} for NDHL. Both values were close to the PDHL (ΔH_P^o = -9.4 ± 0.7 kJ mol^{-1}, ΔS_P^o = -26 ± 2 J mol^{-1} K^{-1}) and 2-PhPDHL (ΔH_P^o = -9.4 ± 0.9 kJ mol^{-1}, ΔS_P^o = -26 ± 3 J mol^{-1} K^{-1}) monomers, and it suggests attaching another aromatic ring to the group at the δ-position does not impact polymerization thermodynamics. The negative enthalpy of polymerization of a cyclic monomer results mostly from its ring strain.[115] The enthalpy of NDHL is close to the values reported for DVL (ca. -10 kJ mol^{-1}), but slightly lower than the values reported for δ-decalactones (-17.1 ± 0.6 kJ mol^{-1})[116,117] and other alkyl-substituted δ-lactones (-13 to -19 kJ mol^{-1}).[98] The inclusion of an ether linkage in the pendant group appears to decrease the ring strain as compared to the all-carbon pendant group of alkyl-substituted δ-lactones, which may be due to the increased rotational freedom of the ether group. The entropy of NDHL indicates that it is entropically disfavored as compared to DVL (-15 J mol^{-1} K^{-1}). However, the entropic penalty for polymerization is less than that of alkyl-substituted DVLs (ca. -55 J mol^{-1} K^{-1}), which enables the significant conversions observed in spite of the lower ΔH_P^o. Thermodynamically, both polymers showed (2-PhPDHL and NDHL) similar enthalpy values (ΔH_P^o) for polymerizations, and their entropic penalty for polymerizations were also similar. Both polymers reached equilibrium faster and earlier at higher temperatures. So, two fused aromatic rings at the δ-position (NDHL) does not affect thermodynamics of polymerizations.

Table 4.6. Observed equilibrium monomer concentration ($[M]_{eq}$) at different temperatures

Temperature (°C)	**$[M]_{eq}$ (M)**
20.5	0.385
35	0.484
45	0.561
57.5	0.599

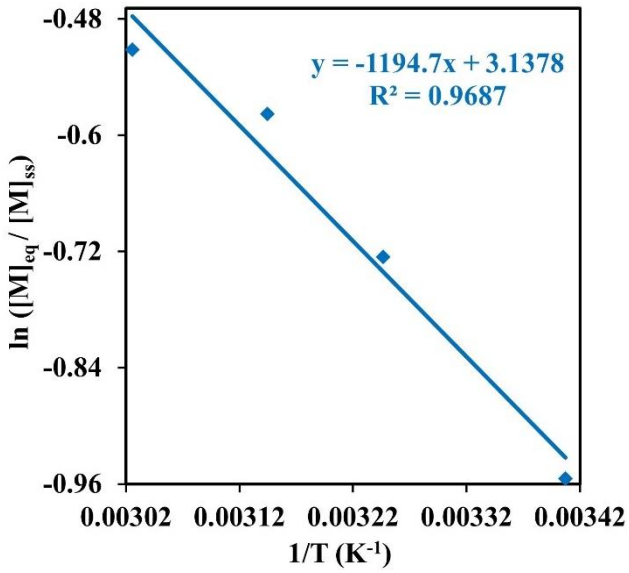

Figure 4.14. Van't Hoff analysis for poly(NDHL) (blue diamond).

4.3.5 Kinetics of polymerization

Characteristics of a living chain-growth polymerization include the first-order kinetics in monomer concentration and a linear relationship between molecular weight and monomer conversion.[118] Deviations from the linear dependence are attributed to the presence of slow initiation or side reactions such as chain transfer and termination reactions. The controlled/living characteristic of

ROP can be confirmed by kinetics experiments. The polymerization kinetics were analyzed for NDHL monomer under optimal catalyst loadings and polymerization conditions determined above, which demonstrated equilibrium polymerization as evidenced by plateauing conversion (Figure 4.15a). Like 2-PhPDHL, a semilogarithmic plot of monomer conversion as a function of reaction time for NDHL was linear. It indicates NDHL polymerization is first-order with respect to monomer concentration (Figure 4.15b). Martello et al. also reported that similar TBD-catalyzed δ-decalactone polymerization followed first order kinetics.[119] The inclusion of two aromatic groups (whether linked as 2-PhPDHL or infused as NDHL) at δ-position does not affect the rate law of polymerization.

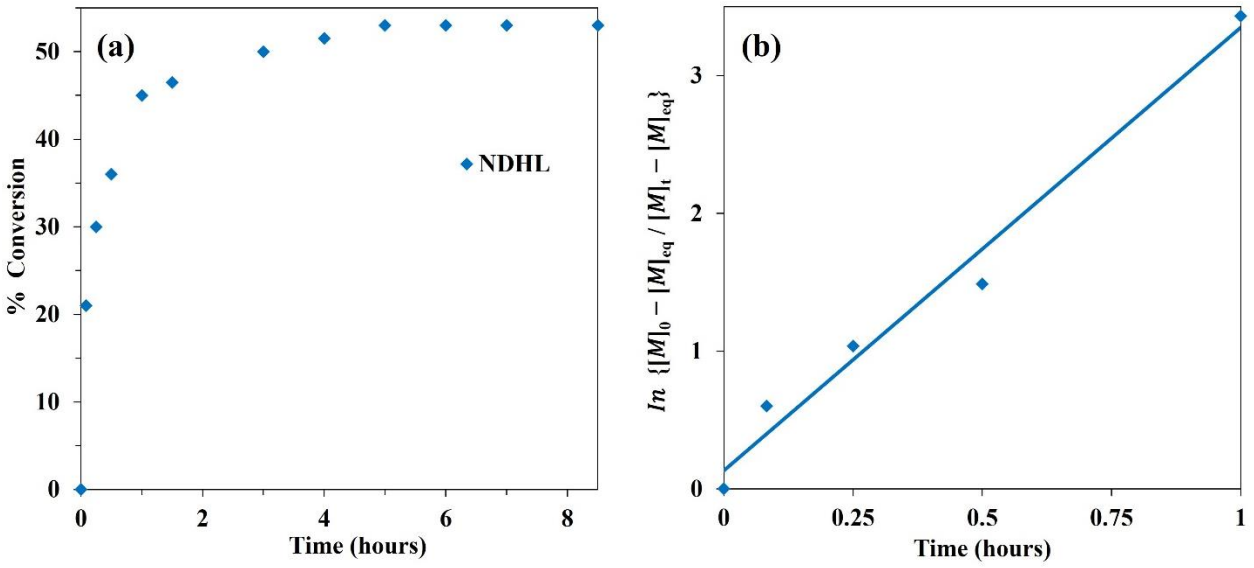

Figure 4.15. a) Monomer conversion as a function of time for polyNDHL b) Linearized kinetics behavior for ROP of NDHL (blue diamond) before reaching equilibrium, where $[M]_{eq}$ is the equilibrium monomer concentration, $[M]_0$ is the initial monomer concentration, $[M]_t$ is the monomer concentration at given a time.

A controlled polymerization reaction would show a linear increase of molecular weight throughout the polymerization reaction until it reaches equilibrium. The molecular weight of poly(NDHL) linearly increased as a function of monomer conversion and the dispersity values ranged from 1.2 to 1.8 (Figure 4.16). Since this was linear relationship, it suggested that all the chains were initiated at the same time. A potential limitation of the data in Figure 4.15b is that separation of these low molecular weight polymers by SEC does not guarantee an accurate result but still showed the separation. Repetition of the kinetics experiments are recommended for future work.

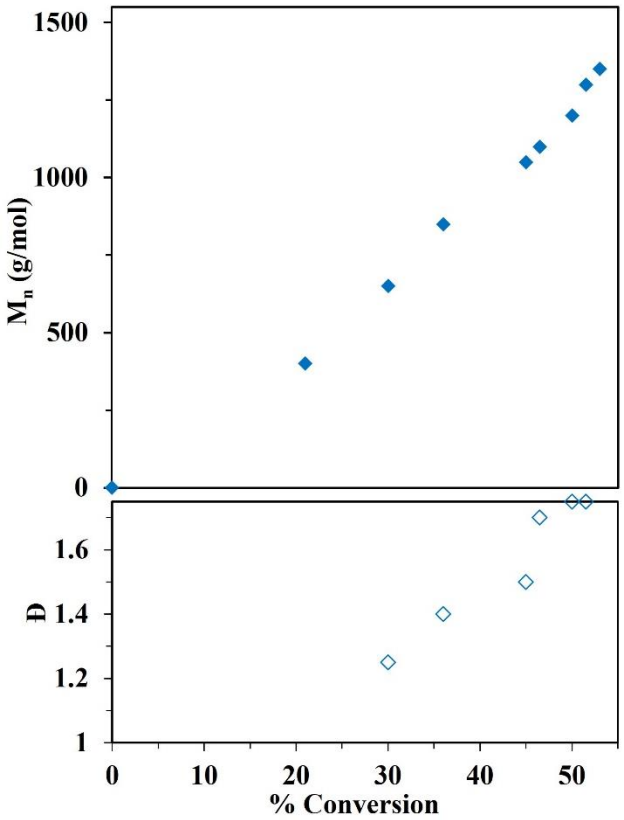

Figure 4.16. Number average molecular weight (M_n) and dispersity (Đ) as a function of monomer conversion for poly(NDHL). Both M_n and Đ measured by SEC. Ratios of $[M]_0/[I]$ = 50/1 for poly(NDHL) used throughout this study.

4.4 Conclusions

The optimum conditions for the polymerization of NDHL was different than the 2-PhDHL monomer. Higher (6.5 times higher than 2-PhPDHL: 20 mol% or 220 mM minimum at the same conditions and monomer concentration) TBD catalyst loading was needed for appreciable conversion in the polymerization due to the more sterically hindered pendant group and the slower secondary alcohol propagating chain end. Higher catalyst loading provoked the TBD catalyst to act as an initiator to initiate and propagate the polymerization. At all $[M]_0/[I]$ ratios, low MW polymers were synthesized due to the role of the TBD catalyst as an initiator. We did not observe similar behavior for PDHL monomer due to the low catalyst loading was needed for the polymerization. The rate of polymerization for NDHL was faster than PDHL as expected due to higher catalyst loading. The T_g observed for poly(NDHL) (37 °C) was close to the poly(2-PhDHL).

CHAPTER 5

SYNTHESIS AND RING-OPENING POLYMERIZATION OF 6-((CYCLOHEXYLOXY)METHYL)OXAN-2-ONE (CDHL)

5.1 Introduction

In the previous chapters, different six-membered lactone monomers bearing different aromatic groups at the δ-position were synthesized and their polymerization conditions were described. The glass transition temperatures (T_gs) increased from -65 to 39.5 °C by introducing these aromatic rings compared to its unsubstituted six-membered polyDVL. The hydrogenated version of these pendant groups at δ-position can give a new library of six-membered monomers (Figure 5.1). The ROP of these new monomers can produce aliphatic polyesters with tunable properties.[39,40,41]

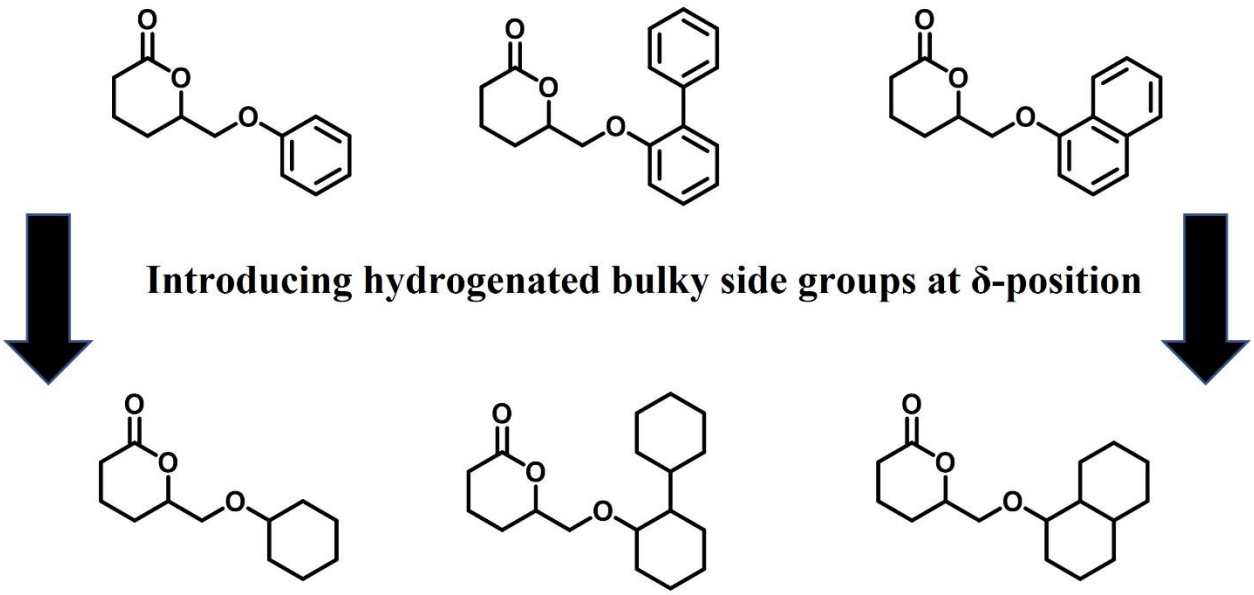

Figure 5.1. Introducing sterically hindered hydrogenated pendant groups at δ-position will produce a new library of monomers with tunable properties

In this chapter, a cyclohexyl group was introduced at the δ-position of the lactone monomer by following six steps reactions (Figure 5.2) and it was polymerized by ROP technique using TBD catalyst at room temperature in 1,4-dioxane. Finally, full thermodynamics and kinetics studies were conducted for the new monomer and polymeric system.

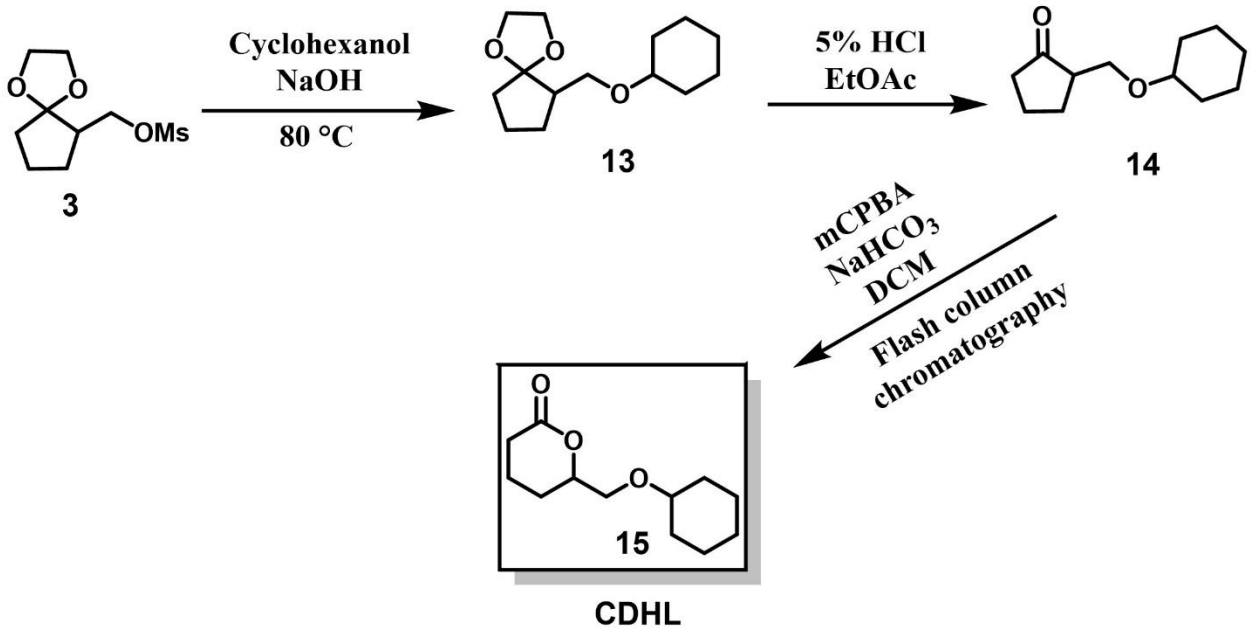

Figure 5.2. Reaction scheme for CDHL monomer synthesis

5.2 Materials and methods

Reagents, including methyl cyclopentanone-2-carboxylate (TCI), p-toluenesulfonic acid (Acros), lithium aluminum hydride (Aldrich), potassium sodium tartrate tetrahydrate (Aldrich), sodium hydride (Acros), methanesulfonyl chloride (Fisher), cyclohexanol (Aldrich), potassium hydroxide (Aldrich), 3-chloroperoxybenzoic acid (Acros), sodium bicarbonate (Fischer), TBD: 1,5,7-triazabicyclo[4.4.0]dec-5-ene (Fisher), benzyl alcohol (Aldrich), 1,4-dioxane (extra dry) (Acros),

dichloromethane (anhydrous) (Acros), and N,N-dimethylformamide (anhydrous) (Aldrich) were used as received. All the other solvents and reagents were used as received from commercial suppliers without further purification unless stated otherwise.

5.2.1 Synthesis of 6-((cyclohexyloxy)methyl)-1,4-dioxaspiro[4.4]nonane (13)

Sodium hydroxide (4.32 g, 0.108 mol) was added to the excess cyclohexanol (110 mL) and stirred for 30 min at reflux temperature (150-160 °C) to deprotonate the cyclohexanol. After deprotonation, **3** (6 g or 0.0254 mol in 20 mL DMF) was added to the mixture and stirred for 36 h at 80 °C. After the reaction time, the mixture was extracted with ethyl acetate (2 x 50 mL) and filtered. The filtrate was concentrated on a rotary evaporator and then distilled under a vacuum to at 80 °C. Cyclohexanol was collected as a distillate and the remaining was collected as product **13** (2.1 g, 35% yield).

^{1}H NMR (Chloroform-*d*) δ (ppm): 3.86 (m, 4H), 3.51 (dd, *J* = 9.25 Hz, 6.1 Hz, 1H), 3.31 (dd, *J* = 9.25 Hz, 8.45 Hz, 1H) 3.18 (m, 1H), 2.17 (m, 1H), 2.15 (m, 1H), 1.87 - 1.22 (m, 16H).

5.2.2 Synthesis of 2-((cyclohexyloxy)methyl)cyclopentanone (14)

In this synthesis, a 5% HCl (20 mL) solution was added into a mixture of **13** (2.1 g**,** 0.0087 mol) in ethyl acetate (30 mL) solvent and stirred overnight at room temperature. Brine solution (50 mL) was poured into the mixture the next morning and extracted with ethyl acetate (3 x 50 mL). The extracted organic layer was dried over Na_2SO_4 and removed on a rotary evaporator to give **14** (0.85 g, 50% yield).

^{1}H NMR (Chloroform-*d*) δ (ppm): 3.59 (dd, *J* = 9.35 Hz, 3.7 Hz, 1H), 3.54 (dd, *J* = 9.25 Hz, 6.15 Hz, 1H) 3.16 (m, 1H), 2.25 (m, 4H), 1.77 - 1.17 (m, 16H).

5.2.3 Synthesis of 6-((cyclohexyloxy)methyl)oxan-2-one (15)

In this synthesis, 3-chloroperoxybenzoic acid (mCPBA, 70%) (1.6 g, 0.0093 mol) and sodium bicarbonate (0.55 g, 0.0065 mol) were added to dichloromethane (50 mL) and stirred for 15 mins at room temperature. **14** (0.85 g, 0.0043 mol) was added into the mixture and stirred overnight. After the reaction time, extra dichloromethane (50 mL) solvent was added to the reaction mixture. The organic layer was washed with saturated Na_2SO_3 (10 mL), saturated $NaHCO_3$ (20 mL), then brine solution (10 mL), and separated. The organic layer was dried over anhydrous Na_2SO_4 and concentrated on a rotary evaporator to get the crude product (δ-substituted 89.5% major and α-substituted 10.5% minor product). The resulting solid was purified via silica gel flash column chromatography using 70:30 hexane:ethyl acetate mobile phase. After running flash column chromatography, 0.35 g of pure CDHL (**15**) was collected at a 38% yield.

^{1}H NMR (Chloroform-*d*) δ (ppm): 4.41 (m, 1H), 3.6 (dd, *J* = 10.2 Hz, 4.6 Hz, 1H), 3.55 (dd, *J* = 10.25 Hz, 5.35 Hz, 1H), 3.27 (m, 1H), 2.55 (m, 1H), 2.47 (m,1H) 1.95 - 1.25 (m, 14H).

^{13}C NMR (Chloroform-*d*) δ (ppm): 171.45, 79.32, 78.28, 69.75, 32.08, 29.74, 25.74, 24.83, 23.92, 18.25.

5.2.4 Polymerization materials and methods

Vials and magnetic stir bars used for polymerization reactions were dried in an oven at 100 °C overnight before use. The CDHL monomer was dried overnight before use in the room temperature vacuum oven. TBD was dried overnight in the antechamber of a nitrogen glovebox and kept in the glovebox under nitrogen after received. Vials, caps, syringes, spatulas, and all other materials used

to set up polymerization reactions were dried in the antechamber of the glovebox overnight before use.

5.2.5 General polymerization procedure for CDHL

Polymerization of CDHL proceeded as follows. Two different stock solutions of initiator and catalyst were prepared by adding 3 μL benzyl alcohol in 300 μL 1,4-dioxane and 7 mg TBD in 100 μL 1,4-dioxane separately in an N_2 filled glovebox. First, the stock solution of benzyl alcohol (20 μL, 0.00188 mmol) and then the stock solution of TBD (9.5 μL, 0.00471 mmol) were added using glass syringes to CDHL monomer (20 mg, 0.0942 mmol) dissolved in dioxane solvent (35.5 μL) already in 2 mL vial with a septum. The homogenous mixture was stirred for the desired reaction time at ambient temperature. The polymerization was quenched by adding excess benzoic acid (9 mg, 0.0738 mmol). A typical polymerization led to ca. 47% conversion of CDHL. The inactive catalyst was removed by precipitation of the pure polymer into diethyl ether.

5.2.6 Polymerization kinetics experiments

Polymerization kinetics experiments were carried out at ambient temperature for CDHL monomers. The experiment was conducted using benzyl alcohol (BnOH) as an initiator and TBD as a catalyst. For measurement of the CDHL polymerization kinetics, the stock solution of benzyl alcohol (34 μL, 0.0033 mmol) and the stock solution of TBD (16 μL, 0.0081 mmol) were added using glass syringes to CDHL monomer (34.5 mg, 0.163 mmol) dissolved in dioxane solvent (72 μL) in 2 mL vial with a septum. The homogenous mixture was stirred until the polymerization reached equilibrium and aliquots were collected throughout the polymerization. The aliquots were

quenched by adding 30 molar excess benzoic acid and monomer conversions were determined using ^{1}H NMR spectroscopy.

For the polymerization kinetics experiments, the [Monomer]$_0$:[Initiator] and [Monomer]$_0$:[Catalyst] ratios were fixed. The polymerization appeared to reach equilibrium, as indicated by a plateau in monomer conversion as a function of time. Pseudo first-order behavior was verified by fitting the kinetics data to Equation 5.1,[120] which describes monomer concentration as a function of time for an equilibrium polymerization:

$$\ln\left(\frac{[M]_0-[M]_{eq}}{[M]_0-[M]_t}\right) = k_{app}t \qquad \text{(Equation 5.1)}$$

where $[M]_{eq}$ is the equilibrium monomer concentration, $[M]_0$ is the initial monomer concentration, $[M]_t$ is the monomer concentration at given a time, and k_{app} is the apparent rate constant.

5.2.7 Polymerization thermodynamics experiments

For the polymerization thermodynamics experiments, the setup was the same as for the kinetics experiments, but the polymerizations were stirred in an oil bath at a range of temperatures. The temperature was varied for CDHL from 20 to 45 °C. The polymerizations achieved different equilibrium monomer concentrations ($[M]_{eq}$) at different temperatures. Aliquots were collected after sufficient reaction time to reach equilibrium (typically 24 h for CDHL) and quenched with excess benzoic acid. The polymerization progress was tracked using ^{1}H NMR spectroscopy. To ensure the polymerizations reached equilibrium, the reactions were kept running for at least another 12 h after reaching equilibrium. To estimate enthalpy (ΔH_p) and entropy (ΔS_p) for the

polymerization, the equilibrium monomer concentration was plotted as a function of inverse temperature and fit using a van 't Hoff analysis:

$$\ln\left(\frac{[M]_{eq}}{[M]_{ss}}\right) = \frac{\Delta H_p}{RT} - \frac{\Delta S_p}{R} \qquad \text{(Equation 5.2)}$$

where T is the polymerization temperature, R is the ideal gas constant, and $[M]_{ss}$ is a standard state monomer concentration that was set to 1 M.

5.2.8 Analysis of polymer products

^{1}H NMR and ^{13}C NMR spectra were obtained either using Varian Inova 400 MHz and Bruker Avance NEO 500 MHz NMR spectrometers using $CDCl_3$ as a solvent. Size exclusion chromatography (SEC) was conducted in dimethylformamide (DMF) containing 0.5 wt% LiBr as the mobile phase with a flow rate of 1 mL min^{-1} at 70 °C. SEC analysis was performed by three Phenogel columns (Phenomenex) in series with different pore sizes (50, 10^3, and 10^6 Å), using a refractive index detector (35 °C) and calibration curves from linear polystyrene standards.

The crude polymer was dissolved in dichloromethane and precipitated in cold diethyl ether (1:5). The purified polymers were dried in a vacuum oven. The T_g of different polymers was measured using a differential scanning calorimeter (DSC, TA Instruments DSC2500) at a rate of 10 °C min^{-1} over a range from -90 to 100 °C using ~1.5 mg sample in a heat/cool/heat experiment under an N_2 atmosphere. The T_g were reported from the second heating cycle and analyzed with TA TRIOS software (v5.0.0).

5.3 Results and discussion

The typical Williamson ether synthesis conditions (NaH as a base and DMF as a solvent) mentioned in Chapters 2 through 4 gave an elimination product (Figure 5.3) for this synthesis. Christopher Stewart reported in his thesis work that decreased acidity of cyclohexanol compared to phenol made the desired reaction more susceptible to elimination side reactions and NaH base reacted with the solvent (DMF) during the reaction.[121] However, changing solvent system to 1,4-dioxane still gave the elimination product and a flash chromatography column was necessary to separate the pure product from the reaction mixture. The overall yield was reported at about 10%.

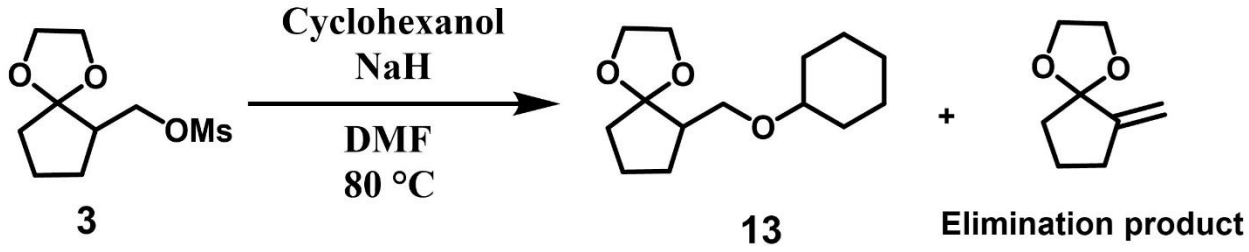

Figure 5.3. Reaction scheme for etherification reaction which resulted in overall low yield

Cyclohexanol was used both as the nucleophile and solvent in this work. Sodium hydroxide was used as a base to deprotonate the cyclohexanol at a reflux temperature. The successful etherification was confirmed by ^{1}H NMR spectroscopy. The appearance of multiplets at 3.18 ppm confirmed the successful etherification reaction (Figure 5.4). The singlet peak at 3 ppm was disappeared and the protons next to the ether linkage were shielded (3.51 ppm and 3.31 ppm). Excess cyclohexanol was removed by distillation under vacuum. The yield was increased to 35%.

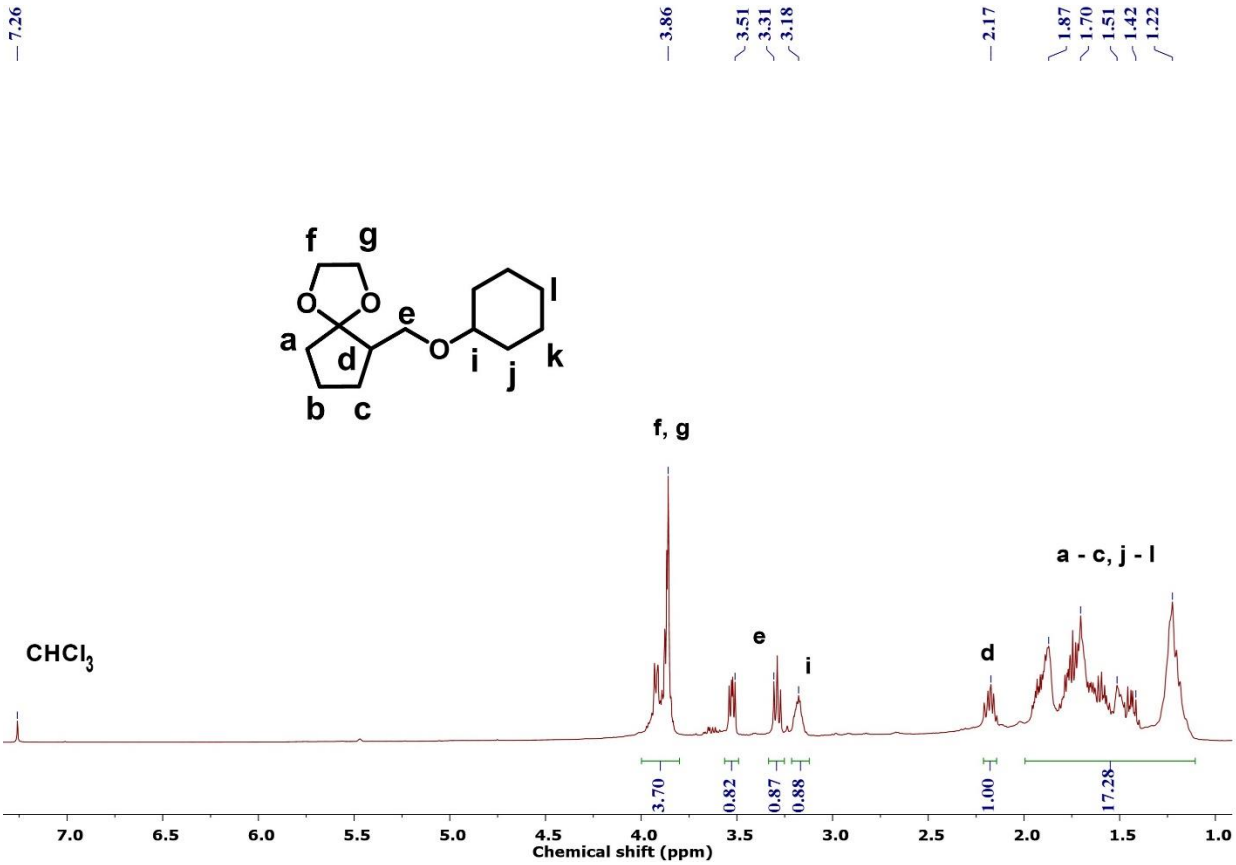

Figure 5.4. ^{1}H NMR spectrum of 6-((cyclohexyloxy)methyl)-1,4-dioxaspiro[4.4]nonane (13).

The protecting acetal group was removed in the next step in the presence of an acidic solution. Hydrochloric acid (5%) was used to remove the acetal group. The removal of the acetal group was confirmed by the disappearance of peaks at 3.86 ppm (Figure 5.5). The protons next to the ether linkage were affected mostly due to the removal of the acetal group and those protons showed a de-shielding effect in the ^{1}H NMR spectrum.

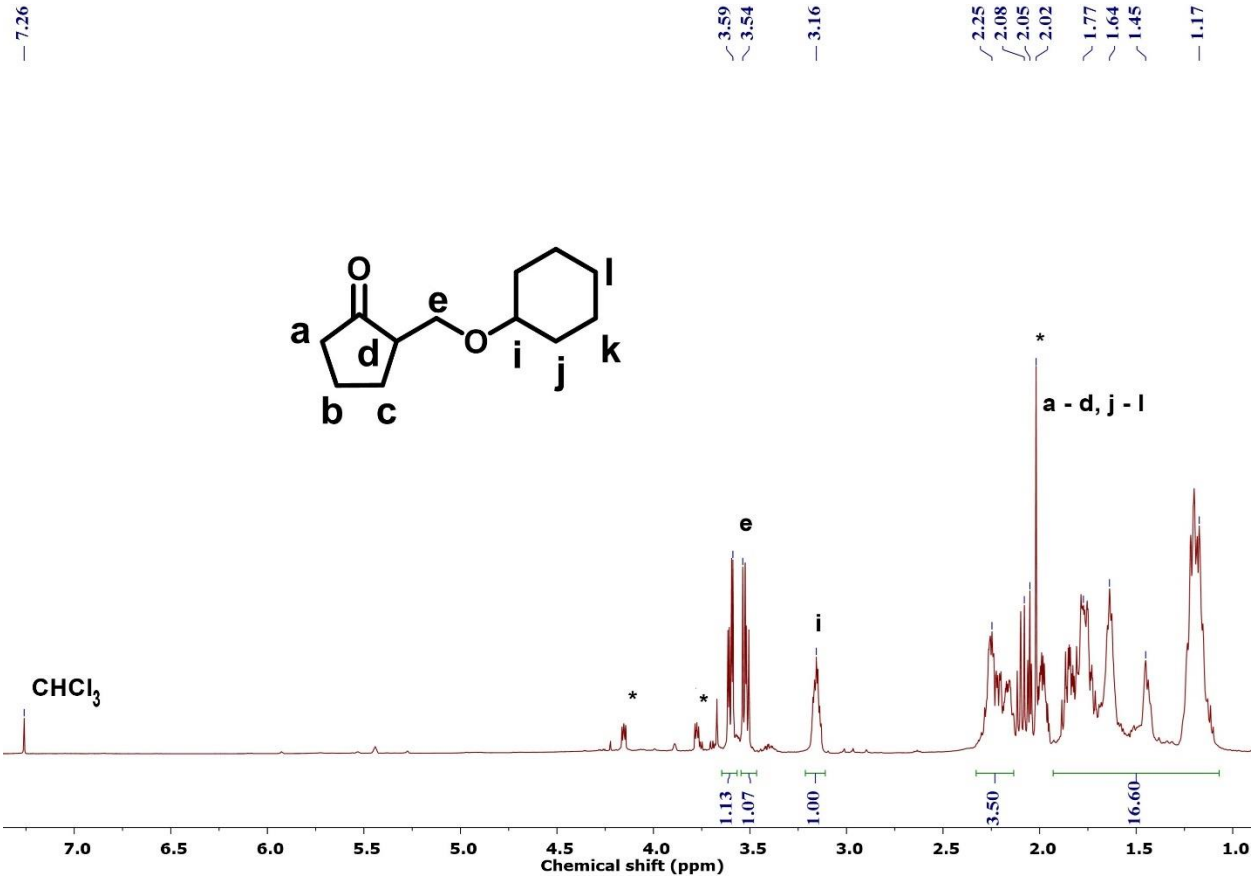

Figure 5.5. ^{1}H NMR spectrum of 2-((cyclohexyloxy)methyl)cyclopentanone (14). *Ethyl acetate and ethylene glycol.

A Baeyer-Villiger oxidation reaction was used to synthesize six membered lactones from the five-membered cyclic ketones. 3-Chloroperoxybenzoic acid (mCPBA) was used as a peroxyacid source. Both α-substituted and δ-substituted products were observed in the ^{1}H NMR spectrum due to the unsymmetrical cyclic ketone. δ-substituted product (89.5%) was the major product in the synthesis due to the higher migratory aptitude of the tertiary alkyl group over the secondary alkyl group. The peak of protons next to the ester group confirmed the successful six-membered lactone synthesis at 4.39 ppm for the major product (Figure 5.6). After this step, a mixture of major and minor products was obtained in the presence of 3-chlorobenzoic acid as a by-product. For ROP

and controlled polymerizations, pure CDHL was separated. Flash column chromatography was used to separate the pure CDHL monomer. Pure CDHL was separated successfully by using more non-polar hexane solvent. A 70:30 hexane and ethyl acetate mixture was used as a mobile phase. The products were tracked by thin layer chromatography (R_f = 0.25 for δ-substituted product and R_f = 0.4 for α-substituted product) primarily. The pure CDHL was confirmed by both ^{1}H and ^{13}C NMR spectroscopy (Figure 5.7 - 5.8).

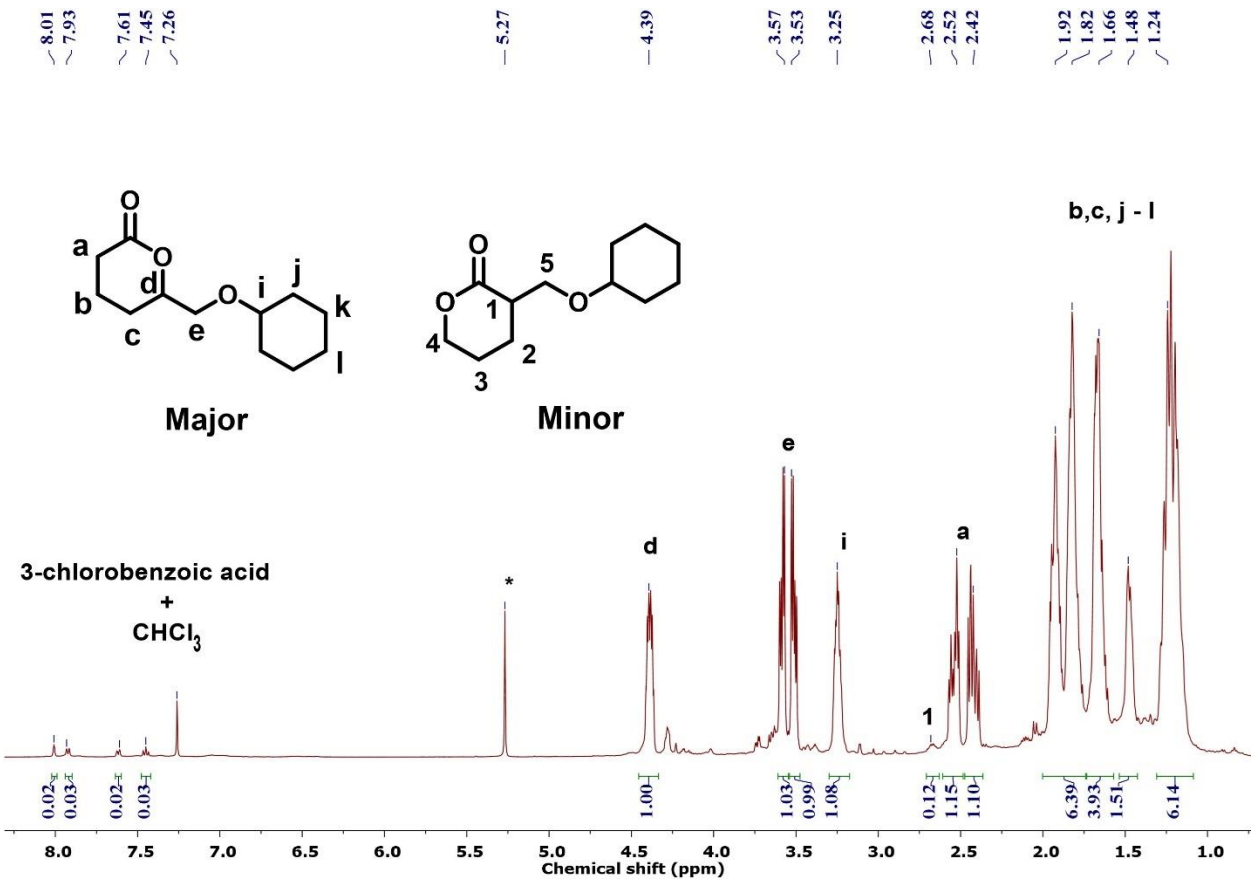

Figure 5.6. ^{1}H NMR spectrum of a crude mixture of 6-((cyclohexyloxy)methyl)oxan-2-one (15), *DCM solvent.

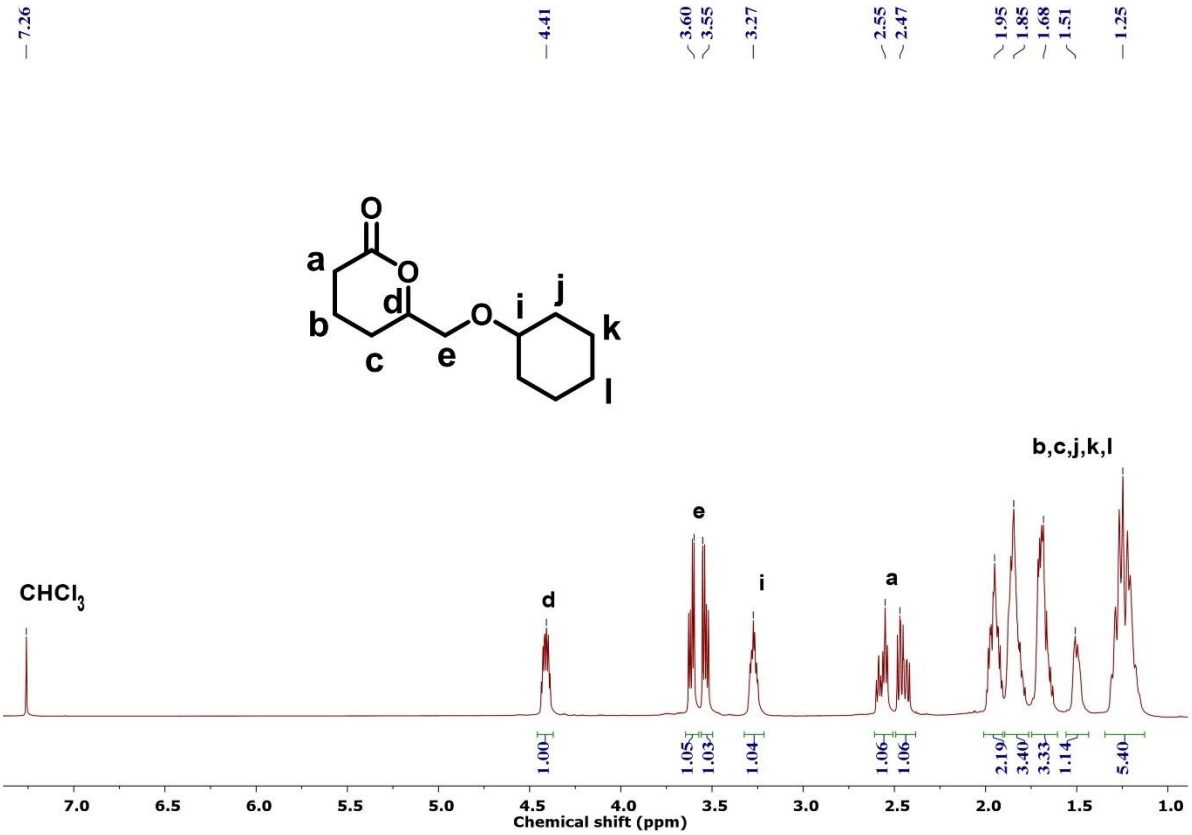

Figure 5.7. ^{1}H NMR spectrum of pure 6-((cyclohexyloxy)methyl)oxan-2-one (15), collected after flash column chromatography.

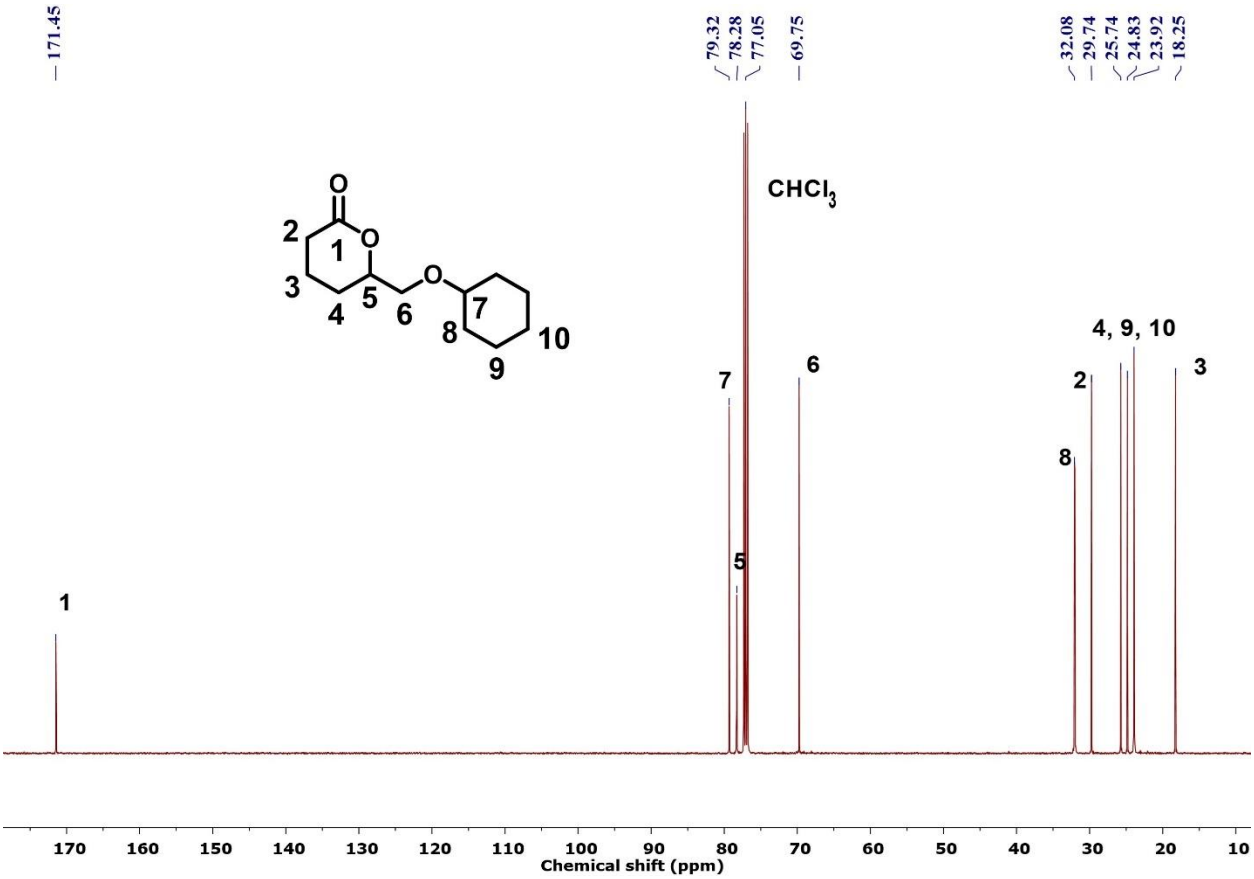

Figure 5.8. ^{13}C NMR spectrum of pure 6-((cyclohexyloxy)methyl)oxan-2-one (15).

5.3.1 Ring-opening polymerization of CDHL lactone

Finding the optimum conditions for the polymerization reaction are necessary for the new CDHL monomer system. The objectives of the optimization reactions were to obtain a higher conversion, to find a catalytic system for polymerizing the new monomer in a controlled manner, and to get high molecular weight polymers. The general scheme for the ring opening polymerization of CDHL is shown in Figure 5.9 below.

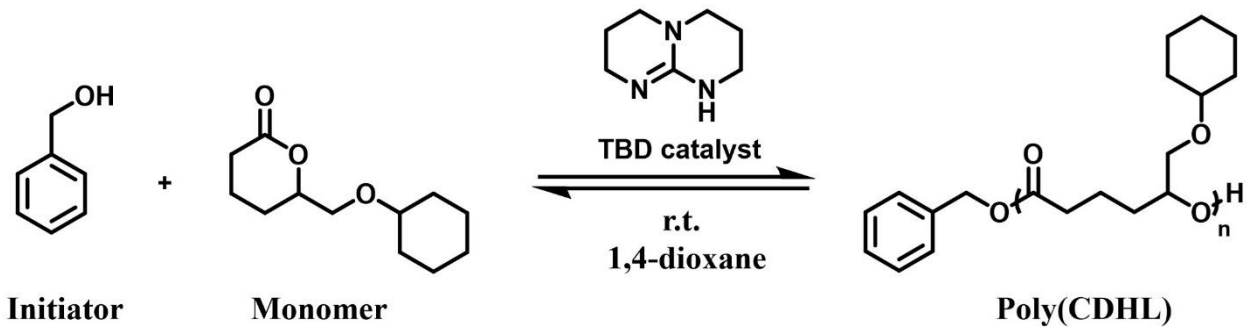

Figure 5.9. Polymerization scheme for the ring-opening polymerization of CDHL

Initially, the CDHL monomer was polymerized at room temperature using benzyl alcohol (BnOH) as the initiator and basic TBD (0.3 mol%) as a catalyst in 1,4-dioxane while keeping the initial monomer concentration at $[M]_0$ = 1.1 M as reported in Chapter 1 for PDHL monomer. The initiator initiated the polymerization successfully, but no propagation was observed from the ^{1}H NMR spectroscopy. The conversion was less than 5% until 5 mol% catalyst (based on monomer moles) was used to achieve higher conversion in the polymerization of CDHL (Table 5.1). Similar behavior was found for polymerizing 2-PhPDHL and NDHL in Chapters 3 and 4 using TBD as a catalyst due to the presence of more sterically hindered groups at the δ-position

5.3.2 Controlling the molecular weight of poly(CDHL)

The CDHL monomer was polymerized at room temperature using benzyl alcohol (BnOH) as the initiator and TBD as a catalyst. The conversion was tracked by taking aliquots from the reaction and analyzing them using ^{1}H NMR spectroscopy (Figure 5.10). The methylene protons of the BnOH initiator shifted from 4.7 to 5.09 ppm, confirming that the monomer was initiated by BnOH. The methine protons of CDHL (4.41 ppm) shifted to 4.94 ppm, corresponding to the lactone ring opening and the successful polymerization.

Table 5.1. Effect of TBD catalyst loadings for ROP of CDHL

Catalyst (mol%)[a]	**Catalyst (mM)[b]**	**%Conversion[c]**
0.3	3.3	<5%
0.5	5.5	<5%
1	11	<5%
3	33	<5%
5	55	47%

[a]Based-on monomer moles; [b]Calculated by the moles of the catalyst over total volume; [c]Conversion measured by ^{1}H NMR spectroscopy. Ratios of $[M]_0/[I]$ = 50/1 for the polymerization used throughout this study where initial monomer concentration, $[M]_0$ = 1.1 M

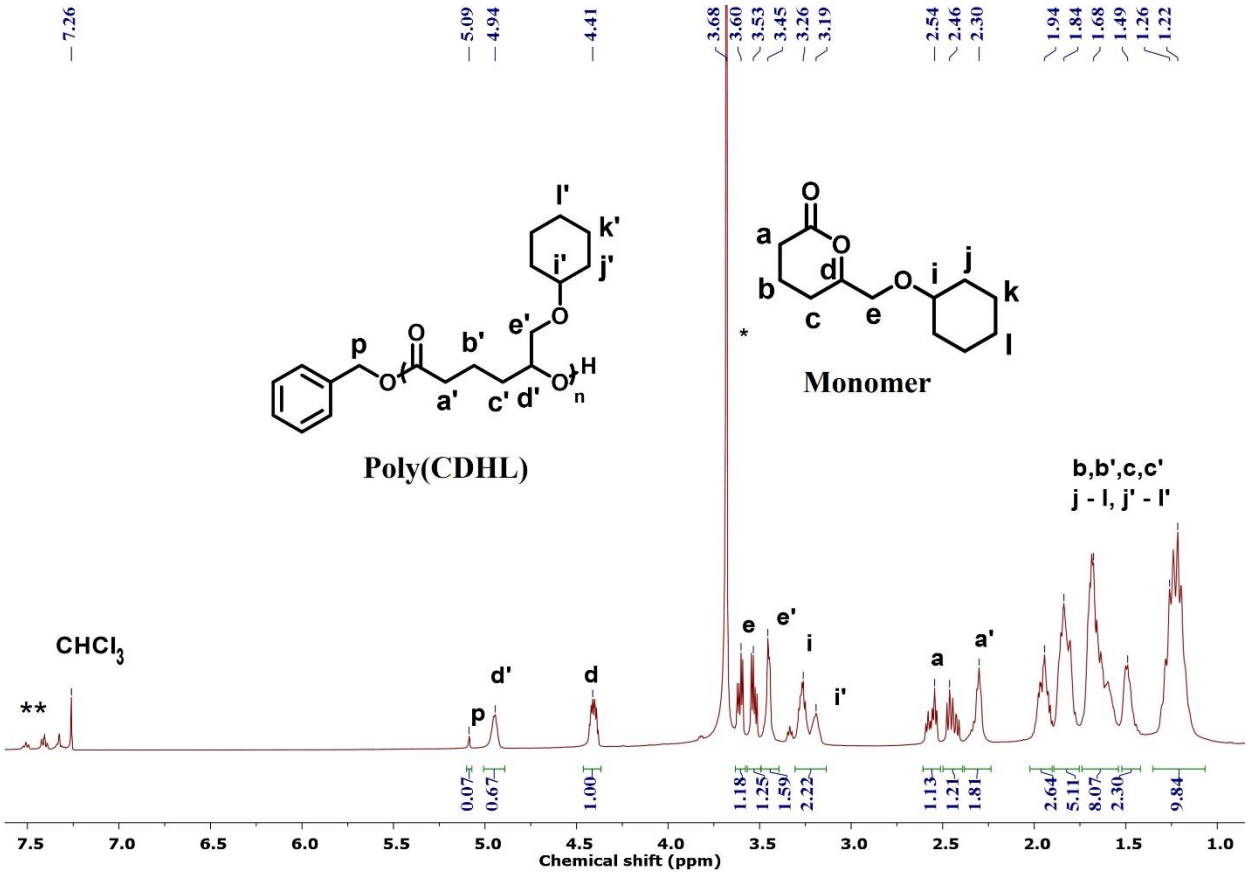

Figure 5.10. ^{1}H NMR spectrum of crude poly(CDHL). ^{1}H NMR spectrum was collected after the polymerization reached equilibrium on day three. *1,4-Dioxane solvent, **3-chlorobenzoic acid.

Table 5.2 summarizes the results obtained from different polymerizations. As mentioned above, the minimum 5 mol% TBD catalyst (55 mM) is needed to propagate the polymerization of CDHL. The equilibrium monomer conversion of CDHL was about 45%. The molar mass distributions were not unimodal for all the polymers (Figure 5.11), which indicated low molecular weight polymers forming at the same time.

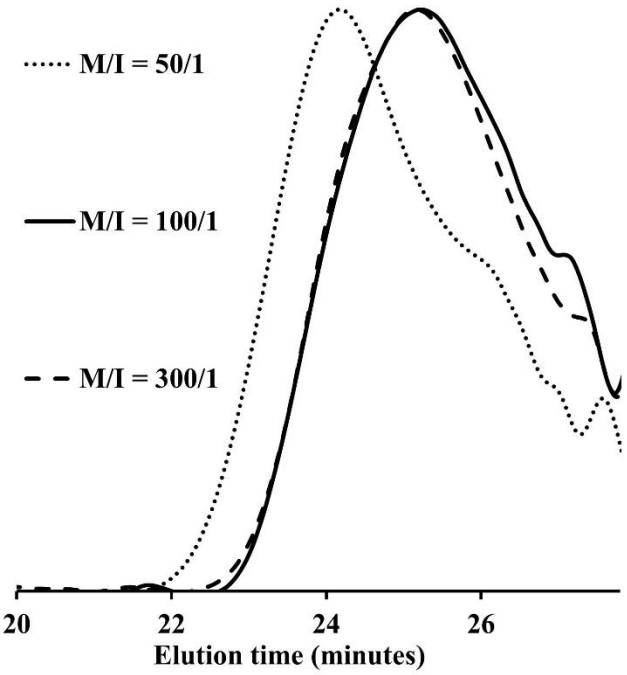

Figure 5.11. SEC elution curves for ROP of CDHL after reaching equilibrium conversion at different $[M]_0/[I]$ ratios. Molecular weights ($M_{n,\ SEC}$) and dispersity are in Table 5.2.

The experimental M_n values from size exclusion chromatography (SEC) differed from the calculated expected values. Unlike PDHL, the $M_{n,SEC}$ of poly(CDHLs) differed from the expected values at different $[M]_0/[I]$ ratios (Table 5.2, entries 1-3). The $M_{n,SEC}$ values should increase by increasing $[M]_0/[I]$ for poly(CDHL). However, the $M_{n,SEC}$ value still deviated significantly from the $M_{n,\ expected}$ value while we increased the $[M]_0/[I]$ ratio from 50 to 100 or 100 to 300 (Table 5.2, entries 1-3). Though size exclusion chromatographic technique cannot deliver actual MW of the polymers due to the calibration of the RI detector with polystyrene (PS) standards, a nearly two to three-fold increase in the $M_{n,sec}$ values were expected while changing the $[M]_0/[I]$ ratios. It suggests a failure in the controlled polymerization and that BnOH is not initiating all the chains. Broader dispersities were expected due to the higher catalyst loading as we mentioned in the NDHL monomer section in Chapter 4 (Table 5.2, entries 1-3). Besides acting as a catalyst, TBD can

initiate ROP process as shown in Chapters 3 and 4. It was not possible to confirm whether the polymerization initiated by the TBD from ^{1}H NMR spectrum because some of the polymer proton peaks might overlap with the TBD initiated proton peaks (3.25 ppm) as shown in Chapters 3 and 4. And precipitation of pure polymer from the crude was very difficult due to the low molecular weight and low conversion. End group studies by matrix assisted laser desorption/ionization (MALDI) are needed to confirm the initiation process by TBD.

Table 5.2. Results for TBD catalyzed ROP of CDHL

Monomer	**Entry**	**$[M]_0/[I]/[C]$**	**Time (days)**	**Conv.[b] (%)**	**$M_{n,\ expected}$[c] (kg/ mol)**	**$M_{n,\ SEC}$[d] (kg/ mol)**	**Đ[d]**
CDHL[a]	1	50/1/2.5	3	47	5.0	3.2	1.7
	2	100/1/5	5	43	9.0	1.0	1.87
	3	300/1/15	5	43	27.0	1.0	1.9

[a]1,4-dioxane as solvent, $[M]_0$ = 1.1 M; where $[M]_0$ = Initial monomer concentration. [b]Conversion measured by ^{1}H NMR spectroscopy. [c]Calculated from $[M]_0/[I]$ × monomer conversion × MW of CDHL. [d]Measured by SEC in DMF with 0.5 wt% LiBr as the mobile phase, using linear polystyrene standards with a refractive index detector.

5.3.3 Glass transition temperature (T_g) of poly(CDHL)

The glass transition temperature (T_g) was measured by DSC from the second heating cycle for poly(CDHL) (Figure 5.12), The bulky cyclohexyl group at the δ-position showed a T_g of -19 °C which was higher than unsubstituted six-membered poly(δ-valerolactone) (-65 °C) [122,123] and seven-membered poly(ε-caprolactone) (-60 °C) reported in the literature.[124] However, the T_g was lower than poly(PDHL) (6 °C) reported in Chapter 2. The pure polymers could not be precipitated out from the reaction due to low molecular weight. The monomers could have the plasticizing effect to lower the T_g. At the same time, T_g of a polymer depends on the molecular weight and it

increases rapidly with increasing molecular weight and plateaus at higher values. Whether the T_g already hit the plateaus for poly(CDHL) could not be tested due to the unavailability of high molecular weight polymers. Additionally, the poly(CDHL) did not crystallize above its T_g due to the racemic mixture, and the catalysts afforded no stereochemical preference.

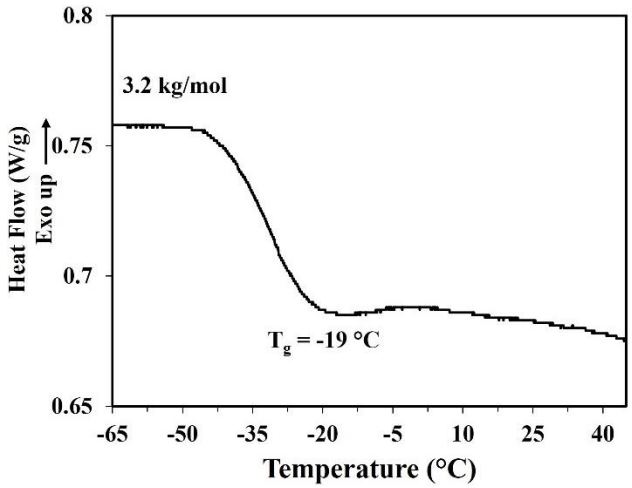

Figure 5.12. DSC thermograms of poly(CDHL). Curves are shifted vertically to provide clarity.

5.3.4 Thermodynamics of polymerization

The polymerizations achieved different equilibrium monomer concentrations ($[M]_{eq}$) at different temperatures and Table 5.3 shows the $[M]_{eq}$ values obtained by running the polymerization at different temperatures. The thermodynamics of the ROP was examined by performing a van't Hoff analysis to calculate the entropy and enthalpy of polymerization and to learn how monomer structure impacts polymerization thermodynamics (Figure 5.13). The enthalpy of polymerization (ΔH_P^o) was -5.6 ± 1.0 kJ mol^{-1} and the entropy of polymerization (ΔS_P^o) was -15 ± 3 J mol^{-1} K^{-1} for CDHL. Both values were different from PDHL monomer (ΔH_P^o = -9.4 ± 0.7 kJ mol^{-1}, ΔS_P^o = -26 ± 2 J mol^{-1} K^{-1}), and it suggests attaching cyclohexyl group at the δ-position impacts the

polymerization thermodynamics. The negative enthalpy of polymerization of a cyclic monomer results mostly from its ring strain.[125] The enthalpy of CDHL is lower than the values reported for phenyl substituted monomers in Chapters 2 to 4. The entropic penalty for polymerization of CDHL is less than all the monomers reported in the previous chapters (PDHL, 2-PhPDHL and NDHL). However, low conversion was observed due to the low enthalpic value for polymerization of CDHL.

Table 5.3. Observed equilibrium monomer concentration ($[M]_{eq}$) at different temperatures

Temperature (°C)	**$[M]_{eq}$ (M)**
20	0.593
23	0.605
35	0.638
45	0.719

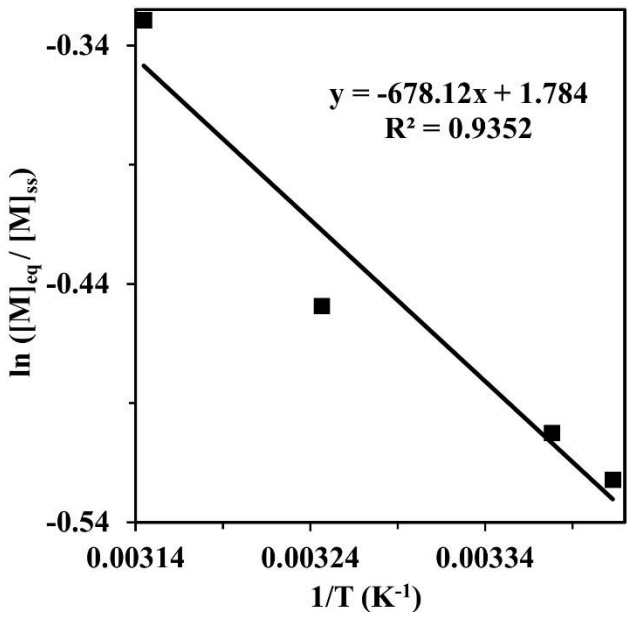

Figure 5.13. Van't Hoff analysis for poly(CDHL) (black rectangle).

5.3.5 Kinetics of polymerization

The controlled/living characteristic of ROP can be confirmed by kinetics experiments. The polymerization kinetics were analyzed for CDHL monomer under optimal catalyst loadings and polymerization conditions determined above, which demonstrated equilibrium polymerization as evidenced by plateauing conversion (Figure 5.14a). Like PDHL in Chapter 1, a semilogarithmic plot of monomer conversion as a function of reaction time for CDHL was linear. It indicates CDHL polymerization is first-order with respect to monomer concentration (Figure 5.14b). Martello et al. also reported that similar TBD-catalyzed δ-decalactone polymerization followed first order kinetics.[126]

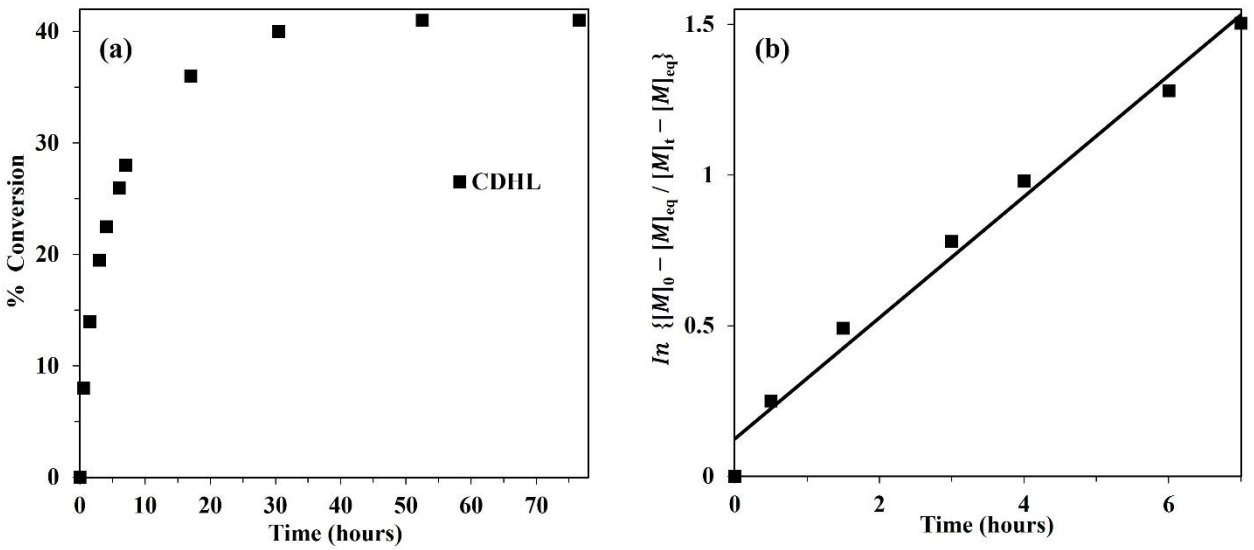

Figure 5.14. a) Monomer conversion as a function of time for polyCDHL b) Linearized kinetics behavior for ROP of CDHL (black rectangle) before reaching equilibrium, where $[M]_{eq}$ is the equilibrium monomer concentration, $[M]_0$ is the initial monomer concentration, $[M]_t$ is the monomer concentration at given a time.

A controlled polymerization reaction would show a linear increase of molecular weight throughout the polymerization reaction until it reaches equilibrium. The molecular weight of poly(CDHL) linearly increased as a function of monomer conversion and the dispersity values ranged from 1.07 to 1.5 (Figure 5.15). The low molecular weight of polymers and high dispersity suggest something else was initiating the polymerization. The pure polymers could not be precipitate out and end group analysis by ^{1}H NMR could not be done to check other initiation sources (TBD initiation or self-initiation). Further studies are needed to confirm the origin of low molecular weight polymer.

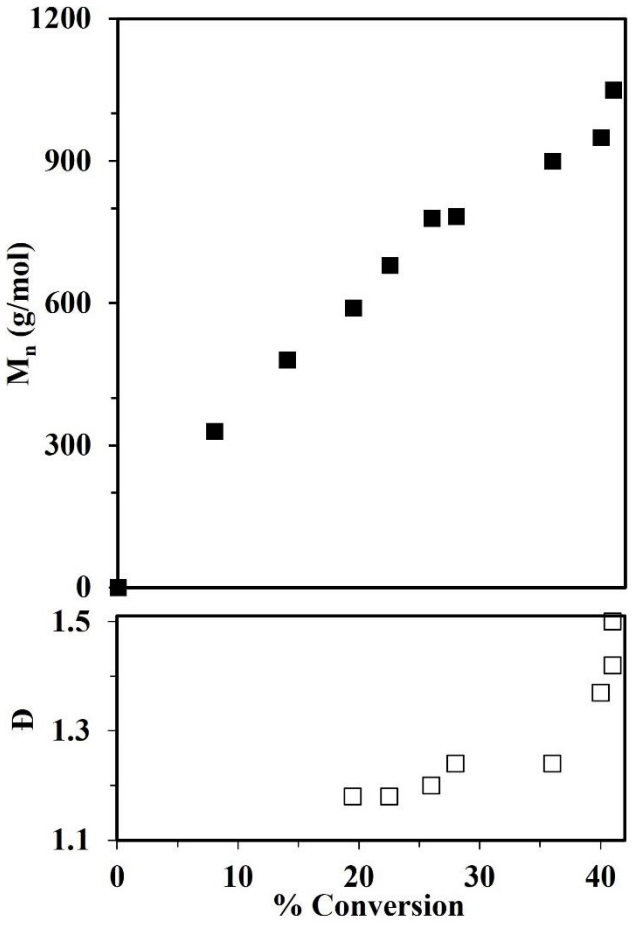

Figure 5.15. Number average molecular weight (M_n) and dispersity (Đ) as a function of monomer conversion for poly(CDHL). Both M_n and Đ measured by SEC. Ratios of $[M]_0/[I]$ = 50/1 for poly(CDHL) used throughout this study.

5.4 Conclusions

The optimum conditions for the polymerization of CDHL showed a significant difference than the PDHL monomer. Higher (16 times higher than PDHL: 5 mol% or 55 mM minimum at the same conditions and monomer concentration) TBD catalyst loading was needed for appreciable conversion in the polymerization due to the more sterically hindered pendant group and the slower

secondary alcohol propagating chain end. Further studies are needed to prove TBD catalyst is acting as an initiator to initiate the polymerization as shown in Chapters 3 and 4. At all $[M]_0/[I]$ ratios low molecular weight polymers were observed unlike PDHL monomer system. The T_g observed for poly(CDHL) was lower than poly(PDHL) (6 °C) reported in Chapter 2. The impurities present with the poly(CDHL) might have the plasticizing effect to get the lower T_g.

CHAPTER 6

FUTURE WORK

More bulky pendant groups at the δ-position of the six-membered lactone monomers can be introduced by synthesizing new monomers following the robust procedures described in previous chapters. As shown in Chapter 3 and 4 that two aromatic rings at the δ-position showed higher T_g polymer properties, attaching another aromatic ring will increase the T_g in a controlled manner. Attaching fused aromatic ring in the synthesis process (NDHL – Chapter 4) was found more difficult than the phenyl phenol ring (PhPDHL – Chapter 3). Synthesizing monomers like PhPDHL will be easier and high T_g polymer can be synthesized from these lactone monomers (Figure 6.1).

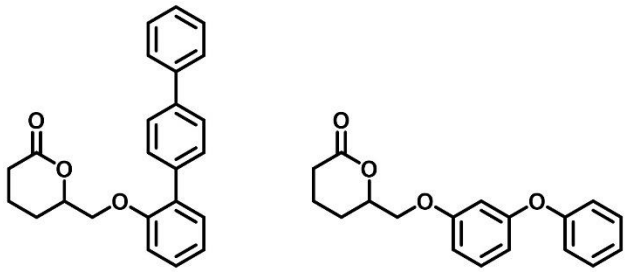

Figure 6.1. New recommended monomer structures for future work

More work can be done with the existing monomers especially hydrogenated version of these aromatic rings (CDHL – Chapter 5). Due to low ring strain, the conversion from monomer to polymer was low and the T_g for CDHL had some plasticizing effect from the monomer impurity as it was hard to precipitate the pure polymer. Finding an appropriate catalyst to get high and

control molecular weight of poly(CDHL) is necessary and it will give the true properties (T_g, mechanical properties, moisture resistance) data for the CDHL and one can decide whether working with hydrogenated version of these monomers will be beneficial or not (Figure 6.2).

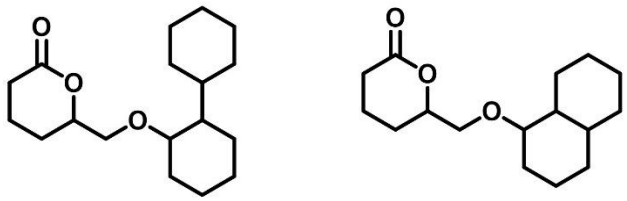

Figure 6.2. Hydrogenated version of proposed different new monomers

Only full catalyst screening was done for PDHL monomer in Chapter 2 (Section 2.3.1) by using different acidic to basic organo-catalysts. As higher TBD loading was needed for propagation of PhPDHL, NDHL and CDHL monomers (Sections 3.3.1, 4.3.1 and 5.3.1) and higher catalyst loadings provoked TBD initiated polymerization. Finding a new catalyst system which will not initiate the polymerization is necessary for future work. As mentioned in the first Chapter different catalysts can be screened like PDHL monomer. Less sterically hindered phosphazene catalyst like t-BuP_2 can be tested also (Figure 6.3).[127,128] Thiourea and IMes co-catalysts system showed successful polymerization of PDHL monomer in Section 2.3.1. No other synthesized monomers in this work have been tried with this catalyst system. This catalyst system can be tested for the polymerization of higher MW polymers.

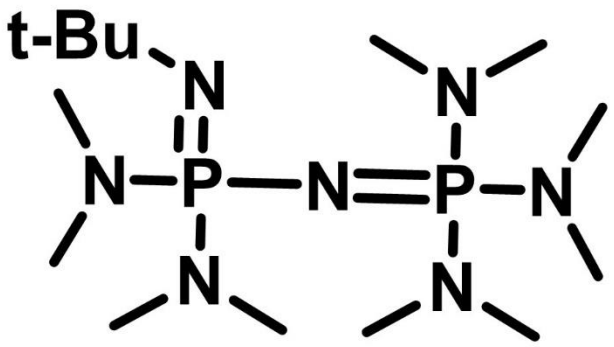

Figure 6.3. Phosphazene base t-BuP_2 catalyst

The problem with TBD catalyst system as shown earlier that it initiated the polymerization along with BnOH initiator. Figuring out the catalysts, which will not initiate the polymerization, is necessary for synthesizing high MW polymers. New catalysts system (t-BuP_2) or existing catalyst system (thiourea and IMes) should be tried as new experiments with and without BnOH initiation system. Different mechanistic studies can be done in future to figure out why some of the catalysts could polymerize these new monomers and some could not. One of the experiments would be find out the pK_a values of these lactone monomers and match with the pK_a values of different catalysts. The synthesized polymers in this work would be valuable in different applications. Copolymerization with different non-biodegradable polymers would introduce cleavable link in the polymers and bio-degradable properties can be achieved.

BIBLIOGRAPHY

[1]Thompson, R. C.; Swan, S. H.; Moore, C. J.; vom Saal, F. S., Introduction: Our Plastic Age. *Philosophical Transactions: Biological Sciences* **2009,** *364* (1526), 1973-1976.

[2]Corcoran, P. L.; Moore, C. J.; Jazvac, K., An anthropogenic marker horizon in the future rock record. *GSA Today* **2014,** *24* (6), 4-8.

[3]Delidovich, I.; Hausoul, P. J. C.; Deng, L.; Pfützenreuter, R.; Rose, M.; Palkovits, R. Alternative Monomers Based on Lignocellulose and Their Use for Polymer Production. *Chem. Rev.* **2016**, *116* (3), 1540–1599.

[4]Mohanty, A. K.; Misra, M.; Drzal, L. T. Sustainable Bio- Composites from Renewable Resources: Opportunities and Challenges in the Green Materials World. J. Polym. Environ. 2002, 10, 19− 26.

[5]O'Dea, R. M.; Willie, J. A.; Epps, T. H., 100th Anniversary of Macromolecular Science Viewpoint: Polymers from Lignocellulosic Biomass. Current Challenges and Future Opportunities. *ACS Macro Letters* **2020,** *9* (4), 476-493.

[6]Geyer, R.; Jambeck, J. R.; Law, K. L. Production, use, and fate of all plastics ever made. Sci. Adv. 2017, 3 (7), No. e1700782.

[7]Lebreton, L.; Slat, B.; Ferrari, F.; Sainte-Rose, B.; Aitken, J.; Marthouse, R.; Hajbane, S.; Cunsolo, S.; Schwarz, A.; Levivier, A.; Noble, K.; Debeljak, P.; Maral, H.; Schoeneich-Argent, R.; Brambini, R.; Reisser, J. Evidence that the Great Pacific Garbage Patch is rapidly accumulating plastic. Sci. Rep. 2018, 8 (1), 4666.

[8]Galbis, J. A.; García-Martín, M. de G.; de Paz, M. V.; Galbis, E. Synthetic Polymers from Sugar-Based Monomers. *Chem. Rev.* **2016**, *116* (3), 1600–1636

[9]Gandini, A. Polymers from Renewable Resources: A challenge for the future of macromolecular materials. Macromolecules 2008, 41, 9491−9504.

[10]Li, Z.; Yang, J.; Loh, X. J. Polyhydroxyalkanoates: Opening Doors for a Sustainable Future. *NPG Asia Mater.* **2016**, *8* (4), 1–20.

[11]Vahabi, H.; Michely, L.; Moradkhani, G.; Akbari, V.; Cochez, M.; Vagner, C.; Renard, E.; Saeb, M. R.; Langlois, V. Thermal Stability and Flammability Behavior of Poly(3-Hydroxybutyrate) (PHB) Based Composites. *Materials (Basel).* **2019**, *12* (14), 1–14.

[12]Lambert, S. As Biodegradable Plastics. **2015**, 1–9.

[13]Motagamwala, A. H.; Huang, K.; Maravelias, C. T.; Dumesic, J. A., Solvent system for effective near-term production of hydroxymethylfurfural (HMF) with potential for long-term process improvement. *Energy & Environmental Science* **2019,** *12* (7), 2212-2222.

[14]Gallo, J. M. R.; Alonso, D. M.; Mellmer, M. A.; Dumesic, J. A., Production and upgrading of 5-hydroxymethylfurfural using heterogeneous catalysts and biomass-derived solvents. *Green Chemistry* **2013,** *15* (1), 85-90.

[15]He, J.; Liu, M.; Huang, K.; Walker, T. W.; Maravelias, C. T.; Dumesic, J. A.; Huber, G., Production of levoglucosenone and 5-hydroxymethylfurfural from cellulose in polar aprotic solvent-water mixtures. *Green Chemistry* **2017**.

[16]Anderson, E. M.; Stone, M. L.; Katahira, R.; Reed, M.; Beckham, G. T.; Román-Leshkov, Y., Flowthrough Reductive Catalytic Fractionation of Biomass. *Joule* **2017,** *1* (3), 613-622.

[17]Schutyser, W.; Renders, T.; Van den Bosch, S.; Koelewijn, S. F.; Beckham, G. T.; Sels, B. F., Chemicals from lignin: an interplay of lignocellulose fractionation, depolymerisation, and upgrading. *Chemical Society Reviews* **2018,** *47* (3), 852-908.

[18]Jampa, S.; Puente-Urbina, A.; Ma, Z.; Wongkasemjit, S.; Luterbacher, J. S.; van Bokhoven, J. A., Optimization of Lignin Extraction from Pine Wood for Fast Pyrolysis by Using a γ-Valerolactone-Based Binary Solvent System. *ACS Sustainable Chemistry & Engineering* **2019,** *7* (4), 4058-4068.

[19]Shuai, L.; Amiri, M. T.; Questell-Santiago, Y. M.; Héroguel, F.; Li, Y.; Kim, H.; Meilan, R.; Chapple, C.; Ralph, J.; Luterbacher, J. S., Formaldehyde stabilization facilitates lignin monomer production during biomass depolymerization. *Science* **2016,** *354* (6310), 329.

[20]Buntara, T.; Noel, S.; Phua, P. H.; Melián-Cabrera, I.; de Vries, J. G.; Heeres, H. J., Caprolactam from Renewable Resources: Catalytic Conversion of 5-Hydroxymethylfurfural into Caprolactone. *Angewandte Chemie International Edition* **2011,** *50* (31), 7083-7087.

[21]Yoshida, N.; Kasuya, N.; Haga, N.; Fukuda, K., Brand-new Biomass-based Vinyl Polymers from 5-Hydroxymethylfurfural. *Polymer Journal* **2008,** *40* (12), 1164-1169.

[22]Tong, X.; Li, Y. Efficient and Selective Dehydration of Fructose to 5- Hydroxymethylfurfural Catalyzed by Brønsted-Acidic Ionic Liquids. *Chem. Sus. Chem* 2010, 3 (3), 350–355

[23]Carniti, P.; Gervasini, A.; Biella, S.; Auroux, A. Niobic Acid and Niobium Phosphate as Highly Acidic Viable Catalysts in Aqueous Medium: Fructose Dehydration Reaction. Catal. Today 2006, 118

[24]Schwartz, T. J.; Bond, J. A Thermodynamic and Kinetic Analysis of Solvent-Enhanced Selectivity in Monophasic and Biphasic Reactor Systems. *Chem. Commun*. 2017, 53, 8148–8151

[25]Román-Leshkov, Y.; Dumesic, J. A. Solvent Effects on Fructose Dehydration to 5-Hydroxymethylfurfural in Biphasic Systems Saturated with Inorganic Salts. *Top. Catal.* 2009, 52 (3), 297–303

[26]W. Diono, S. Machmudah, S.M. Goto, Utilization of sub and supercritical water reactions in resource recovery of biomass wastes, Eng. J. 17 (2013), 1-12.

[27]Kleinert, M.; Barth, T. Phenols from Lignin. *Chemical Engineering & Technology* 2008, 31 (5), 736–745.

[28]Binder, J. B.; Gray, M. J.; White, J. F.; Zhang, Z. C.; Holladay, J. E. Reactions of Lignin Model Compounds in Ionic Liquids. Biomass and Bioenergy 2009, 33 (9), 1122–1130.

[29]Caballero, J. A.; Font, R.; Marcilla, A. Comparative Study of the Pyrolysis of Almond Shells and Their Fractions, Holocellulose and Lignin. Product Yields and Kinetics. Thermochimica Acta 1996, 276, 57–77.

[30]S. Mukkamala, M.C. Wheeler, A.R.P. van Heiningen, W.J. DeSisto, Formate-Assisted Fast Pyrolysis of Lignin, Energy Fuels, 26 (2012) 1380-1384.

[31]S.H. Beis, S. Mukkamala, N. Hill, J. Joseph, C. Baker, B. Jensen, E.A. Stemmler, M.C. Wheeler, B.G. Frederick, A.R.P. van Heiningen, A.G. Berg, W.J. DeSisto, Fast Pyrolysis of Lignins, Bioresources, 5 (2010) 1408-1424.

[32]A.E. Vithanage, E. Chowdhury, L.D. Alejo, P.C. Pomeroy, W.J. DeSisto, B.G. Frederick, W.M. Gramlich, Renewably sourced phenolic resins from lignin bio-oil, J. Appl. Polym. Sci., 2017, 134

[33]Allen, M. C.; Hoffman, A. J.; Liu, T.-w.; Webber, M. S.; Hibbitts, D.; Schwartz, T. J., Highly Selective Cross-Etherification of 5-Hydroxymethylfurfural with Ethanol. *ACS Catalysis* **2020,** *10* (12), 6771-6785.

[34]Álvarez-Chávez, C. R.; Edwards, S.; Moure-Eraso, R.; Geiser, K., Sustainability of bio-based plastics: general comparative analysis and recommendations for improvement. *Journal of Cleaner Production* **2012,** *23* (1), 47-56.

[35]Farah, S.; Anderson, D. G.; Langer, R., Physical and mechanical properties of PLA, and their functions in widespread applications — A comprehensive review. *Advanced Drug Delivery Reviews* **2016,** *107*, 367-392.

[36]Singhvi, M.; Gokhale, D., Biomass to biodegradable polymer (PLA). *RSC Advances* **2013,** *3* (33), 13558-13568.

[37]Nguyen, H. T. H.; Qi, P.; Rostagno, M.; Feteha, A.; Miller, S. A., The quest for high glass transition temperature bioplastics. *Journal of Materials Chemistry A* **2018,** *6* (20), 9298-9331

[38]Galbis, J. A.; García-Martín, M. d. G.; de Paz, M. V.; Galbis, E., Synthetic Polymers from Sugar-Based Monomers. *Chemical Reviews* **2016,** *116* (3), 1600-1636.

[39]Liu, T.; Simmons, T. L.; Bohnsack, D. A.; MacKay, M. E.; Smith, M. R., III; Baker, G. L., Synthesis of Polymandelide: A Degradable Polylactide Derivative with Polystyrene-like Properties. *Macromolecules (Washington, DC, United States)* **2007,** *40* (Copyright (C) 2013 American Chemical Society (ACS). All Rights Reserved.), 6040-6047.

[40]Fiore, G. L.; Jing, F.; Young, J. V. G.; Cramer, C. J.; Hillmyer, M. A., High Tg aliphatic polyesters by the polymerization of spirolactide derivatives. *Polymer Chemistry* **2010,** *1* (6), 870-877.

[41]Marcincinova-Benabdillah, K.; Boustta, M.; Coudane, J.; Vert, M., Novel Degradable Polymers Combining d-Gluconic Acid, a Sugar of Vegetal Origin, with Lactic and Glycolic Acids. *Biomacromolecules* **2001,** *2* (4), 1279-1284.

[42]Gandini, A., The irruption of polymers from renewable resources on the scene of macromolecular science and technology. *Green Chemistry* **2011,** *13* (5), 1061-1083.

[43]Holmberg, A. L.; Stanzione, J. F.; Wool, R. P.; Epps, T. H., A facile method for generating designer block copolymers from functionalized lignin model compounds. *ACS Sustainable Chemistry & Engineering* **2014,** *2*, 569-573.

[44]Kim, H.; Olsson, J. V.; Hedrick, J. L.; Waymouth, R. M., Facile synthesis of functionalized lactones and organocatalytic ring-opening polymerization. *ACS Macro Letters* **2012,** *1*, 845-847.

[45]Kumar, A.; von Wolff, N.; Rauch, M.; Zou, Y.-Q.; Shmul, G.; Ben-David, Y.; Leitus, G.; Avram, L.; Milstein, D., Hydrogenative Depolymerization of Nylons. *Journal of the American Chemical Society* **2020,** *142* (33), 14267-14275.

[46]Kamber, N. E.; Jeong, W.; Waymouth, R. M.; Pratt, R. C.; Lohmeijer, B. G. G.; Hedrick, J. L., Organocatalytic Ring-Opening Polymerization. *Chemical Reviews* **2007,** *107* (12), 5813-5840.

[47]Alemán, C.; Betran, O.; Casanovas, J.; Houk, K. N.; Hall, H. K., Thermodynamic Control of the Polymerizability of Five-, Six-, and Seven-Membered Lactones. *The Journal of Organic Chemistry* **2009,** *74* (16), 6237-6244.

[48]Schneiderman, D. K.; Hillmyer, M. A., Aliphatic polyester block polymer design. *Macromolecules* **2016,** *49*, 2419-2428.

[49]Kamber, N. E.; Jeong, W.; Waymouth, R. M.; Pratt, R. C.; Lohmeijer, B. G. G.; Hedrick, J. L. Organocatalytic Ring-Opening Polymerization. *Chem. Rev.* **2007**, *107* (12), 5813–5840.

[50]Odian, G. Principles of Polymerization, 4th ed.; Wiley-Interscience: Hoboken, NJ, 2004.

[51]Gazeau-Bureau, S.; Delcroix, D.; Martín-Vaca, B.; Bourissou, D.; Navarro, C.; Magnet, S. Organo-Catalyzed ROP of ϵ-Caprolactone: Methanesulfonic Acid Competes with Trifluoromethanesulfonic Acid. Macromolecules **2008**, 41 (11), 3782–3784.

[52]Kamber, N. E.; Jeong, W.; Waymouth, R. M.; Pratt, R. C.; Lohmeijer, B. G. G.; Hedrick, J. L. Chem. ReV. **2007**, 107, 5813–5840.

[53]Lin, B.; Waymouth, R. M. Urea Anions: Simple, Fast, and Selective Catalysts for Ring-Opening Polymerizations. *J. Am. Chem. Soc.* **2017**, *139* (4), 1645–1652.

[54]Lohmeijer, B. G. G.; Pratt, R. C.; Leibfarth, F.; Logan, J. W.; Long, D. A.; Dove, A. P.; Nederberg, F.; Choi, J.; Wade, C.; Waymouth, R. M.; Hedrick, J. L. Guanidine and Amidine Organocatalysts for Ring-Opening Polymerization of Cyclic Esters. *Macromolecules* **2006**, *39* (25), 8574–8583.

[55]Zhang, L.; Pratt, R. C.; Nederberg, F.; Horn, H. W.; Rice, J. E.; Waymouth, R. M.; Wade, C. G.; Hedrick, J. L. Acyclic Guanidines as Organic Catalysts for Living Polymerization of Lactide. *Macromolecules* **2010**, *43* (3), 1660–1664.

[56]Nederberg, F.; Connor, E. F.; Moller, M.; Glauser, T.; Hedrick, J. L. Angew. Chem., Int. Ed. 2001, 40 (14), 2712–2715.

[57]Fastnacht, K. V.; Spink, S. S.; Dharmaratne, N. U.; Pothupitiya, J. U.; Datta, P. P.; Kiesewetter, E. T.; Kiesewetter, M. K. Bis- and Tris-Urea H-Bond Donors for Ring-Opening Polymerization: Unprecedented Activity and Control from an Organocatalyst. *ACS Macro Lett.* **2016**, *5* (8), 982–986.

[58]Spink, S. S.; Kazakov, O. I.; Kiesewetter, E. T.; Kiesewetter, M. K. Rate Accelerated Organocatalytic Ring-Opening Polymerization of l-Lactide via the Application of a Bis(Thiourea) H-Bond Donating Cocatalyst. *Macromolecules* **2015**, *48* (17), 6127–6131.

[59]Makiguchi, K.; Satoh, T.; Kauchi, T., Diphenyl Phosphate as an Efficient Cationic Organocatalyst for Controlled/Living Ring-Opening Polymerization of δ-Valerolactone and ε-Caprolactone. *Macromolecules* **2011,** *44*, 1999-2005.

[60]Kiesewetter, M. K.; Scholten, M. D.; Kirn, N.; Weber, R. L.; Hedrick, J. L.; Waymouth, R. M. Cyclic Guanidine Organic Catalysts: What Is Magic About Triazabicyclodecene? *J. Org. Chem.* **2009**, *74* (24), 9490–9496

[61]Dove, A. P. Organic Catalysis for Ring-Opening Polymerization. *ACS Macro Lett.* **2012**, *1* (12), 1409–1412

[62]Kiesewetter, M. K.; Shin, E. J.; Hedrick, J. L.; Waymouth, R. M. Organocatalysis: Opportunities and Challenges for Polymer Synthesis. *Macromolecules* **2010**, *43* (5), 2093–2107

[63]Chuma, A.; Horn, H. W.; Swope, W. C.; Pratt, R. C.; Zhang, L.; Lohmeijer, B. G. G.; Wade, C. G.; Waymouth, R. M.; Hedrick, J. L.; Rice, J. E. The Reaction Mechanism for the Organocatalytic Ring-Opening Polymerization of l-Lactide Using a Guanidine-Based Catalyst: Hydrogen-Bonded or Covalently Bound? *J. Am. Chem. Soc.* **2008**, *130* (21), 6749–6754

[64]Pratt, R. C.; Lohmeijer, B. G. G.; Long, D. A.; Waymouth, R. M.; Hedrick, J. L. Triazabicyclodecene: A Simple Bifunctional Organocatalyst for Acyl Transfer and Ring-Opening Polymerization of Cyclic Esters. *J. Am. Chem. Soc.* **2006**, *128* (14)

[65]Simón, L.; Goodman, J. M. The Mechanism of TBD-Catalyzed Ring-Opening Polymerization of Cyclic Esters. J. Org. Chem. 2007, 72 (25), 9656–9662.

[66]Olsén, P.; Odelius, K.; Albertsson, A.-C., Thermodynamic Presynthetic Considerations for Ring-Opening Polymerization. *Biomacromolecules* 2016**,** *17* (3), 699-709.

[67]Duda, A.; Kowalski, A. Handbook of Ring-Opening Polymerization 2009, 1−51.

[68]Dainton, F. S.; Ivin, K. J. Q. Rev., Chem. Soc. 1958, 12, 61.

[69]Schneiderman, D. K.; Hillmyer, M. A., Aliphatic polyester block polymer design. *Macromolecules* **2016,** *49*, 2419-2428.

[70]Dainton, F. S.; Ivin, K. J. Nature 1948, 162, 705.

[71]Dainton, F. S.; Ivin, K. J. Proc. R. Soc. London, Ser. A 1952, 212, 207.

[72]Dainton, F. S.; Ivin, K. J. Proc. R. Soc. London, Ser. A 1952, 212, 96.

[73]Odian, G. Principles of Polymerization, 4th ed.; Wiley-Interscience: Hoboken, NJ, 2004.

[74]Trost, B. M. Science 1991, 254, 1471.

[75]Fastnacht, K. V.; Spink, S. S.; Dharmaratne, N. U.; Pothupitiya, J. U.; Datta, P. P.; Kiesewetter, E. T.; Kiesewetter, M. K. Bis- and Tris-Urea H-Bond Donors for Ring-Opening Polymerization: Unprecedented Activity and Control from an Organocatalyst. *ACS Macro Lett.* **2016**, *5* (8), 982–986.

[76]Cywar, R. M.; Zhu, J.-B.; Chen, E. Y.-X. Selective or Living Organopolymerization of a Six-Five Bicyclic Lactone to Produce Fully Recyclable Polyesters. *Polym. Chem.* 2019, *10* (23), 3097–3106.

[77]Kiesewetter, M. K.; Shin, E. J.; Hedrick, J. L.; Waymouth, R. M. Organocatalysis: Opportunities and Challenges for Polymer Synthesis. Macromolecules 2010, *43* (5), 2093–2107.

[78]Lin, B.; Waymouth, R. M. Urea Anions: Simple, Fast, and Selective Catalysts for Ring-Opening Polymerizations. J. Am. Chem. Soc. 2017, *139* (4), 1645–1652.

[79]Hu, S.; Dai, G.; Zhao, J.; Zhang, G. Ring-Opening Alternating Copolymerization of Epoxides and Dihydrocoumarin Catalyzed by a Phosphazene Superbase. *Macromolecules* **2016**, *49* (12), 4462–4472.

[80]Flanders, M. J.; Gramlich, W. M., Reversible-addition fragmentation chain transfer (RAFT) mediated depolymerization of brush polymers. *Polymer Chemistry* **2018,** *9* (17), 2328-2335.

[81]Williams, C. K., Synthesis of functionalized biodegradable polyesters. *Chemical Society Reviews* **2007,** *36* (10), 1573-1580.

[82]Zhao, J.; Hadjichristidis, N., Polymerization of 5-alkyl δ-lactones catalyzed by diphenyl phosphate and their sequential organocatalytic polymerization with monosubstituted epoxides. *Polymer Chemistry* **2015,** *6*, 2659-2668.

[83]Neitzel, A. E.; Haversang, T. J.; Hillmyer, M. A., Organocatalytic Cationic Ring-Opening Polymerization of a Cyclic Hemiacetal Ester. *Industrial & Engineering Chemistry Research* **2016,** *55* (45), 11747-11755.

[84]Kasyapi, N.; Bhowmick, A. K., Nanolamellar triblock of poly-d,l-lactide–δ-valerolactone–d,l-lactide with tuneable glass transition temperature and crystallinity for use as a drug-delivery vesicle. *RSC Advances* **2014,** *4* (52), 27439-27451.

[85]Aubin, M.; Prud'homme, R. E., Preparation and properties of poly(valerolactone). *Polymer* **1981,** *22* (9), 1223-1226.

[86]Yang, H.; Ge, J.; Huang, W.; Xue, X.; Chen, J.; Jiang, B.; Zhang, G., Facile synthesis of biodegradable and clickable polymer. *RSC Advances* **2014,** *4* (45), 23377-23381.

[87]Kim, H.; Olsson, J. V.; Hedrick, J. L.; Waymouth, R. M., Facile synthesis of functionalized lactones and organocatalytic ring-opening polymerization. *ACS Macro Letters* **2012,** *1*, 845-847.

[88]Martello, M. T.; Burns, A.; Hillmyer, M. A., Bulk ring-opening transesterification polymerization of the renewable d-decalactone using an organocatalyst. *ACS Macro Letters* **2012,** *1*, 131-135.

[89]Shi, Y.; Cao, X.; Luo, S.; Wang, X.; Graff, R. W.; Hu, D.; Guo, R.; Gao, H., Investigate the Glass Transition Temperature of Hyperbranched Copolymers with Segmented Monomer Sequence. *Macromolecules* **2016,** *49* (12), 4416-4422.
[90]Flanders, M. J.; Gramlich, W. M., Reversible-addition fragmentation chain transfer (RAFT) mediated depolymerization of brush polymers. *Polymer Chemistry* **2018,** *9* (17), 2328-2335.

[91]Alamri, H.; Zhao, J.; Pahovnik, D.; Hadjichristidis, N. Phosphazene-Catalyzed Ring-Opening Polymerization of ε-Caprolactone: Influence of Solvents and Initiators. Polym. Chem. 2014, 5 (18), 5471–5478.

[92]Pascual, A., Sardón, H., Ruipérez, F., Gracia, R., Sudam, P., Veloso, A. and Mecerreyes, D. (2015), Experimental and computational studies of ring-opening polymerization of ethylene brassylate macrolactone and copolymerization with ε-caprolactone and TBD-guanidine organic catalyst. J. Polym. Sci. Part A: Polym. Chem., 53: 552-561.

[93]Simón, L.; Goodman, J. M., The Mechanism of TBD-Catalyzed Ring-Opening Polymerization of Cyclic Esters. *The Journal of Organic Chemistry* **2007,** *72* (25), 9656-9662

[94]Jaffredo, C. G.; Carpentier, J.-F.; Guillaume, S. M. Controlled ROP of β-Butyrolactone Simply Mediated by Amidine, Guanidine, and Phosphazene Organocatalysts. *Macromolecular Rapid Communications* **2012**, *33* (22), 1938–1944.

[95]Kasyapi, N.; Bhowmick, A. K., Nanolamellar triblock of poly-d,l-lactide–δ-valerolactone–d,l-lactide with tuneable glass transition temperature and crystallinity for use as a drug-delivery vesicle. *RSC Advances* **2014,** *4* (52), 27439-27451.

[96]Aubin, M.; Prud'homme, R. E., Preparation and properties of poly(valerolactone). *Polymer* **1981,** *22* (9), 1223-1226.

[97]Yang, H.; Ge, J.; Huang, W.; Xue, X.; Chen, J.; Jiang, B.; Zhang, G., Facile synthesis of biodegradable and clickable polymer. *RSC Advances* **2014,** *4* (45), 23377-23381.

[98]Schneiderman, D. K.; Hillmyer, M. A., Aliphatic polyester block polymer design. *Macromolecules* **2016,** *49*, 2419-2428.

[99]Duda, A.; Kowalski, A.; Penczek, S.; Uyama, H.; Kobayashi, S. Kinetics of the Ring-Opening Polymerization of 6-, 7-, 9-, 12-, 13-, 16-, and 17-Membered Lactones. Comparison of Chemical and Enzymatic Polymerizations. *Macromolecules* **2002**, *35* (11), 4266–4270.

[100]Makiguchi, K.; Satoh, T.; Kauchi, T., Diphenyl Phosphate as an Efficient Cationic Organocatalyst for Controlled/Living Ring-Opening Polymerization of δ-Valerolactone and ε-Caprolactone. *Macromolecules* **2011,** *44*, 1999-2005.

[101]Olsén, P.; Odelius, K.; Albertsson, A.-C., Thermodynamic Presynthetic Considerations for Ring-Opening Polymerization. *Biomacromolecules* **2016,** *17* (3), 699-709.

[102]Kamber, N. E.; Jeong, W.; Waymouth, R. M.; Pratt, R. C.; Lohmeijer, B. G. G.; Hedrick, J. L. Organocatalytic Ring-Opening Polymerization. *Chem. Rev.* **2007**, *107* (12), 5813–5840.

[103]Martello, M. T.; Burns, A.; Hillmyer, M. A., Bulk ring-opening transesterification polymerization of the renewable d-decalactone using an organocatalyst. *ACS Macro Letters* **2012,** *1*, 131-135.

[104]Tavana, J.; Faysal, A.; Vithanage, A.; Gramlich, W. M.; Schwartz, T. J. Pathway to Fully-Renewable Biobased Polyesters Derived from HMF and Phenols. *Polym. Chem.* **2022**.

[105]Camacho-Zuñiga, C.; Ruiz-Treviño, F. A. A New Group Contribution Scheme To Estimate the Glass Transition Temperature for Polymers and Diluents. *Ind. Eng. Chem. Res.* **2003**, *42* (7), 1530–1534.

[106]Flanders, M. J.; Gramlich, W. M., Reversible-addition fragmentation chain transfer (RAFT) mediated depolymerization of brush polymers. *Polymer Chemistry* **2018,** *9* (17), 2328-2335.

[107]Alamri, H.; Zhao, J.; Pahovnik, D.; Hadjichristidis, N. Phosphazene-Catalyzed Ring-Opening Polymerization of ε-Caprolactone: Influence of Solvents and Initiators. Polym. Chem. 2014, 5 (18), 5471–5478.

[108]Simón, L.; Goodman, J. M., The Mechanism of TBD-Catalyzed Ring-Opening Polymerization of Cyclic Esters. *The Journal of Organic Chemistry* **2007,** *72* (25), 9656-9662

[109]Zhao, J., Hadjichristidis, N., & Gnanou, Y. (2014). Phosphazene-promoted anionic polymerization. *Polimery*, *59*(1), 49-59.

[110]Ntetsikas, K.; Alzahrany, Y.; Polymeropoulos, G.; Bilalis, P.; Gnanou, Y.; Hadjichristidis, N. Anionic Polymerization of Styrene and 1,3-Butadiene in the Presence of Phosphazene Superbases. *Polymers* **2017**, *9*, 538.

[111]Kasyapi, N.; Bhowmick, A. K., Nanolamellar triblock of poly-d,l-lactide–δ-valerolactone–d,l-lactide with tuneable glass transition temperature and crystallinity for use as a drug-delivery vesicle. *RSC Advances* **2014,** *4* (52), 27439-27451.

[112]Aubin, M.; Prud'homme, R. E., Preparation and properties of poly(valerolactone). *Polymer* **1981,** *22* (9), 1223-1226.

[113]Yang, H.; Ge, J.; Huang, W.; Xue, X.; Chen, J.; Jiang, B.; Zhang, G., Facile synthesis of biodegradable and clickable polymer. *RSC Advances* **2014,** *4* (45), 23377-23381.

[114]Schneiderman, D. K.; Hillmyer, M. A., Aliphatic polyester block polymer design. *Macromolecules* **2016,** *49*, 2419-2428.

[115]Duda, A.; Kowalski, A.; Penczek, S.; Uyama, H.; Kobayashi, S. Kinetics of the Ring-Opening Polymerization of 6-, 7-, 9-, 12-, 13-, 16-, and 17-Membered Lactones. Comparison of Chemical and Enzymatic Polymerizations. *Macromolecules* **2002**, *35* (11), 4266–4270.

[116]Makiguchi, K.; Satoh, T.; Kauchi, T., Diphenyl Phosphate as an Efficient Cationic Organocatalyst for Controlled/Living Ring-Opening Polymerization of δ-Valerolactone and ε-Caprolactone. *Macromolecules* **2011,** *44*, 1999-2005.

[117]Olsén, P.; Odelius, K.; Albertsson, A.-C., Thermodynamic Presynthetic Considerations for Ring-Opening Polymerization. *Biomacromolecules* **2016,** *17* (3), 699-709.

[118]Kamber, N. E.; Jeong, W.; Waymouth, R. M.; Pratt, R. C.; Lohmeijer, B. G. G.; Hedrick, J. L. Organocatalytic Ring-Opening Polymerization. *Chem. Rev.* **2007**, *107* (12), 5813–5840.

[119]Martello, M. T.; Burns, A.; Hillmyer, M. A., Bulk ring-opening transesterification polymerization of the renewable d-decalactone using an organocatalyst. *ACS Macro Letters* **2012,** *1*, 131-135.

[120]Flanders, M. J.; Gramlich, W. M., Reversible-addition fragmentation chain transfer (RAFT) mediated depolymerization of brush polymers. *Polymer Chemistry* **2018,** *9* (17), 2328-2335.

[121]Hesek, D.; Lee, M.; Noll, B. C.; Fisher, J. F. Complications from Dual Roles of Sodium Hydride as a Base and as a Reducing Agent. **2009**, No. 3, 2567–2570.

[122]Kasyapi, N.; Bhowmick, A. K., Nanolamellar triblock of poly-d,l-lactide–δ-valerolactone–d,l-lactide with tuneable glass transition temperature and crystallinity for use as a drug-delivery vesicle. *RSC Advances* **2014,** *4* (52), 27439-27451.

[123]Aubin, M.; Prud'homme, R. E., Preparation and properties of poly(valerolactone). *Polymer* **1981,** *22* (9), 1223-1226.

[124]Yang, H.; Ge, J.; Huang, W.; Xue, X.; Chen, J.; Jiang, B.; Zhang, G., Facile synthesis of biodegradable and clickable polymer. *RSC Advances* **2014,** *4* (45), 23377-23381.

[125]Duda, A.; Kowalski, A.; Penczek, S.; Uyama, H.; Kobayashi, S. Kinetics of the Ring-Opening Polymerization of 6-, 7-, 9-, 12-, 13-, 16-, and 17-Membered Lactones. Comparison of Chemical and Enzymatic Polymerizations. *Macromolecules* **2002**, *35* (11), 4266–4270.

[126]Martello, M. T.; Burns, A.; Hillmyer, M. A., Bulk ring-opening transesterification polymerization of the renewable d-decalactone using an organocatalyst. *ACS Macro Letters* **2012,** *1*, 131-135.

[127]Zhao, J.; Hadjichristidis, N.; Schlaad, H. Polymerization Using Phosphazene Bases. In *Anionic Polymerization: Principles, Practice, Strength, Consequences and Applications*; Hadjichristidis, N., Hirao, A., Eds.; Springer Japan: Tokyo, 2015; pp 429–449.

[128]Ren, C.; Zhu, X.; Zhao, N.; Shen, Y.; Chen, L.; Liu, S.; Li, Z. Polystyrene Beads Supported Phosphazene Superbase as Recyclable Organocatalyst for Ring-Opening Polymerization of δ-Valerolactone. *European Polymer Journal* **2019**, *119*, 130–135.

BIOGRAPHY OF THE AUTHOR

Atik Faysal was born in Dhaka, Bangladesh on August 02, 1994. He was raised in Dhaka, Bangladesh and graduated from University of Dhaka in 2016 with a bachelor's degree in Applied Chemistry and Chemical Engineering. After receiving his degree, Atik will be joining MilliporeSigma, to begin his career in the field of polymer chemistry as an R&D Scientist. Atik is a candidate for the Doctor of Philosophy degree in Chemistry from the University of Maine in May 2022.